**Ph.D. Dissertation of Sport Science**

# REFERENT CONTROL OF HUMAN PREHENSION

**– Synergies and Hierarchical Organization of Control Variables for Translational and Rotational Equilibrium in Multi-digit Prehension –**

**August 2022**

**Graduate School of Seoul National University**
**Department of Physical Education**
**Human Biomechanics Major**

**Junkyung Song**

# REFERENT CONTROL OF HUMAN PREHENSION

## – Synergies and Hierarchical Organization of Control Variables for Translational and Rotational Equilibrium in Multi-digit Prehension –

**Advisor Jaebum Park**

**Submitting a Ph.D. Dissertation of Sport Science**

**June 2022**

**Graduate School of Seoul National University**
**Department of Physical Education**
**Human Biomechanics Major**

**Junkyung Song**

**Confirming the Ph.D. Dissertation written by Junkyung Song**

**June 2022**

| | | |
|---|---|---|
| Chair | Seonjin Kim | (Seal) |
| Vice Chair | Jooeun Ahn | (Seal) |
| Examiner | Jae Kun Shim | (Seal) |
| Examiner | Woojin Park | (Seal) |
| Examiner | Jaebum Park | (Seal) |

# Abstract

Stabile prehensile action is a basic function commonly required in daily lives. Static equilibrium during prehension can be achieved by an infinite combination of digit forces and moments. Thus, the multi-digit prehension is mechanically redundant. This dissertation aimed to extend the understanding of human prehension mechanisms, known mainly as mechanical variables such as digit forces and moments, to a control level based on the referent control hypothesis. According to the referent control, the mechanical effects of digit in the isometric condition emerge by specifying the digit referent position and apparent stiffness as hypothetical control variables. We devised two types of motorized handle apparatus that could induce the handle displacement to quantify a set of the control variables for translational and rotational equilibrium, separately. It was found that the control variables were hierarchically organized in a way to stabilize mechanical effects during static prehension. This organizing pattern of the control variables differed depending on given external constraints. We confirmed the evidence that the functional implications of the two control variables may be different. The referent variable is related to the direction and magnitude of desired net mechanical effects, while the apparent stiffness reflects the stability properties for the effectors and given tasks. Further, the control variables for translation and rotation could be organized independently, consistent with the principle of superposition in human prehension. Overall, these results implied that the neuromotor system generates the motor commands required for static prehension, reflecting the external constraints of the task, the desired mechanical effect, and the stability properties of effectors. Our findings add to current literature on human prehension control and will explore the control mechanisms of various human movements by supplementing the current framework of the referent control hypothesis.

***Keyword*****:** Multi-digit prehension, Equilibrium-point hypothesis, Referent control, Human motor control, Motor redundancy, Motor synergy

***Student Number*****:** 2017-31990

# Table of Contents

# List of Figures

## Chapter 1



## Chapter 2



## Chapter 3

## Chapter 4

# List of Tables

## Chapter 3

# Chapter 1. General Introduction

## 1.1. Problem Statement

Stable grasping and manipulating an object by exerting forces on them using five digits (i.e., multi-digit prehension) is a basic function commonly required in our daily lives. For static prehension, the central nervous system (CNS) has to adjust the mechanical effect of the individual digit to produce the required resultant force and moment. This process is mechanically redundant—the resultant forces and moments that satisfy the static prehension can be achieved by different sets of individual digit forces (Park, Kim, & Shim, 2010; Pataky, Latash, & Zatsiorsky, 2004a; Shim, Latash, & Zatsiorsky, 2003; Zatsiorsky, Gregory, & Latash, 2002b). Further, recent developments of the equilibrium-point hypothesis (the *lambda*-model) to the referent control have suggested that even a single effector makes mechanically non-redundant has redundancy at the level of control in isometric condition (Feldman, 2015; Latash, 2020a). In this framework, two control variables, the threshold position (referent coordinate, *RC*; referent angle, $R_\theta$) and apparent stiffness ($k$), co-varied each other to stabilize desired mechanical outcome (Ambike, Mattos, Zatsiorsky, & Latash, 2016).

By intuitive inference rather than empirical observation, recent studies proposed a set of hypothetical control variables, *Referent aperture*, *Referent orientation (angle)*, and *Referent vertical coordinate*, commensurate with prehension mechanics to describe the control of grasping objects (Ambike, Paclet, Zatsiorsky, & Latash, 2014; Latash, Friedman, Kim, Feldman, & Zatsiorsky, 2010). It is assumed

that designates the referent aperture ensures the grip stability (i.e., horizontal translation constraint), and setting the referent orientation allows the generation of a desired net moment of force to satisfy rotational equilibrium constraint. However, no attempt has been made to experimentally quantify the variables of referent aperture and referent orientation during prehensile action. For the first time, quantification and reconstruction of these hypothetical control variables is the primary purpose of this dissertation.

Based on the referent control hypothesis, the current dissertation will specifically address the following topics: 1) *Synergies and hierarchical organization of the hypothetical control variables for static prehensile action*. According to the referent control hypothesis, the defined higher-level control variables produce high-dimensional lower-level variables, and this sequence of few-to-many mapping is based on the task-specific stability, characteristics of a biological system (Latash, 2020a). This hierarchical control scheme has not yet been tested in a prehensile action consisting of two levels of the control hierarchy (i.e., the task is shared between the thumb and a virtual finger at the upper hierarchy; at the lower hierarchy, the effect of the virtual finger is combined by four fingers). 2) *Effect of external mechanical constraints on synergies within the space of control variables*. The CNS is known to use different strategies during multi-digit prehension depending on various internal (Hager-Ross & Schieber, 2000) and external constraints (Park, Kim, et al., 2010). However, these studies addressed mechanical variables such as digit force and moment production, and it is still largely unknown how mechanical constraints influence the organizing patterns of the control level variables. 3) *Principle of superposition in the space of control variables describing translation*

*and rotation of grasping object.* According to the principle of superposition, translation and rotation equilibrium for static prehension can be decomposed into independently controlled sub-action (Arimoto & Nguyen, 2001). Since several studies have confirmed this decoupled strategy is effective in human grasping tasks (Shim, Latash, & Zatsiorsky, 2005b; Zatsiorsky, Latash, Gao, & Shim, 2004), we expect to be also preserved in the space of the control variable ensuring grip stability and rotational equilibrium. It is hoped that the outcomes of this dissertation will add to the current literature on prehension control and help to understand the neuromotor system that designates the control variables reflecting various external and internal constraints to ensure stable prehensile actions.

## 1.2. Study Objectives

This dissertation has the following objectives.

1) To quantify the referent aperture and investigate the hierarchical organization of referent coordinate ($RC$) and the apparent stiffness ($k$) as hypothetical control variables for grip force production (chapter 3).

2) To test a hypothesis on the stability properties in the space of control variables $\{RC, k\}$ depending on external constraints (chapter 3).

3) To quantify the referent orientation for digit moment production and identify the hierarchical organization of referent angle ($R_\theta$) and apparent rotational stiffness ($k_\theta$) depending on magnitude and direction of moment production (chapter 4).

4) To identify the validity of the principle of superposition and extend it into the

space of control variables during multi-digit moment production (chapter 4).

## 1.3. Organization of Dissertation

In chapter 2, the following issues on previous works of literature are reviewed and discussed: the motor redundancy and abundance, equilibrium-point hypothesis, referent control of motor action, mechanics of static prehension, and prehension control. The current dissertation consists of two sub-studies that are related to translation and rotation equilibrium control of human prehension (Figure 1.1).

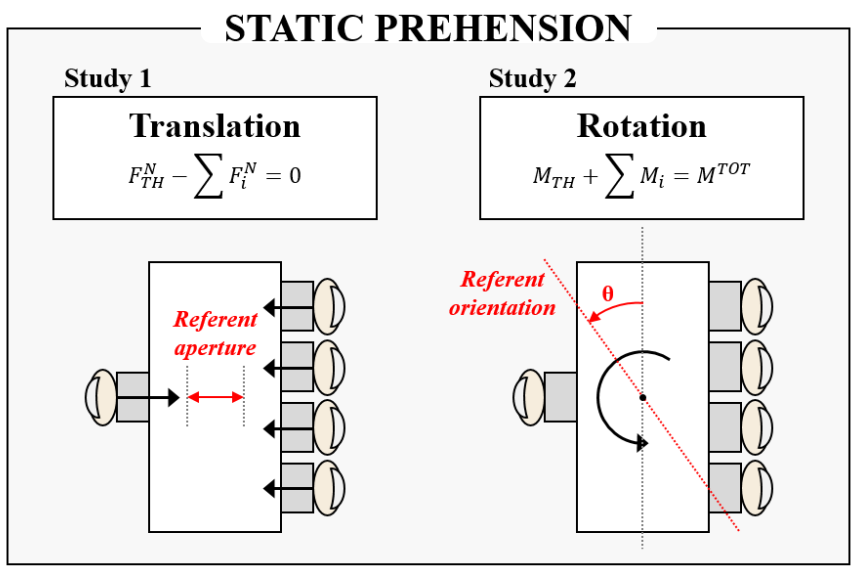


**Figure 1.1.** A diagram for organization of current dissertation. $F^N_{TH}$: normal forces of thumb; $F^N_i$: normal forces of individual fingers; $M_{TH}$: moment of thumb; $M_i$: moment of individual fingers; $M_{TOT}$: total moment.

**1) Study 1 (chapter 3)**

**Translational equilibrium control**: *hierarchical and synergistic organization of control variables (RC, k) during multi-digit grasp of a free and an externally fixed object.*

**2) Study 2 (chapter 4)**

**Rotational equilibrium control**: *hierarchical and synergistic organization of control variables ($R_\theta$, $k_\theta$) for magnitude and direction of multi-digit moment production.*

# Chapter 2. Background of Literature Review

## 2.1. Motor Redundancy & Motor Abundance

In general, human movement has more elements contributing to performance than are necessary to solve corresponding motor tasks. For example, a person trying to reach his hand to an object, the possible configuration of the arm has more degrees of freedom (DOF) than is needed to organize the spatial position and orientation of the hand. Moreover, the number of muscles that create a joint at a certain angle within the task space easily exceeds the DOF of the joint—i.e., every level of analysis of the human movement system is redundant. Therefore, the CNS has to deal with more DOF than what is prescribed in the task space. This problem of motor redundancy has been recognized as a central issue in the field of motor control. Through a famous study involving Blacksmith, Bernstein stated that the CNS does not find a unique solution by removing redundant DOF but instead tries to use an apparently redundant set of elements to stabilize the performance of the task (Bernstein, 1930, 1947, 1966).

Several assumptions and approaches explaining how the CNS solves the redundancy problem have been suggested. Some researchers have considered that the controller tries to find a unique solution based on optimization approaches, which essentially need to select a cost function (Mussaivaldi & Hogan, 1991; Todorov, 2004). These approaches applying optimization principles were based on certain mechanical, psychological, or complex cost functions (Rosenbaum, Loukopoulos, Meulenbroek, Vaughan, & Engelbrecht, 1995; Seif-Naraghi & Winters, 1990). An

alternative approach to the problem of motor redundancy was based on the principle of motor abundance (Gelfand & Latash, 1998; Latash, 2012). In this principle, the controller does not generate a single optimal solution to cope with the redundancy problem. Rather, it facilitates families of solutions that can equally solve the task with acceptable accuracy, which is in line with Bernstein's view. These families reflect the preferred sharing of the redundant element for stability of action and have been referred to as a "synergy". The following section addresses the concept of motor synergy related to the central content of this dissertation.

### 2.1.1. Motor Synergy

Movement does not repeat itself due to motor variability in the characteristics of neuromuscular elements, even if the control pattern and the external conditions remain unchanged (Bernstein, 1966). Nevertheless, human movements have properties that stabilize certain variables that can be specific effectors, outcome forces, whole-body COM, etc. Ensuring the stability for task-specific variables in the presence of internal and environmental variability is important feature of biological systems. Many researchers confirmed this characteristic of action stability (Latash, 2017), starting from the aforementioned classical study of professional blacksmiths—it showed that the variability in the trajectory of the hammer across repetitive strikes has relatively lower than the variability of the joint trajectories (Bernstein, 1930). The important notion of *task-specific stability* was introduced as a characteristic of the movement system (Schoner, 1995). This notion suggests that the redundant element system is able to reorganize interactions among elements leading to stability of certain performance variables but

not others, depending on the task and intention of the actor. The definition of motor synergy includes this notion of task-specific stability, and incorporating redundant factors into these synergies has been viewed as a means of mitigating problem of motor redundancy by reducing the number of variables manipulated by CNS (Latash, Scholz, & Schoner, 2007).

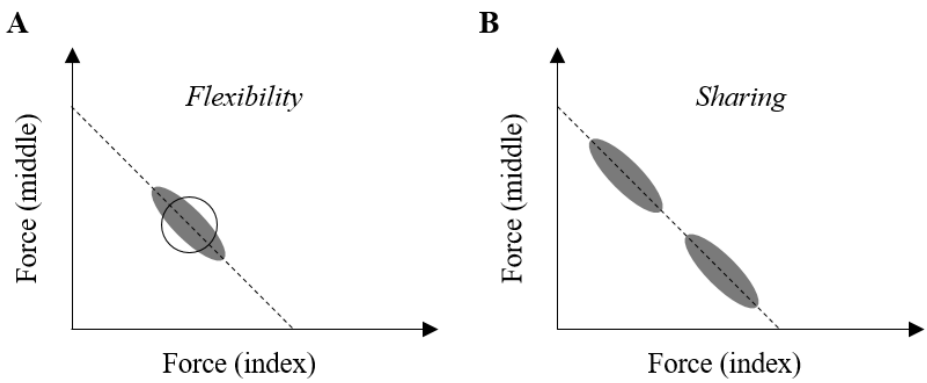


**Figure 2.1.** An illustration of two features of synergy, flexibility and sharing.

Flexibility and sharing are important features of synergies (Latash, 2008). For example, when generating a certain resultant force with index and middle fingers, the forces by individual fingers vary from trial to trial. The inclined dashed lines in Figure 2.1 represent the perfect solution space ensuring the prescribed resultant force by all possible combinations of two-finger forces. The data distributions over repetitive trials can be formed circles or ellipses, as shown in Figure 2.1A. In general, smaller than expected finger forces are compensated by other finger forces (i.e., negative co-variation). Thus, the data cloud can appear in the form of an ellipse; it represents the flexibility that a co-variation pattern between finger forces reflects

how well the synergy stabilized the performance variable. Further, the average distribution of finger forces can possibly differ from person to person. Figure 2.1B describes an example of two sharing patterns—forces of the index finger may be relatively greater than the middle finger and vice versa. The average location of the data distribution (sharing) and the shape of the distribution (stability/flexibility) are generally independent and are therefore considered two basic characteristics of synergy. The flexibility reflects the stability properties within the space of a redundant system, and sharing is considered the preferred pattern for the controller to organize redundant DOFs for successful performance.

### 2.1.2. Uncontrolled Manifold Approach

A method to analyze the structure of the variability has been developed within the framework of the uncontrolled manifold (UCM) hypothesis (Scholz & Schoner, 1999). It is used in many studies of various tasks involving multi-finger pressing and prehension tasks (Park, Han, & Shim, 2015; Park, Singh, Zatsiorsky, & Latash, 2012; Park, Zatsiorsky, & Latash, 2010; Shim, Latash, & Zatsiorsky, 2005a; Shim et al., 2005b; Song, Kim, & Park, 2021) and for impaired populations (Jo et al., 2016; Kong, Kim, Joung, Chung, & Park, 2019; Latash & Huang, 2015; Park, Lewis, Huang, & Latash, 2013; Park, Wu, Lewis, Huang, & Latash, 2012; Song, Shin, Kim, & Park, 2021). The UCM hypothesis is based on the principle of motor abundance, stabilizing task-specific performance variables through the benefit of redundant elements instead of selecting a unique solution.

The synergy can be quantified by UCM analysis that separates the variance in the space of elemental variables into two sub-spaces. The first sub-space, UCM,

yields no changes in the given performance variables. The second sub-space was the orthogonal component (ORT) to the UCM, of which the variances within the ORT space affect the changes in the performance variables. The relative difference between the variance within UCM ($V_{UCM}$) and ORT ($V_{ORT}$) is used as a synergy index as follows.

$$\text{synergy index } (\Delta V) = \frac{(V_{UCM}/DOF_{UCM} - V_{ORT}/DOF_{ORT})}{(V_{TOT}/DOF_{TOT})} \qquad (2.1),$$

where the $V_{TOT}$ represents the sum of $V_{UCM}$ and $V_{ORT}$ (total variance), and all variance are computed per dimension in the corresponding space (i.e., normalized by their DOF of each space). Note that the synergy index is influenced by both variance components, $V_{UCM}$ and $V_{ORT}$; the magnitude of synergy index cannot be attributed to change in one component (Karol et al., 2011). The index of synergy provides information on how actively the CNS uses motor redundancy. The intentional increase in $V_{UCM}$ can be evidence that the system can explore a variety of solutions under unusual or uncertain conditions (Freitas & Scholz, 2009; Yang, Scholz, & Latash, 2007).

## 2.2. Equilibrium-Point Hypothesis

The equilibrium-point (EP) hypothesis, especially the lambda (λ) model, has become a steadily increasing theoretical framework in the field of motor control. The EP hypothesis is the only theory that the CNS uses physiological variables as control variables without the necessity to pre-program mechanical variables and motor commands. The term ‘parametric control’ also reflects this feature, and it was demonstrated empirically in humans and animals (Archambault, Mihaltchev, Levin,

& Feldman, 2005; Asatryan & Feldman, 1965; Feldman, 2015; Feldman & Orlovsky, 1972; Foisy & Feldman, 2006; Matthews, 1959). The parameter, λ, is the activation threshold of alpha ($\alpha$) motoneuron specified in the dimension of muscle length—central signal defines the λ as the spatial range where the muscle activity initiates and generates length-dependent active muscle force (Asatryan & Feldman, 1965; Feldman, 1966, 1986). Changing such parameters shift the equilibrium state by the interaction between the organism and the environment. Consequently, changes in mechanical properties and motor commands emerge due to a natural cooperative tendency of the neuromuscular system to reach equilibrium (Feldman, Goussev, Sangole, & Levin, 2007). This particular form of parametric control can be considered as the foundation of a physiologically feasible theory of the human movement system, and this section first addresses how the influence from the descending and spinal centers on $\alpha$-motoneuron are transformed into spatial variables.

### 2.2.1. Physiological Origin for Threshold Properties of $\alpha$-motoneuron

One of the well-known biological features of skeletal muscle is the dependence of active muscle force on muscle length (i.e., tonic stretch reflex (Liddell & Sherrington, 1924)). If the inactive muscle slowly stretches from its initial length and the central influence remains unchanged, the length-dependent afferent inputs from muscle receptors (i.e., muscle spindles) facilitate motoneuron, the membrane potential of corresponding motoneuron increases (Matthews, 1972). Then, when the electrical threshold is reached, the motoneuron is recruited, and this point of muscle length is the threshold of the stretch reflex.

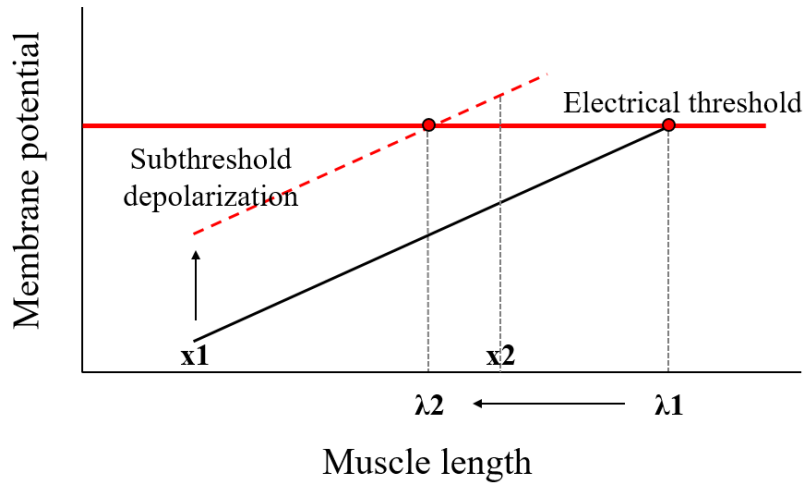


**Figure 2.2.** Physiological origin of threshold position control.

Figure 2.2 is a simple example of threshold position control for a single $\alpha$-motoneuron. The motoneuron is in a subthreshold state at resting muscle length (x1), and membrane potential increase with passive muscle lengthening by facilitating afferent feedback. The $\alpha$-motoneuron is recruited where it reaches the electrical threshold (horizontal red line), and this muscle length is the threshold of muscle length ($\lambda$1). The membrane potential can be enhanced through direct ($\alpha$-inputs) or indirect ($\gamma$-inputs) effects on the $\alpha$-motoneuron. As a result, the $\alpha$-motoneuron will be recruited at a shorter muscle length ($\lambda$2). The $\alpha$-motoneuron can be recruited without passive muscle lengthening. When the muscle length is x2, and the threshold position is set to $\lambda$1, it is silent because the $\alpha$-motoneuron is in a state of subthreshold. At this time, if the threshold position is shifted to $\lambda$2 by central facilitation, the corresponding $\alpha$-motoneuron can be recruited at x2 length. Unlike afferent input, the central input to motor neurons is independent of muscle length so that the central

input can enhance membrane potential at any muscle length. Further, threshold muscle length can be changed via some influences descending from the brainstem, which influence the electrical threshold of $\alpha$-motoneurons (Fedirchuk & Dai, 2004; Heckman, Johnson, Mottram, & Schuster, 2008; Krawitz, Fedirchuk, Dai, Jordan, & McCrea, 2001). It is known that tonic bulbo-spinal stimulation changes the electrical thresholds of $\alpha$-motoneurons resulting shift in the spatial thresholds for muscle activation. In the state of minimal supraspinal and spinal influences, the threshold is higher than the upper limit of biomechanical muscle length, so the muscle can be relaxed at all joint angles within the biomechanical range (Feldman, 2019).

Various sources, as well as the central drive, can influence setting the threshold of muscle activation. According to the EP hypothesis, the muscle is activated when the difference between the actual muscle length and the threshold length is greater than zero ($x - \lambda^* > 0$; $\lambda^*$ is the net dynamic threshold of muscle activation). The dependency of the threshold length on stretch velocity ($v$) can also affect setting $\lambda^*$ (Pilon & Feldman, 2006). As the muscle is lengthened at a rapid rate, the membrane potential increases more steeply, and the $\alpha$-motoneuron is recruited at a shorter muscle length. These features are formulated with the first approximation as follows.

$$\lambda^* = \lambda - \mu v + \rho + \varepsilon \qquad (2.2),$$

where the $\lambda$ is a central component of the threshold of muscle length, the $v$ represents velocity ($v>0$ for lengthening and $v<0$ for shortening), the $\mu$ stands for dynamic sensitivity of the motoneuronal pool, and it defined via the activity of dynamic $\gamma$-motorneuron that innervate muscle spindle (Matthews, 1972). The $\rho$ represents the component of the threshold that from heteronymous proprioceptive and cutaneous

afferent influences on motoneuron, and $\varepsilon$ is a component representing the history-dependent intrinsic properties of the motoneuron.

In summary, the motoneuron functions in a one-dimensional spatial frame of reference, which is the length of the muscle. This referent point in this frame of reference is the threshold position of muscle activation ($\lambda^*$), and the activity of the motoneurons depends on the difference between the current length and the threshold length of the muscle. The referent point can be changed by supraspinal and spinal input, and the velocity of changes in muscle length and intermuscular interaction also influence it. Any deviation of the muscle length from the threshold length, elicited by central resetting or external forces, causes a change in proprioceptive signals to $\alpha$-motoneuron. The proprioceptive response also induces the activation of interneurons in the reflex loops, some of which mediate interactions between muscles. Gelfand and Tsetlin (1971) suggested that the response of the neuromuscular system to any imposed activity and interactions is driven by the *Principle of minimal interaction*. According to this principle, the system seeks to reduce the imposed activity by bringing the body into a state that minimizes all possible interactions in the system within limits defined by external forces. It implies that the neuromuscular elements act individually or collectively to reduce the imposed activity and interaction by minimizing the gap between the actual and threshold position (Feldman et al., 2007).

### 2.2.2. Threshold Position Control with EP for Single Muscle and Joint

Threshold determines where the muscle begins to be activated and produces nonlinear force-length characteristics (Asatryan & Feldman, 1965). This

characteristic is called invariant (ICs: invariant characteristics). Shifting λ does not prescribe changes in any mechanical variables such as muscle force, length, and even level of muscle activation (i.e., EMG) that can change differently depending on the characteristics of external force. The EP represents a specific combination of positions in body segments where muscles and external forces or torques are balanced. Since EP is characterized by the interactions between the organisms and environment, the CNS can only influence but cannot predetermine it.

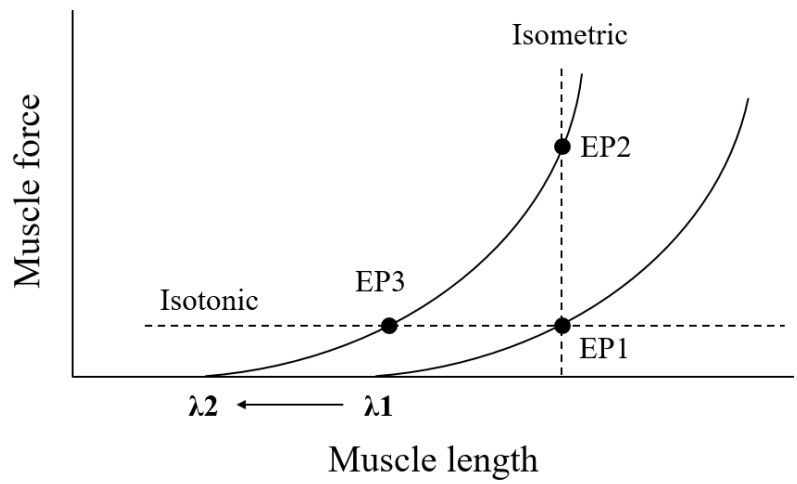


**Figure 2.3.** Force-length characteristics for single muscle.

In Figure 2.3, the λ defines the spatial range where the muscle begins to produce active force. Then, the EP is located at a specific muscle length along the IC curve where external load and active muscle force are balanced (EP1). If the threshold position is shifted under the isometric condition (from λ1 to λ2), the EP reaches a new balance point along the shifted IC curve where requires greater active muscle force (EP2). When the external force does not change and there is no factor

limiting the change in the length of the muscle (i.e., isotonic condition), the shifting of λ changes the EP to the shorter muscle length and induces movement (EP3). In other words, within the EP hypothesis, movement (i.e., changes in muscle length) can emerge following changes in the external load or a shift in the central parameter, λ.

External perturbation can cause deflections of the system from the EP. If perturbations are transient, the reflection may be sufficient to restore the previous EP (i.e., equifinality). However, if the system cannot tolerate the transient perturbation, it can restore stability by switching to a new, stable EP (e.g., stepping forward in response to sudden tilting of the platform). Several researchers falsely rejected the EP hypothesis based on the perturbation-induced violation of the equifinality (Lackner & Dizio, 1994). However, the EP hypothesis does not predict that the equifinality should be observed in response to any transient perturbation (Feldman & Latash, 2005).

Muscles are usually controlled cooperatively as a group of agonists and antagonists, and it means that the controller changes in the spatial threshold of several muscles. Figure 2.4 is a simple example of an agonist and antagonist muscle spanning a single joint. In the case of the joint level involved agonist and antagonist muscles, there are two commands that effectively change each threshold of muscle length (λ), the reciprocal (R) command and co-activation (C) command (Feldman, 1980, 1986).

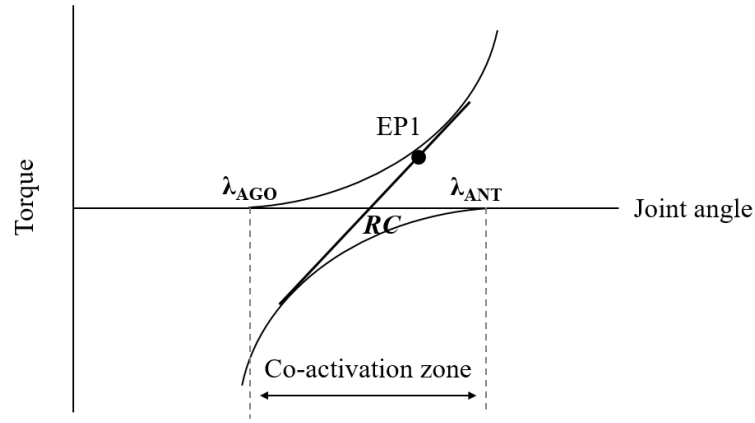


**Figure 2.4.** Torque-angle characteristics for single joint.

Control of a single joint can be explained with two parameters of the threshold of the tonic stretch reflex for the agonist ($\lambda_{AGO}$) and antagonist ($\lambda_{ANT}$). Each muscle's IC (thin solid curve) defines torque-angle characteristics (thick solid line) by the algebraic sum of the two IC. The mid-point between the two λs is called referent coordinate or referent configuration (*RC*), representing spatial referent angle involved joint (Feldman, 2015; Reschechtko & Latash, 2017). This location is defined by the R-command. The C-command defines the spatial range (co-activation zone between two λs) where both muscles are activated. Therefore, the slope of the torque-angle characteristics, which are stiffness-like properties of joint, is defined by C-command. Note that despite the linearizing action of the stretch reflex, the individual ICs (i.e., force-length curve) are generally non-linear. However, the overall torque-angle characteristics become closer to linear within the co-activation range when nonzero co-contraction of agonist and antagonist muscles—indeed, nonzero co-activation of antagonist muscle is commonly observed even during simple isometric steady-state force production (Corcos, Agarwal, Flaherty, &

Gottlieb, 1990; Ghez & Gordon, 1987). The EP is located along with the defined torque-angle characteristics at the point where external and internal torque is balanced (EP1), and the level of activation of each muscle is proportional to the differences between the joint angle and each λ.

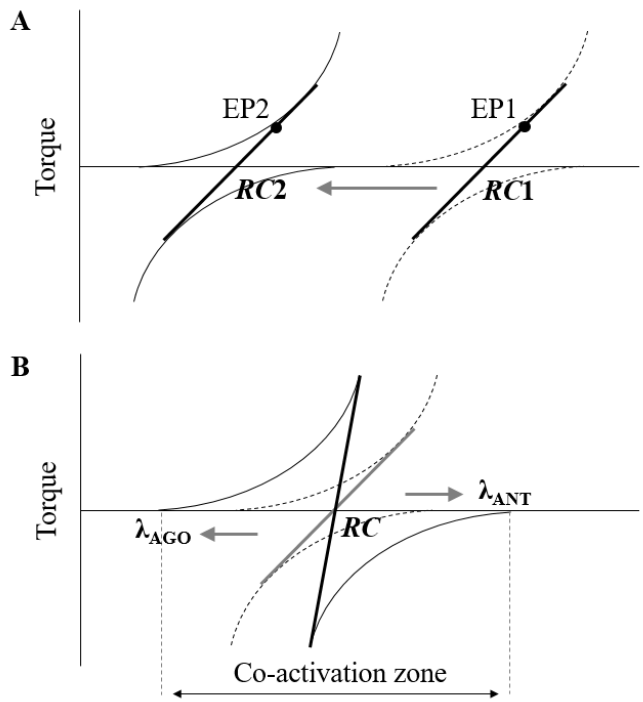


**Figure 2.5.** Role of (A) R- and (B) C-command for control the single joint.

According to the EP hypothesis, control of an effector can be described with the time profile of two basic commands. The joint movement occurs as *RC* is shifted by the R-command (Figure 2.5A). The R-command that adjusts the involved λs in the reciprocal direction can effectively change the position of the *RC*, and a new EP is formed at the new joint angle (EP2), as shown in Figure 2.5A. Physiologically, the

shift *RC* implies the reciprocal central influences—depolarization for agonist $\alpha$-motoneuron and hyperpolarization for antagonist one. The C-command defines the common spatial activation zones of muscles leading to change in the apparent stiffness ($k$) of the joint (Latash & Gottlieb, 1991). As shown in Figure 2.5B, when the two λs moves toward the shorter muscle length (i.e., co-facilitation of $\alpha$-motoneuron of agonist and antagonist), the co-activation zone can be increased regardless of the location of the *RC*. Then, the slope of the net torque-angle characteristics of the joint is enhanced. If the actual joint angle locates outside of the co-activation zone, only one muscle will be activated. In fact, the central effect on the threshold of agonist and antagonist can be achieved alone by affecting only the flexor or extensor muscles (Sangani, Raptis, & Feldman, 2011). The width of the co-activation zones can be controlled independently of the R-command (Figure 2.5B), while the location of co-activation zones depends on the R-command—when the *RC* is shifted, the co-activation zone is shifted with it. Therefore, the R-command is considered the primary central command responsible for the shift in the EP.

In the framework of the EP hypothesis, gradual shifts in λ are characteristics of the movement. The magnitudes of changes in the level of muscle activation and active joint torque depend on the distance between the actual joint angle and *RC* of the joint. Therefore, the controller can influence the movement speed and extent by adjusting the rate and duration of changes *RC* (Pilon & Feldman, 2006; StOnge, Adamovich, & Feldman, 1997). The rate of changes in *RC* is defined by the speed of propagation of excitation along a neuronal ensemble projecting to $\alpha$-motoneuron and spinal interneuron (Adamovich, Burlachkova, & Feldman, 1984). The nervous system cannot entirely predetermine the equilibrium position and its trajectory (Flash

& Hogan, 1985), rather it just changes the equilibrium state of the neuromuscular system in a feed-forward way, and the nervous system and environment (external forces) are equal contributors in designating the course and pattern of changes in the EP and motor actions. Threshold control is a means of shifting the EP, but it is inappropriate to say that the nervous system pre-programs or directly specifies the EP shifting or equilibrium trajectory (Latash, 2021).

## 2.3. Referent Control of Motor Action

EP hypothesis is based on the idea of parametric control (Latash, 2020a). According to the concept of parametric control, movement is created by changing physiological parameters, and as a result of changes in these parameters and the interaction of the effector with an external force field, measurable mechanical variables appear. Indeed, recent experiments which apply transcranial magnetic stimulation (TMS) to the primary motor cortex (Ilmane, Sangani, & Feldman, 2013; Raptis, Burtet, Forget, & Feldman, 2010) and vestibular (Zhang, Feldman, & Levin, 2018) have suggested that the descending signals from brain structures cannot encode muscle activation and movement mechanics but changes in parameter λ. Producing actions with time changes in parameters λ has been generalized to explain the control of multiple joints, limbs, and whole-body motion in the form of referent control hypothesis. The ‘Reference’ can be considered the origin of each spatial reference frame from which the movement is generated—in that case, the EP is an emergent property of referent control, but the EP characterizes important features of the organism-environment interaction and remains an integral part of the referent control hypothesis.

Already described referent variables of single joint (*RC*) and single muscle (λ) could be applied more global forms of referent variables, such as referent arm configuration for reaching tasks (Archambault et al., 2005; Pilon, De Serres, & Feldman, 2007), referent body orientation for postural stability (Mullick et al., 2018; Zhang et al., 2018), and referent aperture for producing grip force on holding an object (Ambike, Zhou, Zatsiorsky, & Latash, 2015; Frenkel-Toledo, Yamanaka, Friedman, Feldman, & Levin, 2019; Latash et al., 2010). These global factors are defined in the spatial frame of task level for desired motor action, and they can be used to guide multi-muscle and multi-joint action. Thus, it is assumed that the nervous system controls multiple muscles as coherent units (Feldman, 2015).

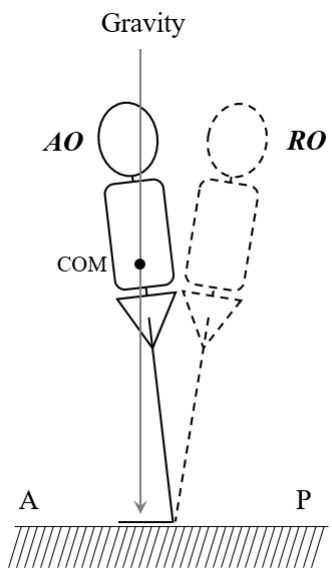


**Figure 2.6.** An illustration of postural control with the referent body orientation.

For a simple example, while leaning the body forward and quiet standing

on the ground, we can maintain this leaning posture without difficulty (actual body orientation: *AO* in Figure 2.6). The body tries to fall forward by gravity, but the counterbalanced torque generated by the plantar flexor allows us to maintain an equilibrium state. In the referent control scheme, there are neurons that receive afferent inputs depending on the body orientation. Independent central inputs to these neurons can predetermine the threshold value (referent body orientation: *RO*) at which they begin to be recruited. Proper projections of these neurons to $\alpha$-motoneuron of postural muscles, including plantar flexor, are organized to specify the threshold length of each muscle corresponding to defined referent orientation. In other words, the common threshold (referent orientation) can be transformed into a one-dimensional threshold length ($\lambda$s) of involved muscles at which muscles are silent but become activated depending on the deviation of the *AO* from the *RO*. The common threshold (*RO*) can be shifted by central influences so that the body can sway back and forth. A recent study has found that rhythmic oscillation of the referent orientation leads to body sway, and the activity of the postural muscles is minimized when the actual and referent orientation instantaneously overlap (Mullick et al., 2018). The stability of such a posture can be reinforced by C-command. It facilitates $\alpha$-motoneurons of paired muscles such that the co-activation occurs within a certain range of referent orientation. In principle, referent control does not accomplish with computations of joint torque, muscle force, and level of muscle activation, rather the stability requirement is met by defining the referent orientation and range of co-activation, which bring about the sense of balance based on somatosensory signals (Feldman, 2011). Thus, the referent control is accomplished during learning to perform desired motor tasks in new environments (i.e., new force fields). The following sections address the hierarchical features of referent control in

which global referent factors (e.g., referent body orientation) formed at the task level are mapped to the threshold length of individual muscles.

### 2.3.1. Hierarchical Organization of Control Variables

The concept of hierarchical organization of the control movements dates back more than a century with the classic work of Hughlings Jackson (1889). Control of redundant sets of lower-level elements such as multi-joint or multi-muscle systems has been recently considered built on a set of fewer variables manipulated at a hierarchically higher level. These variables have been addressed as modes (Danion et al., 2003) or synergies (Ivanenko, Cappellini, Dominici, Poppele, & Lacquaniti, 2005; Ivanenko, Poppele, & Lacquaniti, 2004). The referent control hypothesis has been naturally combined with the idea of a hierarchical control scheme and synergic organization of the abundant element. Every movement begins with defining the trajectories of low-dimensional global referent variables for task-specific variables. High-dimensional referent variables at hierarchically lower levels emerge down to threshold length for involved muscles (Figure 2.7). At each level of the hierarchy, the input is lower dimension compared to the output (e.g., the λs of the individual muscle need to be specified have a greater number than the *RC*s of the involved joints). Hence, each hierarchical level deals with an apparent problem of redundancy (see section 2.1 for more details). After specifying the central referent variable and mechanical constraints, the neuromuscular system tries to achieve a state of minimal muscle activation, called the principle of minimal final action (Latash, 2010). It is derived from the famous principle of minimal interaction (Gelfand & Tsetlin, 1971), which suggested that The interaction between the

elements of a multi-element system is structured to minimize external input to each individual element while maintaining the overall output of the system, which is compatible with the command signal from the hierarchically higher controller.

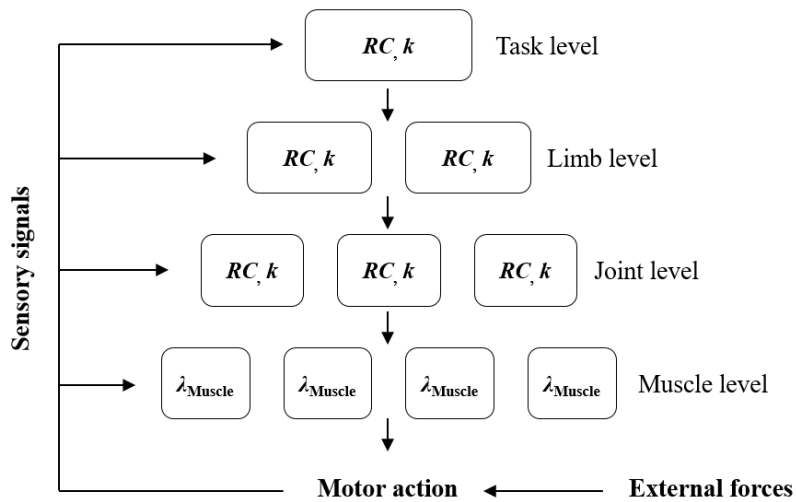


**Figure 2.7.** Hierarchical scheme for specifying control variables.

Imagine that a person tries to perform arm-reaching motion into a target. Figure 2.7 is a hypothetical scheme for mapping control variables at each level. The top-level corresponds to the task, and the lowest level involves setting stretch reflex thresholds (λ) for the participating muscles (e.g., flexor and extensor muscles of elbow and wrist). The task-level control variables may be associated with the end-point position, and the two-dimensional variables, a referent configuration (*RC*) and level of co-activation (*k*) (apparent stiffness) are defined. The *RC* is specified where the end-point can remain in the equilibrium state, and the *k* specifies the resistance to perturbation. Note that the EP of the actual end-point reached by specified

reference is determined by the interaction with the external forces. Specifying higher-level control variables then generates the pairs control variable at hierarchically lower levels such as those of limbs, individual joints, and muscles (λ) via a sequence of few-to-many mappings. This sequence of few-to-many mappings produces problems of motor redundancy. Regarding this issue, Latash (2010) suggested that control using referent variables may be viewed as based on a hierarchy of synergistic control—synergies of neural organization ensure the stabilization of higher-level control variable by covaried adjustment within a redundant set of lower-level variables (Latash et al., 2007). Note that the scheme of hierarchical organization of control variables in Figure 2.7 does not involve any computational processes. The synergistic organization has been assumed to involve the physiological tunable back-coupling loops within the CNS and peripheral receptors (Latash, Shim, Smilga, & Zatsiorsky, 2005; Martin, Scholz, & Schoner, 2009), such as the recurrent inhibition, which has been considered as a mechanism stabilizing the output of $\alpha$-motoneuronal pool, and the stretch reflex loop, which functions to stabilize the equilibrium state of the system.

### 2.3.2. Control of Finger Force Production in Isometric Condition

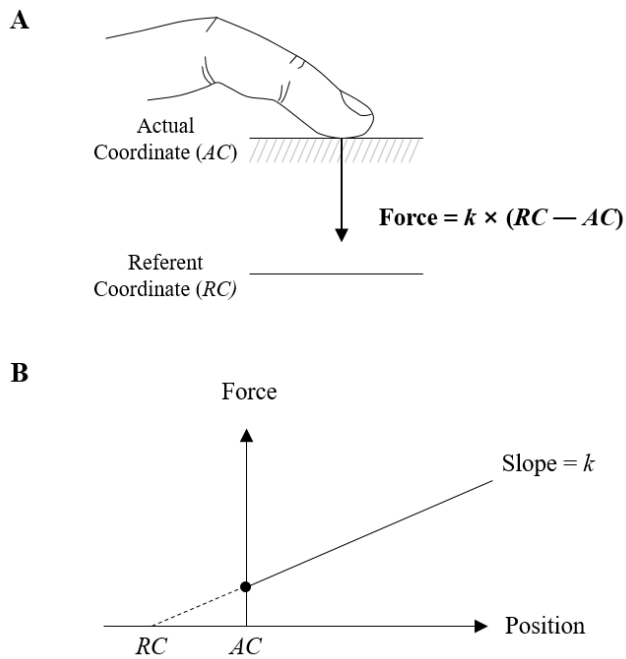


**Figure 2.8.** Schematic for isometric finger forces production in framework of referent control hypothesis.

According to the referent control hypothesis, movement initiates by setting the referent position of the effector, and the activation level of the muscle is determined in proportion to the difference between the referent position and the actual position of the effector. In the isometric condition, the production of finger force can be done by specifying the referent position of the fingertip in the direction in which the force is to be generated. Previous studies denominated this control variable as a "referent coordinate" to describe the control of finger force production (Ambike et al., 2016; Cuadra, Gilmore, & Latash, 2020; Cuadra, Wojnicz, Kozinc, & Latash, 2020; de Freitas, Freitas, Lewis, Huang, & Latash, 2018; Martin, Budgeon, Zatsiorsky, & Latash, 2011; Mattos, Schoner, Zatsiorsky, & Latash, 2015; Reschechtko & Latash, 2017, 2018). The normal forces generated by fingertip is

proportional to the difference between referent coordinate (*RC* in Figure 2.8A) defined by R-command and actual fingertip coordinate (*AC* in Figure 2.8A), while the C-command determines the extent to which the finger flexor and extensor co-activate. In other words, the changes in the R-command lead to a shift in the intercept point of the spring-like properties (*RC* in Figure 2.8B), and changes in C-command lead to changes in the slope (apparent stiffness, *k*, in Figure 2.8B). In linear approximation, the produced finger normal forces in the isometric condition can be represented by the function: $Force = k \times (RC - AC)$ (Ambike et al., 2016). Therefore, the magnitude of the normal finger force depends on the position of the referent coordinate (i.e., the relative difference between *RC* and *AC*) and the apparent stiffness, and the control of finger force is associated with setting neural parameters that translate into *RC* and *k*.

The presence of two control variables, *RC* and *k* defining by R- and C-command, make redundancy in the level of control even at the single effector that mechanically non-redundant. It means that one can use an infinite number of {*RC*, *k*} combinations to produce a certain force magnitude. For across trials, typical data points of {*RC*, *k*} during prescribed finger force production are organized in the form of a hyperbola (Ambike et al., 2016). This hyperbolic line represents UCM space in which a certain magnitude of finger force is ensured even when the two control variables vary. Earlier studies have reported that the two control variables covaried to stabilize outcome forces—intertrial variability of {*RC*, *k*} was much larger along the hyperbolic UCM line compare to the direction orthogonal to the UCM (Ambike et al., 2016; Latash, 2020a). These results provide evidence that control variables can be organized synergistic way to stabilize salient performance variables, which may

be an inherent characteristic of the nervous system to control movement (Latash, 2017).

Further, the stability properties of the *RC* and *k* can be different. In a pressing task that used four fingers to produce prescribed total forces, Reschechtko and Latash (2018) showed that the synergistic behavior was only present in the *RC*, not the *k*. This result was interpreted as supporting the hypothesis that the R-command is primarily responsible for the control of action, whereas the C-command is subordinate to the R-command—there may be a hierarchical relationship between control variables, *RC* and *k*. A well-known typical muscle response is an increase in the level of activation of the agonist and antagonist muscles (i.e., co-activation) after rapid movement; then it slowly subsides without a change in the effector position (Gottlieb, Corcos, & Agarwal, 1991; Yamazaki, Ohkuwa, Itoh, & Suzuki, 1994). These findings have been interpreted that the R- and C-commands have a hierarchical relationship. The R-command has been assumed to be hierarchically higher so that the C-command was obligated to change following the change of the R-command, whereas the change of the C-command was not expected to lead to a mandatory adjustment of the R-command (Feldman, 2015). In other words, the changes in *k* being subordinate to the changes in *RC*. This idea was supported by previous findings that the *RC* had higher intra-class correlation values than the *k* during accurate finger force production tasks (de Freitas et al., 2018), and the changes in the *k* not automatically accompanied by adjustments in the hierarchically higher *RC* (Cuadra, Wojnicz, et al., 2020).

## 2.4. Prehension Mechanics

Precision grip is to hold an object using five tips of the digits with the thumb and other fingers facing each other. When holding a prismatic object with a precision grip, all grasping surfaces are parallel to each other, and the normal digit forces are in the grip plane (Zatsiorsky & Latash, 2008). The effects of the fingers can be reduced to a single united effector as a virtual finger (VF) that produces an equivalent mechanical effect (Arbib, Iberall, & Lyons, 1985; Iberall, 1997). In other words, the VF produces the same mechanical effect as a set of actual fingers. For the control aspects, there are two levels of the hierarchy—the upper-level is coordinated by thumb and VF, while four fingers are organized in the lower-level to generate a desired outcome of the VF.

### 2.4.1. Forces and Moments for Prehensile Action

To keep the holding object steady or to move it, the forces and moments of force applied by individual digits should be coordinated. Two types of forces, *manipulation force* and *internal force*, describe the prehension mechanics. The digit forces exerted on an object are expressed to three components of resultant force and moment along the three orthogonal axes corresponding task space. These six components of the vector of the force and moment influence the object's position and orientation and are called the manipulation force. The internal force is a set of forces without disturbing the equilibrium state of objects (Mason, Salisbury, & Parker, 1989; Murray, Li, & Sastry, 2017). Since the internal force vector act in the opposite direction, there are canceled each other so that they cannot contribute to the

manipulation force. This force component is not a single force but a set of forces and moments, creating a zero resultant force and moment. The manipulation forces are prescribed by the task mechanics. For example, to statically hold an object in the air, the vertical forces must have the same magnitude as the weight of the object. On the other hand, the internal forces are the choice of the controller allowing for much freedom and can be of different magnitude (Gao, Latash, & Zatsiorsky, 2005a). Each digit also can produce a three-dimensional force and moment. Therefore, there is an infinite number of ways to adjust thirty forces and moments of digits to satisfy the set of six constraints during a five-digit prehensile action—this obviously makes the multi-digit system redundant (see chapter 2.1 *problem of motor redundancy*).

Mechanically, the interaction of individual digit and object is described as *soft contacts*. This term means that the digit does not stick to the surface of the object and can only be pressed without pulling it. This component of pressed forces perpendicular to the contract surface is the normal force and the force acting in the direction parallel to the contacted surface is the tangential force. Since the application point of the normal force of the four fingers is different, an auxiliary moment is created, which is called a *secondary moment* (Li, Latash, & Zatsiorsky, 1998; Z. N. Li, Latash, Newell, & Zatsiorsky, 1998). When performing a pressing task using four fingers, the secondary moment generated by the normal finger force is generally known to be balanced in the ulnar side of the middle finger (neutral line), and this phenomenon is considered as an additional constraint of the controller—*the principle of minimization of the secondary moment* (Li et al., 1998). This principle ensures that the sharing pattern of the normal forces between the four fingers in the pressing or prehensile task is constant and independent of the magnitude of the total

force.

The tangential force exerted on objects has been considered functional forces that contribute to the manipulation force. This force plays a primary role, especially when manipulating circular objects such as turning a doorknob (Shim & Park, 2007). When grasping a prismatic object, the total tangential force, commonly referred to as the load force, is shared between the thumb and VF, and the VF tangential force is further shared among the four fingers. The load sharing pattern between fingers is independent of the magnitude of the load. Rather, it depends on the direction of the load (Pataky, Latash, & Zatsiorsky, 2004b). Since the robotic gripper does not produce tangential force, the load sharing among the redundant effector is determined by the mechanical structure. However, the anatomical features of the human hand—finger abduction and adduction at the metacarpophalangeal (MCP) joints— enable the production of the active tangential force in the radial and ulnar directions (Pataky, Latash, & Zatsiorsky, 2008). Indeed, there are several studies related to the tangential digit forces that the CNS actively controls (Shim & Park, 2007; Song, Kim, et al., 2021).

Both the normal and tangential digit forces can contribute to the moment production on the object. Unlike the tangential force, the normal forces have a different moment arm (lever arm) about the thumb being the axis of rotation. Thus the same magnitude of normal finger forces exerted by different fingers creates different moments of force. On the other hand, the tangential finger forces have the same moment arm, producing similar moments in prismatic grasp. One of the features about moment production by normal and tangential digit forces is that the contribution of the moments of the two force component does not depend on the load

or magnitude and direction of the moment, and the percentage contribution of the total moment between its two force component is invariant—their contributions are approximately equal (Zatsiorsky, Gregory, & Latash, 2002a). The small moments about under 0.75Nm are controlled mainly by changes of the relative position of the force application points (i.e., moment arms), and large moments are primarily generated by changes in the magnitude of normal forces (Zatsiorsky et al., 2002a). This implies that the change of the digit contact point to change the moment arm of the normal force can also be regarded as an additional component for moment control.

### 2.4.2. Static Constraints for Grip Stability and Rotational Equilibrium

Consider a grip plane with a person trying to hold a prismatic object to keep it vertical and motionless. Three external constraints that ensure the horizontal, vertical, and rotational equilibrium should be satisfied.

1) *Horizontal translation constraint*: the sum of the individual normal finger forces should be equal and opposite to the thumb force.

$$0 = F_I^N + F_M^N + F_R^N + F_L^N - F_{TH}^N \qquad (2.3)$$

2) *Vertical translation constraint*: the sum of the tangential digit forces should be equal and opposite to the load of the grasping object.

$$L = F_{TH}^T + F_I^T + F_M^T + F_R^T + F_L^T \qquad (2.4)$$

3) *Rotational equilibrium constraint*: the total moment produced by digit forces about axis of rotation should be equal and opposite to the external torque ($T$) exerted on the objects.

$$-T = \sum_i F_i^N \cdot d_i + \sum_i F_i^T \cdot r_i, \quad i = \{I, M, R, L\} \tag{2.5}$$

, where the subscripts *TH*, *I*, *M*, *R*, and *L* stand for the thumb, index, middle, ring, and little finger, respectively; the superscripts *N* and *T* refer to the normal and tangential force, respectively; the *L* is the weight of the object (load); the *T* stands for the external torque; the coefficients *d* and *r* refer to the moment arms of the normal and tangential force, respectively.

When holding a free object (i.e., mechanically unconstrained object), there are two internal forces, *grip force* and the *internal moment* (Gao, Latash, & Zatsiorsky, 2005b). The grip force is a force that is canceled by the normal forces of thumb and VF, ensuring grip stability. Regardless of the task, the grasping must be stable, and grip stability refers to *slip prevention* (i.e., the object should not be dropped). In other words, performers are free to select the magnitudes of normal thumb and VF forces, but the produced forces must be large enough to prevent slippage. The difference of percentage between the actual grip force and the minimal required normal force to prevent slipping is called the *safety margin* (Westling & Johansson, 1984). Slip prevention is mainly achieved by adjusting the grip force. Therefore, slip prevention can be an additional constraint on relations between normal and tangential forces produced by each digit that is defined by the friction coefficients.

The internal moment is that the moment of normal and tangential forces are canceled each other to satisfy the rotational equilibrium when the external torque is not present (Shim et al., 2003). In a non-zero torque task, however, the moment of normal and tangential forces acts in the same direction, assisting each other

(Zatsiorsky, 2002). Further, the notion of *torque agonists* and *torque antagonists* has been introduced (Gao, Latash, & Zatsiorsky, 2006). The fingers that resist external torque and help maintain rotational equilibrium are called torque agonists, and fingers that support external torque are called torque antagonists.

## 2.5. Prehension Control

When a person applies forces to the environment, the magnitude and direction of the force vectors should be controlled. If multi-digits exert force during prehension, the directions and magnitudes of the individual digit forces vary from those of resultant force. The finger force vectors are in different directions and magnitudes but compensate for each other (Gao et al., 2005a). Therefore, the desired direction and magnitude of the resultant force is achieved by a synergic way of the digit forces.

### 2.5.1. Prehension Synergies

The synergy assumes that the neural controller organizes the redundant element system in a task-specific way that reduces the variability of potentially important variables. This neural organization can be assessed quantitatively using indices of co-variation among the redundant elements (Gelfand & Tsetlin, 1966). In this framework, the controller does not remove redundant DOFs, but uses them to ensure stability in performance to solve the redundancy problem. Multi-digit prehension has advantageous for studying the problem of motor redundancy because the experimenters are able to measure all the involved digit forces and displacements

directly. Prehension synergies can be divided into two groups—kinematic and kinetic synergies. An example of kinematic synergy is that the stabilization of the grip aperture. When trying to grasp an object using thumb and index, even if the mechanical perturbation is applied to one of the fingers, the two fingers are quickly adjusted so that the temporal profile of the grip aperture remains relatively unchanged (Cole & Abbs, 1987). It can be seen before the digits make contact with the object. The kinetic synergy is the stabilization of the mechanical action of the hand on the holding object. When a person holds an object statistically, the thumb and VF normal forces fluctuate as a way of in-phase (i.e., positive covariation). On the other hand, fluctuations of four finger forces acting in parallel are more likely to be out-of-phase (i.e., negative covariation) (Park et al., 2015; Santello & Soechting, 2000; Shim et al., 2005b). Many experimental approaches have been used to explore the synergies of prehension, including employing external perturbations (Shim, Huang, Hooke, latash, & Zatsiorsky, 2007; Zatsiorsky, Gao, & Latash, 2006), varying the object geometry and resisted torque or load (Zatsiorsky et al., 2002a, 2002b), studying trial-to-trial variability (Shim et al., 2003, 2005a), and the training effect (Park et al., 2015).

#### *2.5.1.1. Synergies at the Upper Hierarchy (thumb-VF level)*

External constraints for static equilibrium suggest that the correlation between thumb and VF in static prehension may be a strong positive on their normal forces and a strong negative between their tangential force (Shim et al., 2003). These relations are not directly reflective of a neural strategy but are necessitated by mechanical constraints of the task. However, the magnitude of thumb and VF normal

force is chosen by the controller so that their absolute grip force can vary. Likewise, the tangential force of the thumb and VF must be summed to match the weight of the object, but the share of the tangential forces between digits can be chosen by the controller. It is known that the grip force increases when the given external torque is greater for a fixed weight of the handle (Zatsiorsky et al., 2002a), and the sharing pattern of the tangential force shows regular changes with the external torque (Zatsiorsky, Gao, & Latash, 2003a).

The rotational equilibrium equation includes the thumb and VF normal forces that are also involved in the horizontal translation constraint. If these forces are adjusted to meet the rotational equilibrium requirements, the gripping force must also be adjusted. Shim and colleagues (2003) showed that in an experiment using an instrumental handle, the total moment applied by the thumb and VF is actually stabilized, but this is achieved in a way that does not directly affect the grip force. This is consistent with the *principle of superposition* and is covered in the next section.

A study that the two groups of healthy young and elderly performed increase the grip force with maintaining the vertical orientation of the handle confirmed that the elemental variables at the level of thumb-VF are co-vary to stabilize both the grip force and the moment of force applied to the handle (Shim, Latash, & Zatsiorsky, 2004). In that study, the young population had higher indices of force and moment stabilization base on UCM analysis as compared to the elderly population implying that the quantification of the synergy is useful in clinical practice and motor rehabilitation. The elemental variables at the thumb-VF level co-vary each other over across trials to stabilize performance variables as the grip force

and the total moment of force. This means that the data points of repeated attempts in the space of the elemental variables are limited to two null spaces corresponding to the required grip force and the required moment of force.

#### *2.5.1.2. Synergies at the Lower Hierarchy (individual finger level)*

The effect of four fingers have the interdependence, and it is one of the problems in assessing synergistic adjustment in the space of finger forces. When a finger tries to produce force, other fingers also produce unintended force (Kilbreath & Gandevia, 1994; Li et al., 1998; Z. N. Li et al., 1998). The term enslaving has been used to address this problem, and it was discussed as a result of peripheral properties (Leijnse et al., 1993) and neural factors (Schieber & Santello, 2004). Quantification of effects of enslaving during multi-digit prehension was elusive due to a factor—changing the force of just one finger can violate equilibrium constraints and lead to translation or rotation of the holding object. Due to the limitation, quantification of synergies at the individual finger level had been confined to mechanical variables such as forces and moments without consideration possible effect of enslaving.

An important feature of the lower level synergy in multi-digit static prehension is that the stabilization of the grasping performance (i.e., grip stability and rotational equilibrium) is not directly affected by the stabilization or destabilization of the variables in the lower level individual finger. Previous study proposed a synergic chain effect to discuss logical relations of synergies at the two levels of hierarchies (Gorniak, Zatsiorsky, & Latash, 2009). The forces of individual fingers in the lower level are co-vary to satisfy the required mechanical effect of the higher level VF. In other words, VF grip forces are the performance variables of four

fingers grasping action. If the VF normal forces are positively co-vary with the thumb normal forces for ensuring the grip stability, the UCM space (i.e., space of good variance does not affect performance variable) at the upper-level increases. It leads to a decrease in the synergy index at the lower level because the variance of ORT space (i.e., a bad variance that changes the performance variable) in this level increases. This means that the upper-level UCM space and the lower-level ORT space have a conflicting relationship. Indeed, Park et al. (2015) showed the results that the grip force stabilizing synergy only observed in the upper level, while the moment stabilizing synergies are present at both levels of the hierarchy during static prehension.

When generating the moment of force to satisfy rotational equilibrium, effectors (i.e., fingers) located farther away from the axis of rotation (i.e., thumb) generate larger force—*the mechanical advantage hypothesis* (Devlin & Wastell, 1986; Frey & Carlson, 1994; Gielen, van Zuylen, & Denier van der Gon, 1988; Park, Baum, Kim, Kim, & Shim, 2012; Shim et al., 2004; Song, Kim, et al., 2021). It has been known that when the external torque and load change systematically, the effects of lateral fingers (index and little) that have larger moment arm depend mainly on the torque magnitude, whereas the effect of the central fingers (middle and ring) depends on both external load and torque (Zatsiorsky & Latash, 2008). It is also known that this mechanical advantage hypothesis, which affects the force sharing pattern among fingers for net moment production, is effective in fixed-object prehension (Park, Baum, et al., 2012).

### 2.5.2. Principle of Superposition

Through a series of studies, Arimoto and Nguyen (2001) proposed a principle of superposition for controlling robotic hand motion. The main idea of this principle is to separate complex motor tasks into two subtasks controlled by independent controllers. The output signals from the controllers are converged to the same set of actuators that are summed. This control scheme has been considered to reduce the computation time compared to whole action control.

Several studies have generated evidence to support the principle of superposition in human prehensile action (Shim et al., 2005b; Shim & Park, 2007; Zatsiorsky et al., 2004). In the previous study, the subjects were asked to hold an instrumental handle that enables them to change the total load and total external torque (Zatsiorsky, Gao, & Latash, 2003b). Analysis at the thumb-VF level showed that all forces and moments generated by individual digits were dependent on external loads and torque, but analysis of variance showed only the main effects of these two factors without interaction. These results imply that adjustments of digit force and torque to different loads and torque are generated independently of each other. Another study conducted by Shim et al. (2003) demonstrated that the changes in the VF normal force were not correlated with the changes at the moment produced by this force. Because the moment is a product of force and its moment arm, this result can be interpreted that purposeful adjustments of the moment arm eliminate the natural correlation between moment and normal force. In addition, principal component (PC) analysis showed that all elemental variables are formed two PC—the first PC involved the thumb and VF normal forces, and the second PC involved the thumb and VF tangential forces, the moment of normal and tangential forces, and the moment arm of the VF normal force. In follow-up studies, the validity of the

principle of superposition on human prehension is generalized for three-dimensional prehensile action (Shim et al., 2005a) and with circular objects (Shim & Park, 2007). Taken together, these results provide a piece of evidence that the forces and moments during static prehensile action are determined by independent two commands—grip stability and maintain the rotational equilibrium.

### 2.5.3. Referent Variables for Describing Prehensile Action

According to referent control hypothesis, the *RC* (referent configuration or referent coordinate) is a position at which all the involved muscles will be achieved relaxation. Any deviations from this reference lead to muscle activation, so the *RC* can also be addressed as a threshold of body configuration. In general, the actual equilibrium state of body configurations deviates from the defined *RC* due to external forces including the gravity and/or restrictions that may be imposed by external objects (e.g., isometric condition preventing motion of the body segments) and anatomical features of the body (Feldman, 2015).

Pilon et al. (2007) showed that the movement of an object held in hand could result from changes in referent arm-hand configuration with associated anticipatory grip force adjustment. In that study, they suggested the mechanisms of grip force adjustment based on control with referent variable the nervous system changes the threshold position of the hand to produce a grip force. This process begins by defining a referent (threshold) aperture of involved digits. The actual aperture constrained by the shape of the object is wide than the referent aperture that fingers virtually penetrate to the center of the object. The deviation by the object from the threshold position leads to muscle activity (i.e., grip force) that is

proportional to the distance between the actual aperture and referent aperture. Therefore, the grip force toward the center of the object emerges because the object prevents the finger from approaching the referent position. Note that both central modulations in the width of referent aperture and changes in the size of the object (i.e., actual aperture) influence the magnitudes of the grip force (Ambike et al., 2014; Zatsiorsky et al., 2006).

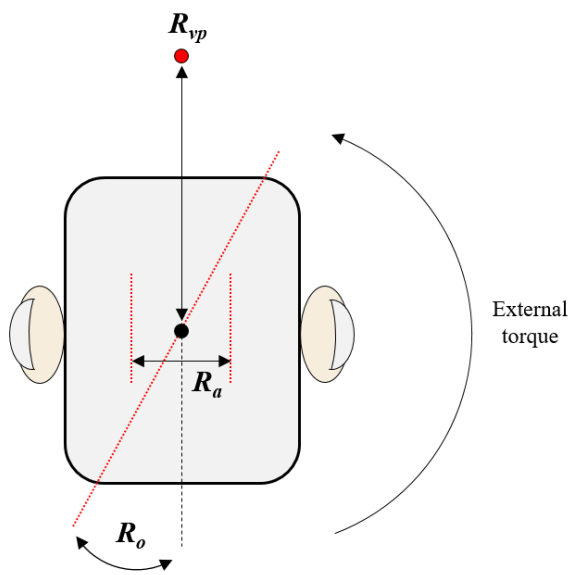


**Figure 2.9.** Three referent variables for describing static free-object prehension by two digits. $R_a$: referent aperture; $R_o$: referent orientation; $R_{vp}$: referent vertical position.

Latash et al. (2010) demonstrated the synergic action of the effectors (fingers) that are directed to a reference position to create a grip force through a novel experimental setup. In addition, in the later study of Ambike et al. (2014), they quantified the apparent stiffness ($k$) of the hand related to the generation of grip force

by using a motorized handle that can adjust the grip width while holding, and this result was interpreted based on the referent control hypothesis. In these studies, they proposed a set of hypothetical referent variables to describe the static prehensile action in the presence of gravity and external torque (Figure 2.9). Such a set includes referent aperture ($R_a$), referent orientation (angle) of the object with respect to the vertical ($R_o$), and referent position in the vertical direction ($R_{vp}$). They further referred midpoint of the referent aperture, assuming that the midpoint of the referent aperture may be located in the center of the object because the two normal forces must be equal and opposite to maintain static equilibrium. They suggested that setting the referent orientation (angle) can lead generation of a resultant moment on the object to compensate for the given external torque, while setting a referent vertical position can balance with the external load by producing the appropriate vertical (tangential) force of involved digits. Given certain external conditions and using these referent variables, the characteristics of the overall behaviors of the hand such as normal forces (i.e., grip forces), tangential forces (i.e., load forces), and resultant moment of forces can be defined.

# Chapter 3. Translational Equilibrium Control:
*Hierarchical and Synergistic Organization of Control Variables During the Multi-digit Grasp of a Free and an Externally Fixed Object*

## 3.1. Introduction

Grasping is a basic human behavior. Humans actively adjust mechanical and physiological variables to satisfy the constraints related to the movement of the object imposed by specific prehensile tasks. This process is governed in part by the central nervous system (CNS) that generates the neuronal command for the proper organization of the mechanical variables involved in the action. In the present work, we use the framework of the referent configurations, based on the equilibrium point hypothesis (Feldman, 2015), to study the control of prehension.

According to the referent control hypothesis, prehension via the opposition of the thumb and fingers is achieved by the specification of the referent aperture ($R_a$) (Ambike et al., 2014; Feldman, 2015; Frenkel-Toledo et al., 2019; Latash, 2010; Latash et al., 2010; Pilon et al., 2007). $R_a$ is located inside the grasped object, and it is related to the referent positions of the digit tips – i.e., the position in space to which the current muscle activation attempts to drive the digit (Figure 3.1A). Grip force at the digit-object interface arises because the object prevents the digits from approaching their corresponding referent positions (Pilon et al., 2007). In previous work, the midpoint of $R_a$ was assumed to be located at the mid-point of the actual grip aperture during static prehension (Ambike et al., 2014; Latash et al., 2010), generating the equal and opposite digit forces necessary for a static grasp. However,

the digit force is determined by the difference in the digit's actual and referent coordinates ($RC$) and the digit apparent stiffness ($k$) (Ambike et al., 2016; Cuadra, Gilmore, et al., 2020; Cuadra, Wojnicz, et al., 2020; Latash, 2020a, 2020b). Therefore, the assumption of the coincidence of the midpoints of $R_a$ and the actual aperture for static grasping implicitly assumed equal apparent stiffnesses of the thumb and the opposing digits. There is some evidence supporting equal $k$ for opposing digits during static prehension (Zatsiorsky et al., 2006), however, this assumption has not been sufficiently tested. In particular, the apparent stiffness can be modulated by adjusting muscle co-contraction, and $k$ is likely a control variable that could influence the stability of the grasp (Latash, 2018).

Therefore, the first goal of this study was to establish that the control of grasp involves modulation of the referent aperture as well as the apparent stiffness. We address this goal by comparing the grasp of a free object, where grasp stability is ensured by the digits, with the grasp of an externally constrained object. Since the digit forces during prehension depend on external mechanical constraints (Park, Baum, et al., 2012; Park, Kim, et al., 2010), it is plausible that the control variables $\{RC, k\}$, are affected by the presence/absence of the external constraints as well. For example, compared to the grip force on an object whose orientation is externally constrained, the grip force for the static prehension of a free object is higher. This increase is due to the higher forces of the lateral (index and little) fingers that assist in maintaining rotational stability of the free object (Park, Baum, et al., 2012). Since the higher grip force was aimed at improving stability, it is probable that the force changes were driven by a higher apparent stiffness. Therefore, we computed the $R_a$ and $\{RC, k\}$ of the digits during static prehension of a free and a constrained object,

while ensuring that the magnitude of the grip force was same in both conditions. Our first hypothesis (H1) was that the apparent stiffness *k* for the digits will be higher when the digit forces are constrained and responsible for grasp stability, i.e., while grasping a free compared to an externally fixed object. Higher *k* will be accompanied by smaller *RC* for the digits so that the grip force is constant. The referent aperture arises from the digit *RC*s (cf. Figure 3.1A), and this would lead to a larger referent aperture while grasping the free object. In addition, our second hypothesis (H2) was that the midpoint of $R_a$ would not be located at the center of the actual aperture, reflecting that *k* for the thumb and the four fingers (combined) are different.

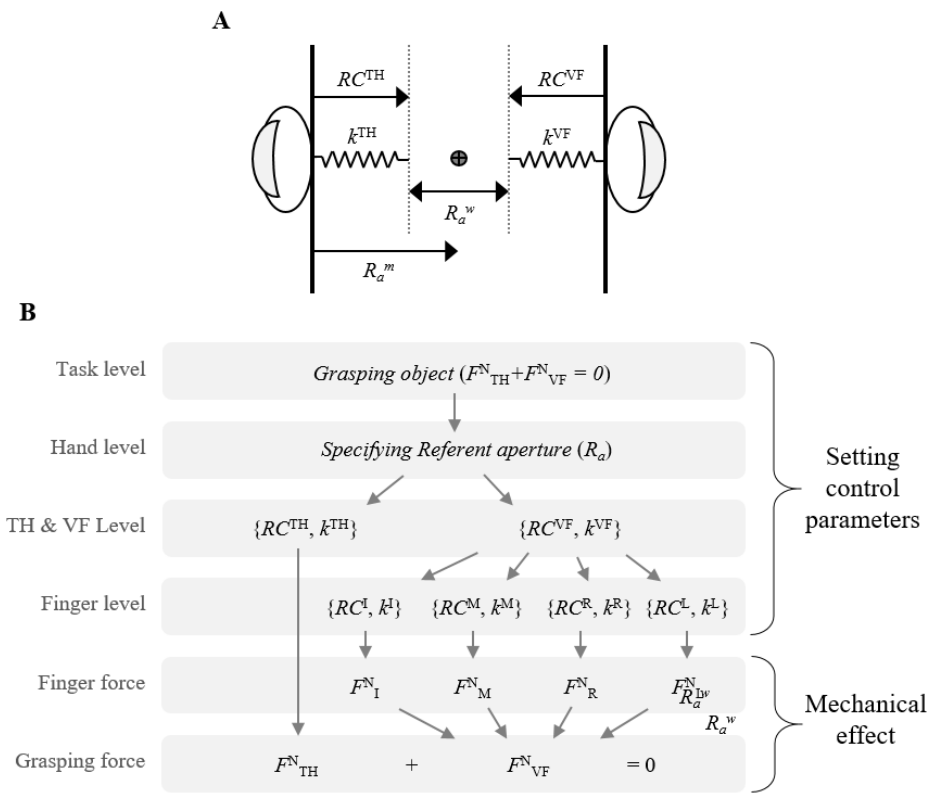

**Figure 3.1.** (A) An illustration of the referent aperture ($R_a$) inside the grasped objects. The $R_a$ is defined by referent coordinate ($RC$) of thumb (TH) and virtual finger (VF). Object prevents the digits from reaching the threshold position $RC$, and a normal force is generated depending upon the digit's apparent stiffness ($k$). $R_a^{w}$: width of referent aperture; $R_a^{m}$: midpoint of referent aperture. (B) A hypothetical scheme of neural control for grasping objects using five digits. $R_a$ as a single control variable for producing grip force is specified at the hand level. At the TH and VF level, the $R_a$ results in the $RC$ and $k$ of both digits. Specified $\{RC, k\}$ in the VF results in the pairs of $\{RC_i, k_i\}$ for the individual fingers ($i$ = I, M, R, and L) at the finger level. Individual normal finger forces ($F^{N}_{i}$) are generated by the corresponding pairs of the $\{RC, k\}$, and the grip force that satisfied the horizontal translation constraint ($F^{N}_{TH}$—$F^{N}_{VF}$ = 0) is produced by the normal forces of the TH and VF.

The second goal of this study was to quantify the synergistic covariation between these control variables during the two types of static prehension. Various mechanical, physiological and control variables involved in motor control are organized in a hierarchy with redundancy at all levels. This hierarchical organization for multi-digit prehension within the referent control hypothesis is presented in Figure 3.1B. The controller designates $R_a$ at the task level, and this leads to defining $\{RC, k\}$ for the higher-level effectors (i.e., the thumb and the virtual finger (Arbib et al., 1985; MacKenzie & Iberall, 1994) — a virtual digit that has the same mechanical effect on the object as the four fingers combined). Since the virtual finger is composed from four fingers, the specified $RC$ and $k$ of the virtual finger arises from $\{RC, k\}$ variables for the individual fingers. Since the number of input variables (at a given level of the hierarchy, called the upper level) is smaller than the number of the output variables (at the adjacent lower level in the hierarchy), there are few-to-many maps linking each pair of consecutive levels of the hierarchy, reflecting the redundancy in the system. This redundancy is exploited by the central controller: the

upper-level variables are stabilized by covaried adjustment within the redundant set of lower-level variables. Such task-specific covariation is quantified using synergy analysis (Ambike et al., 2016). This scheme was verified for manual behaviors when covariation among the control variables of each finger stabilized upper-level variables in a four-finger pressing task (Reschechtko & Latash, 2018). For grasping, however, only stabilization of *mechanical variables* (digit forces and moments) at different levels in the control hierarchy has been reported (Gorniak et al., 2009; Park et al., 2015; Shim et al., 2003, 2005a; Zatsiorsky et al., 2002b; Zatsiorsky & Latash, 2008); no attempt has been made to examine the stabilization of *control variables* in the hierarchy. Therefore, our third hypothesis (H3) was that the control variables in the few-to-many maps presented in Figure 3.1B, including $\{RC, k\}$ and the digit forces, would display synergistic organization. Furthermore, we expected that the synergies in the $\{RC, k\}$ variables and in the digit forces, quantified at the same level, would be correlated since both synergies quantify the same behavior. Finally, our fourth hypothesis (H4) was that the strength of covariation between the variables would be larger during free object prehension compared to fixed object prehension, especially at the higher level of the hierarchy due to the aforementioned external factors. To test these hypotheses, we constructed a motorized handle that changed the grip width and allowed us to estimate $RC$ and $k$ during static prehension.

## 3.2. Methods

### 3.2.1. Subjects

Ten healthy young subjects (8 males and 2 females), age 29.9 ± 3.87 (mean

± SD) years, mass 71.9 ± 6.06 kg, and height 1.72 ± 3.33 m, voluntarily participated in the current experiment. The hand dominance of the subjects was determined using the Edinburgh handedness inventory (Oldfield, 1971), and all subjects were right-handed. They had no history of neurological or musculoskeletal disorder that could affect the completion of the experimental tasks (by self-report). All participants gave informed consent in accordance with the recommendations of the Seoul National University Institutional Review Board (IRB No. 2007/0 02-023).

### 3.2.2. Apparatus

We constructed a motorized handle (Figure 3.2B) that was capable of adjusting the grip width at constant speed. Individual digit forces were measured using five six-component force/torque transducers (Nano-17, ATI Industrial Automation, Garner, NC, USA), which were attached to the motorized-handle (Figure 3.2B). The transducers were aligned in the *x*-*z* plane of the local coordinate system of the handle. 100-grit sandpapers were attached on the contact surfaces of the transducers to provide sufficient friction (Savescu, Latash, & Zatsiorsky, 2008). Also, we confirmed that the position of center of gravity (CoG) of the handle-sensor assembly was along the *z*-axis close to the middle of the grip width (Figure 3.2B). The mass of the handle with transducers was 0.57 kg. All force signals were set to zero before each trial began and sampled at 200 Hz and digitized with an analog-to-digital converter (Gen5, AMTI, Watertown, MA, USA).

Three light-weight spherical reflective markers (4 mm in diameter) were secured to the handle for the measurement of the handle orientation and the horizontal displacement caused by the embedded motor (Figure 3.2B). The marker

positions were recorded at 200 Hz using a motion capture system (OptiTrack, Natural Point Inc., Corvallis, OR, USA). The motion and finger force measurement systems were synchronized. A 24-inch monitor, placed at 0.8 m in front of the subject, provided real-time visual feedback of force (Figure 3.2A). A customized LabVIEW program (National Instruments) was used for acquiring the force data, controlling the motorized handle, and providing real-time visual feedback.

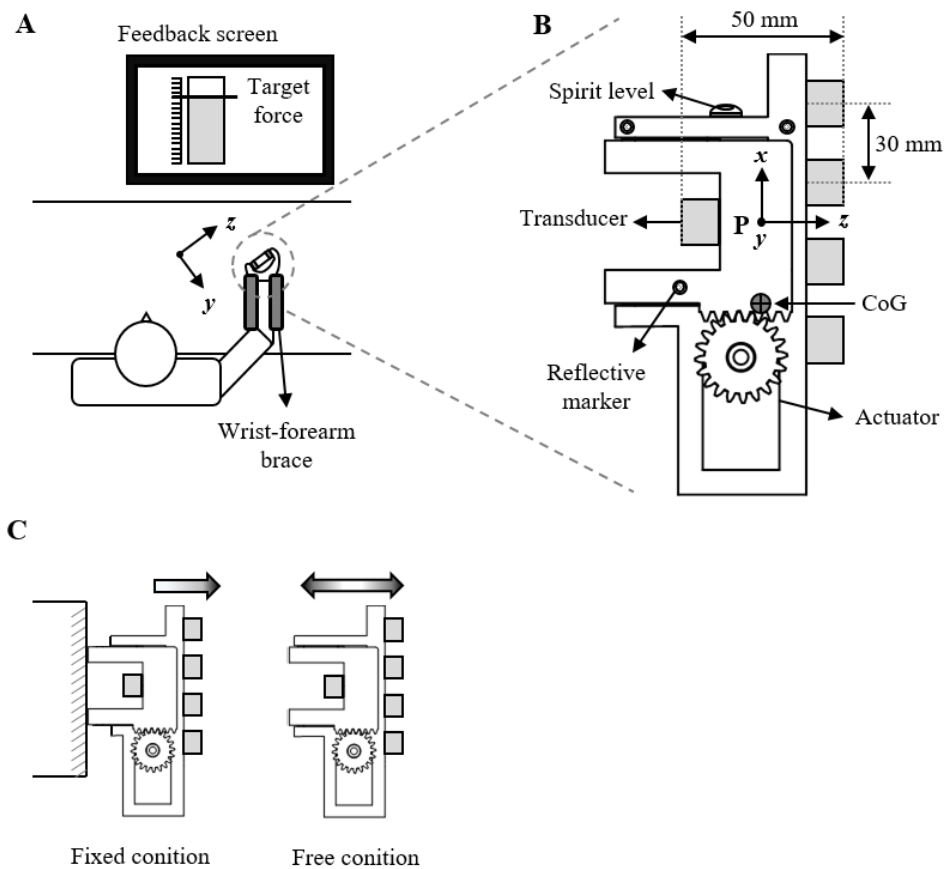

**Figure 3.2.** Experimental setup. (A) Subjects' forearm and wrist were held securely on a rigid brace in a natural grasping hand position. A monitor located at eye level approximately 1 m away from the subjects was used for visual feedback of digit normal forces. Note that the visual force feedback was provided only in the fixed prehension condition. (B) Description of the motorized handle. A handle-fixed coordinate frame was located at point *P*. The distance between the centers of adjacent transducers on the fingers side was 30 mm, and the transducer corresponding to the thumb was located in the center of the middle and ring finger transducers along the *x*-axis. Grip width was 50 mm along the *z*-axis. A servo actuator (Dynamixel MX-64T Robot servos, ROBOTIS, South Korea) was mounted on the frame of the handle to make capable of position and velocity control, and both parts of the handle were connected by two linear guides, allowing the changes of grip width to expand (i.e., moving outward) and contract (i.e., moving inward). A small spirit level and reflective markers were attached to the handle frame. (C) The handle was designed to fix one side of the frame to an immovable steel frame on the table. It made possible fixed-object prehension (FIXED) without mechanical constraints as well as free object prehension (FREE).

### 3.2.3. Experimental Procedure

The subjects sat in a chair, and positioned their right arm as follows: the right forearm and wrist were placed in a rigid forearm brace above the table with their shoulder at approximately 45° abduction and 30° flexion, and the elbow at 60° flexion (Figure 3.2A). In particular, the forearm and wrist were strapped to the arm brace at the neutral position; thus, the motions of flexion-extension and radial-ulnar deviation of the wrist joint were minimized. The main experimental task was to hold the motorized handle with the right hand in two conditions: FREE and FIXED. For the FREE condition, the digits were responsible for maintaining the translational and rotational equilibrium of the handle. In contrast, the handle was firmly fixed to the table in the FIXED condition (Figure 3.2C), so that the digit forces were neither responsible for nor were they able to influence the equilibrium of the handle.

The subjects were instructed to hold the handle with five digits in the grasping plane shown in Figure 3.2A. For the FREE condition, the magnitudes of grip force were not prescribed, and visual grip force feedback was not provided. We instructed the subjects to hold the handle comfortably using "natural" grip force and orient the handle vertically via the spirit level before the onset of the trial. We also instructed the subjects not to make any intentional change in the orientation of the handle when the grip aperture was modulated. The measurement started when the subjects reported a "*ready*" sign and the experimenter confirmed the vertical orientation of the handle. Each trial lasted 15 s. For the first 5 s, the subjects held the handle stationary without any aperture adjustment. At a random time between 5 and 8 s after trial onset, the width of the handle expanded by 20 mm, and then contracted to the initial width at a rate of 20 mm/s (Ambike et al., 2016; Reschechtko & Latash, 2017, 2018). Thus, the initial 50 mm grip width expended to 70 mm and returned to its initial value. The subjects were given the following instructions: "*do not react to the movements of handle*", and "*do not adjust your commands to the hand*" and "*continue holding the handle until the end of the trial*" (Feldman, 1966; Latash, 1994).

For the FIXED condition, the thumb side of the handle was firmly fixed to the table (Figure 3.2C), and the coordinate frame of the fixed handle was aligned with the table-fixed coordinate frame. With this arrangement, the table ensured the static equilibrium of the handle, but the motor was still able to vary the grip aperture. We instructed the subjects to hold the (fixed) handle naturally as if they were grasping a free object. The subjects received visual feedback on the grip force (i.e., the normal force of the thumb; Figure 3.2A), and the target force was equal to the

subject's average normal thumb force over 50 ms of steady state grasping before the handle movement in the FREE condition. This process equalized the average effort of the digits between the two experimental conditions. The measurement started when the subject's grip force matched the prescribed value. Providing real-time visual force feedback when the grip width changed could interfere with the instruction not to voluntarily intervene; therefore, the visual feedback was removed 5 s after trial onset, and the subjects were instructed to hold the handle with the same effort until the end of the trial. Like the FREE condition, the grip width adjustment was initiated at a random time between 5 and 8 s from the onset of the trial.

The FREE and FIXED experimental conditions were conducted over three days. The first day was for familiarizing the subject to the experimental setup and tasks; no data were collected. The second and third day were for the data collection in FREE and FIXED condition, respectively. The subjects performed 30 trials in each condition per day and had a mandatory 45 s rest after the completion of each trial. Also, subjects were required to ask for additional rest if they felt fatigue. None of the subject reported any fatigue. The total duration of the experiment per day was ~ 60 min.

### 3.2.4. Data Analysis

Force and position data were low-pass filtered with a fourth-order, zero-lag Butterworth filter with a cutoff of 10 Hz (Ambike et al., 2015). We restricted the analysis to the *x*-*z* grasping plane (Zatsiorsky et al., 2002a). Therefore, the analysis of digit force data for determination of control variables was limited to the normal forces along the *z* axis. Similarly, we used marker position data along the z axis of

the table-fixed coordinate frame, which was parallel to the direction of aperture adjustment. Since the motorized handle was not fixed in the FREE condition, the handle- and table-fixed *z* axes may get misaligned. Hence, the position data in the FREE condition were visually inspected to ensure that the *z* axes of the two frames were aligned during static prehension and aperture adjustment; we rejected trials in which the alignment between the two *z* axes was more than ± 3°. We also visually inspected the force profiles and rejected trials where we observed significant force drift over time, mismatch in the prescribed and produced force by more than ± 5% at the steady-state force production phase (for the FIXED condition), and abrupt changes in force during the handle expansion phase. The average percentage of accepted trials across the subjects was 92%.

The force and position data for the multiple trials were aligned with respect to $t_0$ – the onset of the motor on the handle (Figure 3.3A). We defined analysis phases as follows: (1) static prehension phase for 50 ms before $t_0$ and (2) the handle expansion phase until the peak digit forces were observed. We confirmed that peak digit forces occurred at the instant of maximum handle expansion. All dependent variables were analyzed at two levels of the control hierarchy: the upper level created by the thumb (TH) and virtual finger (VF), and the lower level created by the four fingers (i.e., index, I; middle, M; ring, R; little finger, L).

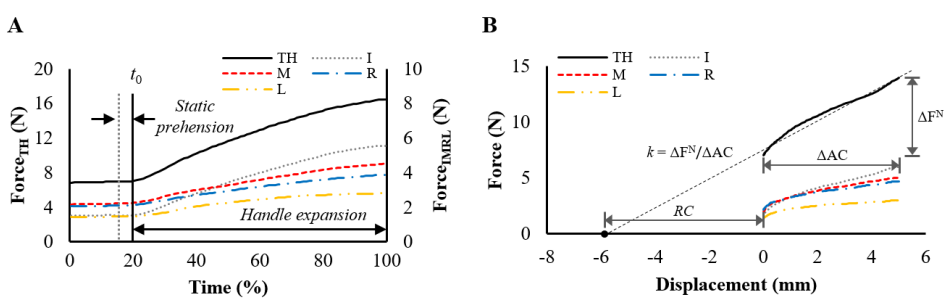

**Figure 3.3.** (A) Representative time-series data of each digit normal forces during static prehension and handle expansion phases. The time is normalized to 100% from the trial onset to when the motorized handle is maximally widened. The scale of the left vertical axis reflects the thumb (TH) force level, and the right axis refers to the force of individual finger (I, M, R, and L). The vertical solid line indicates the time of the onset of the actuator ($t_0$). The dashed vertical line represents the time point before 50 ms of the driving actuator. (B) Example of sensor displacement versus digit normal force data in handle expansion phase. The net change in the normal force ($\Delta F^N$) and digit displacement ($\Delta AC$) of each digit were calculated. The $\Delta F^N$ and $\Delta AC$ were obtained by subtracting the initial value from its final value. The initial values were obtained from the average normal force and corresponding digit position in the static prehension phase, and the final values were computed as the average values during the final 10 ms of handle expansion phase. $k$ of each digit was computed according to Hooke's law, $k = \Delta F^N/\Delta AC$, in unit of N/mm. The $RC$ (in unit of mm) of each digit was computed as $RC = F^N/k$ with the initial digit-tip position (i.e., AC in Equation 3) was defined as zero. Thus, the calculated $RC$ represented the threshold position where the digit normal forces were stationary prior to the handle expansion.

#### *3.2.4.1. Mechanical Constraints of the Task*

For static prehension in the 2D plane, the following constraints must be satisfied in the FREE condition: 1) The sum of the normal forces of the four fingers must equal the normal force of the TH to satisfy the horizontal translation constraint. 2) The sum of the tangential forces produced by all five digits must equal the weight of the grasped object. 3) The resultant moment produced by all five-digit forces must be zero since no external torque acted on the handle. For the FIXED condition, there was no need to satisfy these constraints to maintain static equilibrium.

#### *3.2.4.2. Reconstruction of RC and k at Two Hierarchical Levels*

Our purpose was to quantify the referent aperture, specifically, the width

($R_a^w$) and midpoint ($R_a^m$) of $R_a$. These quantities depend on the *RC* and *k* of TH and VF. Therefore, we computed the *RC* and *k* values for each digit separately using the methods of Reschechtko and Latash (2018). We modeled the normal force of digit *i* along the *z* axis ($F^N_i$) as:

$$F_i^N = k_i \times (AC_i - RC_i), \qquad (3.1)$$

where $AC_i$ is the actual coordinate of the digit-tip along the *z* axis. We assumed a linear relation between the force and the difference in the actual and referent coordinate (see the representative force-displacement profiles for the digits in Figure 3.3B). To validate this assumption, we regressed separately the normal force against the *z*-axis displacement of each digit. We accepted trials in which the *R* values of the regressions for all the digits were above 0.9 (Reschechtko & Latash, 2017). This yielded between 20 and 30 trials for all condition, with an average of 24.2 trials across subjects.

The details of the computation of *RC* and *k* are described in Figure 3.3B. To generate a grasping force, the *RC* of both TH and VF must lie inside the object (Figure 3.1A). Note that the sign of *RC* will depend on the location and orientation of the coordinate frame used for the computation; similarly, the normal force of the TH and VF, when expressed in the same handle-fixed coordinate frame, will be of opposite signs. For further analysis, we used the absolute values of all normal forces, and we expressed *RC*s as positive distances from the actual location of the corresponding digit before the grip width was modulated, as shown in Figure 3.1A. We obtained pairs of digits {*RC*, *k*} for all selected trials. Using the *RC* of TH and VF, we computed width and midpoint of $R_a$ (i.e., $R_a^{\mathrm{w}}$ and $R_a^{\mathrm{m}}$, respectively) as follows:

$$R_a^w = grip\ \ width - \ \ |RC|^{TH} - |RC|^{VF}, \qquad (3.2)$$

$$R_a^m = |RC|^{TH} + \ \frac{R_a^w}{2} = 0.5 \times [grip\ \ width + \ \ |RC|^{TH} - |RC|^{VF}\ \ ], \qquad (3.3)$$

where grip width was 50 mm, and $R_a^m$ was determined from the initial TH position before the grip width changed.

#### *3.2.4.3. Permutation Analysis of RC and k*

We investigated whether the control variables within the referent configuration hypothesis, $\{RC, k\}$, which are called elemental variables (EVs) within the synergy literature, displayed covariation to stabilize task-specific performance variables (PVs). This analysis was conducted separately for FREE and FIXED conditions and for the upper and lower level of the control hierarchy. For the upper level, the total normal force $F^N_{TOT}$ can be expressed as

$$F_{TOT}^N = \ \ |RC|_{TH} \times k_{TH} - |RC|_{VF} \times k_{VF}. \qquad (3.4)$$

Equation 3.4 indicates that the control variables for TH and VF are constrained to produce close to zero total force, so that the handle remains static. For the lower level, the VF normal force ($F^N_{VF}$) arises from the $\{RC, k\}$ for the fingers:

$$F_{VF}^N = \ \sum_i RC_i \times k_i. \qquad (3.5)$$

We quantified the synergy in which $\{RC, k\}$ of the TH and VF covary in a 4-dimensional space to stabilize $F^N_{TOT}$ at the upper level. At the lower level, we quantified the $\{RC, k\}$ synergy in the 8-dimensional space that stabilizes $F^N_{VF}$. Finally, we also quantified the synergy in the corresponding 2-dimensional $\{RC, k\}$ space stabilizing the normal force for the TH and the VF at the upper level, and for

the four fingers (I, M, R, L) at the lower level. For digit *i*, the EVs and PVs are related simply as: $F^N_i = RC_i \times k_i$. This constraint on the EVs is hyperbolic, and the constraints expressed in Equations 4 and 5 are sums of hyperbolas. These constraints are highly non-linear and linearizing these systems for the synergy analyses is questionable. Therefore, we utilized the permutation analysis to identify task-specific covariation in the EVs (Muller & Sternad, 2003). We generated surrogate PVs using the respective constraint equations for each analysis after random permutations of the EVs. The permutation operation removes the task-specific covariation in the EVs; if the variability in the corresponding surrogate PVs is higher than the original PV set, we conclude that the EVs contained task-specific covariation.

The permutation analysis is the technique that creates a set of random surrogate data, which is expected to remove the effect of task specific covariation among the involved variables. This surrogate data set had the same means and standard deviation (SD) as the actual values. We randomly generated $\{RC, k\}$ pairs of surrogate data using each subject's actual $\{RC, k\}$ values within each digit and condition. We then calculated $F^N$ of surrogate data ($F^N_{SUR}$) and subsequently computing average SD of $F^N_{SUR}$ ($SD^F_{SUR}$) over 10,000 times permutations. Finally, the ratio of SD from surrogate and actual data set ($R_{SD}$) was computed by comparing $SD^F_{SUR}$ with SD of the actually observed $F^N$ ($SD^F_{ACT}$) as follow, $R_{SD} = SD^F_{SUR}/SD^F_{ACT}$. We computed the $R_{SD}$, separately for both hierarchies and individual digits. Theoretically, if $R_{SD}$ is more than 1, it means that the *RC* and *k* within original data covaried to stabilize the outcome digit force. However, we applied the more conservative criterion $R_{SD} > 2$ to infer task-specific covariation (Reschechtko & Latash, 2018).

#### *3.2.4.4. UCM-based Analysis of Variance on Digit Normal Forces*

The uncontrolled manifold (UCM) approach was employed to analyze the digit $F^N$ at the two hierarchical levels (Park et al., 2015). For the upper level, the TH and VF normal forces were the EVs, the total normal force was the PV. The TH and VF normal force magnitudes must covary positively so that their difference is stabilized around zero, and the object remains static. Therefore, the EVs and the PV are related by the constraint: $F^N_{TOT} = F^N_{TH} - F^N_{VF}$. The Jacobian relating small changes in the EVs to changes in the PV was [1, -1]. For the lower-level analysis, the individual finger forces were the EVs, the VF normal force was the PV, related by the constraint: $F^N_{VF} = \sum F^N_i$, for $i$ = {I, M, R, L}, and the corresponding Jacobian was [1, 1, 1, 1]. For both analyses, the null space of the corresponding Jacobian defines the uncontrolled manifold (UCM). Changes in the EVs along the UCM do not change the PV; however, changes in the EVs orthogonal to the UCM change the PVs.

For each of these analyses, the across-trial EV data was decomposed into two variance components: one along the corresponding UCM ($V_{UCM}$), and another orthogonal to the UCM ($V_{ORT}$). The synergy index ($\Delta V$) was then calculated using the normalized difference in $V_{UCM}$ and $V_{ORT}$ as follows:

$$\Delta V = \frac{V_{UCM}/DOF_{UCM} - V_{ORT}/DOF_{ORT}}{V_{TOT}/DOF_{TOT}}, \qquad (3.6)$$

where $V_{UCM}$, $V_{ORT}$, and $V_{TOT}$ are further normalized by the degrees of freedom (DOF) of their respective subspaces, allowing comparison of the indices across two subspaces that were observed in different dimensions. The $\Delta V$s were log-

transformed using the Fischer transformation to account for the bounds on the synergy index (Park et al., 2013; Wu, Zatsiorsky, & Latash, 2012).

### 3.2.5. Statistics

Our first and second hypotheses were related to the quantification of {*RC, k*} of individual digits and the midpoint of $R_a$ in the FREE and FIXED conditions. To test the first hypothesis (H1), we performed separate *Digit* × *Type* repeated-measures (RM) ANOVAs on *RC* and *k*. This analysis was performed separately at each hierarchical level. The factor *Digit* had two levels (TH and VF) for the upper-level analysis and four levels (I, M, R, L) at the lower-level analysis. The factor *Type* had two levels (FREE and FIXED) for both analyses. Also, we performed separate paired *t*-tests on $R_a^w$ and $R_a^m$ to determine the effect of *Type* on the referent aperture. To test the second hypothesis (H2), we performed separately for the FREE and FIXED conditions single-sample *t*-tests to compare the computed midpoint of the referent aperture ($R_a^m$) with the value of 25 mm – the midpoint of the actual aperture. The third and fourth hypotheses were about the quantification of the synergies within the control variables and comparison between two prehension conditions. To test the third hypothesis (H3), all the $R_{SD}$ values, quantifying synergistic organization of the control variables, were compared with the critical value of 2 using separate single-sample *t*-tests for all digits in both conditions. Similarly, $\Delta V_Z$ values were compared with the relevant critical values using single-sample *t*-tests. The critical value of $\Delta V_Z$ was 0 for the upper-level $F^N$ analyses and 0.55 for the lower-level $F^N$ analysis since the bounds on the synergy indices were different depending on the nullity of the Jacobian. Also, the correlation analyses between $R_{SD}$ and $\Delta V_Z$ for total normal force

stabilization was performed separately in the FREE and FIXED conditions. Finally, to test the fourth hypothesis, synergies within space of {*RC*, *k*} were analyzed using RM ANOVAs with factors *Hierarchy* (two levels: upper and lower level) and *Type*. Similarly, the $F^N$-stabilizing $\Delta V_Z$ (and corresponding $V_{UCM}$ and $V_{ORT}$) were tested using the same RM ANOVA.

Mauchly's sphericity test was used to confirm the assumptions of sphericity, and their violations were corrected by the Greenhouse-Geisser estimation. All pairwise comparisons with Bonferroni corrections were performed to explore significant interaction effects, or significant main effects when no interaction was observed. The effect size was quantified using partial eta-squared ($\eta p^2$) for the ANOVAs and Cohen's *d* for the t tests. We conducted all statistical analyses using SPSS 24.0 (IBM, Armonk, NY), and the level of significance was set at $p<.05$.

The current experiment measured both normal and tangential digit forces; both groups of forces are essential to ensure a stable static grasp. However, we restricted our analyses to the normal forces. Our results and interpretations would be problematic if there was interaction between the normal and tangential forces. Therefore, we tested the independence of the normal and tangential forces via a principal component analysis (PCA) with variance maximizing rotation to observe the configuration of digit normal ($F^N$) and tangential ($F^T$) forces. This analysis was conducted using four components of digit forces ($F^N_{TH}$, $F^N_{VF}$, $F^T_{TH}$, $F^T_{VF}$) over repeated trials for each subject and condition (FREE and FIXED) separately. The Kaiser Criterion (i.e., extracted PCs should be the eigenvectors with eigenvalues > 1) was employed to define the significant PCs and loading coefficients (Kaiser, 1960).

## 3.3. Results

To determine task performance, we calculated the orientation (angle) of the handle ($\theta_{Handle}$) with respect to the horizontal axis in the *x-z* plane in the FREE condition. There was no significant change in $\theta_{Handle}$ over the time. A single sample t-test showed that the average $\theta_{Handle}$ in the static prehension phase was not significantly different from zero. Thus, the participants were able to maintain the orientation of the handle as instructed.

**Table 3.1.** Loadings of principal components (PC1 and PC2) of digits normal and tangential finger forces in free (FREE) and fixed object (FIXED) conditions.

| | **FREE** | | **FIXED** | |
|---|---|---|---|---|
| | **PC1** | **PC2** | **PC1** | **PC2** |
| $\mathbf{F^N_{TH}}$ | **0.980 (0.005)** | 0.162 (0.028) | **0.769 (0.035)** | 0.067 (0.087) |
| $\mathbf{F^N_{VF}}$ | **0.978 (0.005)** | 0.175 (0.028) | **0.793 (0.037)** | 0.116 (0.053) |
| $\mathbf{F^T_{TH}}$ | 0.118 (0.053) | **0.975 (0.005)** | -0.068 (0.069) | **0.654 (0.164)** |
| $\mathbf{F^T_{VF}}$ | -0.079 (0.054) | **-0.975 (0.004)** | 0.006 (0.049) | **-0.645 (0.169)** |

Averaged loading factors across subjects. The values in parentheses indicate standard errors. Significant loadings (> |0.5|) are shown in bold. $F^N_{TH}$: thumb normal force; $F^N_{VF}$: virtual finger normal force; $F^T_{TH}$: thumb tangential force; $F^T_{VH}$: virtual finger tangential force.

Recall that the analyses of the forces and referent variables is conducted for the normal (*z*) direction, independent of the tangential forces produced by the digits. The PCA with four components of digit forces ($F^N_{TH}$, $F^N_{VF}$, $F^T_{TH}$, $F^T_{VF}$) showed that the first two significant PCs explained more than 99.26 ± 0.27% and 69.85 ± 2.64% of the variance for the FREE and the FIXED conditions, respectively. Average loadings across subject for the FREE and FIXED conditions are listed in Table 3.1, and the

significant loadings (> 0.5) are shown in bold. The normal forces of the TH and VF had large loadings in the PC1, whereas the two tangential force components grouped into PC2. This grouping pattern appeared similarly in the FREE as well as in the FIXED condition. These results suggest the independence of the normal and the tangential digit forces during our tasks.

### 3.3.1. Values of Control Variables, *RC* & *k*

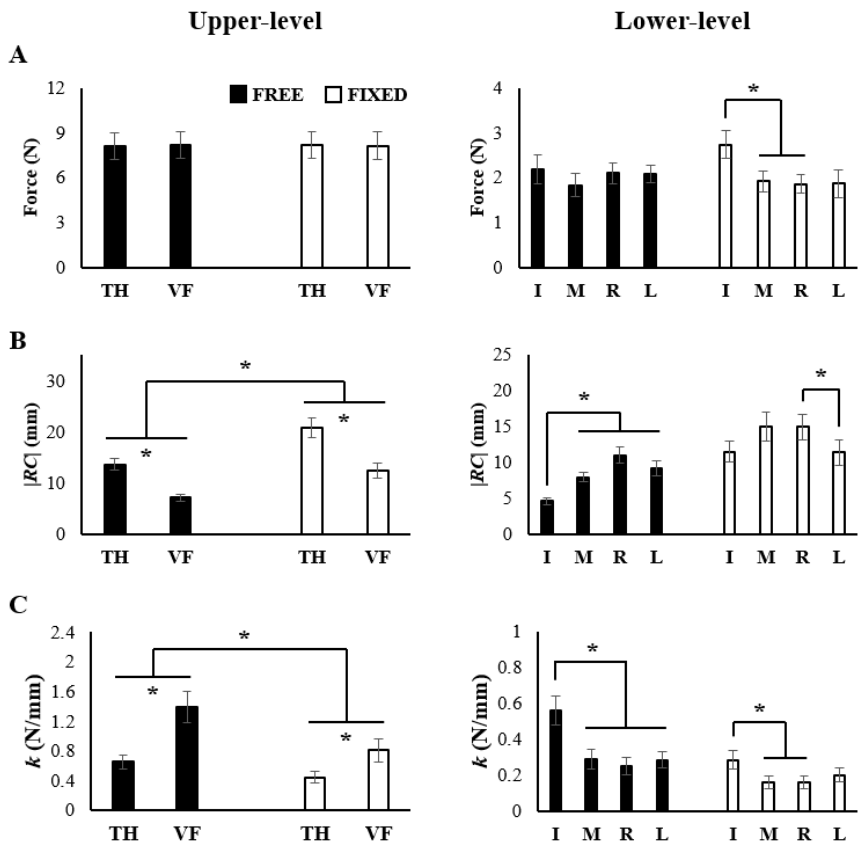

**Figure 3.4.** Across-subject mean and standard errors of (A) digit normal forces, (B) *RC*, and (C) *k* for the upper and lower hierarchies. The upper level (left panel) includes the thumb (TH) and virtual finger (VF), and the lower level (right panel) contains the index (I), middle (M), ring (R), and little (L) finger. The solid bars and the open bars indicate the FREE and FIXED, respectively. The asterisks indicate the presence of statistical differences between digits and conditions.

The upper-level *RC* for TH in both conditions was significantly larger than the VF *RC*, and the *RC* in the FIXED Condition was significantly higher than that of the FREE Condition (Figure 3.4B). In contrast, *k* was significantly larger for the VF than TH, and *k* of TH and VF was larger in the FREE condition (Figure 3.4C). These results were supported by significant main effects of *Digit* (*RC*: $F_{[1,9]}$=87.15, $p$<0.001, $\eta p^2$=0.91; *k*: $F_{[1,9]}$=25.15, $p$=0.001, $\eta p^2$=0.74) and *Type* (*RC*: $F_{[1,9]}$=21.40, $p$=0.001, $\eta p^2$=0.70; *k*: $F_{[1,9]}$=16.98, $p$=0.003, $\eta p^2$=0.65) in the ANOVAs.

The across-finger changes in *RC* and *k* were dissimilar in the FREE and FIXED tasks. This was reflected in significant *Digit* × *Type* interactions for both variables (*RC*: $F_{[3,27]}$=6.02, $p$=0.003, $\eta p^2$=0.40; *k*: $F_{[3,27]}$=9.49, $p$<0.001, $\eta p^2$=0.51). The post-hoc comparisons revealed that in the FREE condition, the *RC* for the index finger was lower than that for the other three fingers, and the opposite pattern appeared for the *k* ($p$<0.05). In the FIXED condition, the *RC* was R > L, and the *k* was I > M and R ($p$<0.05). Further, the *RC* of the I and M was significantly lower in the FREE than the FIXED condition, whereas the *k* of that fingers in the FREE was significantly larger than the FIXED condition ($p$<0.05).

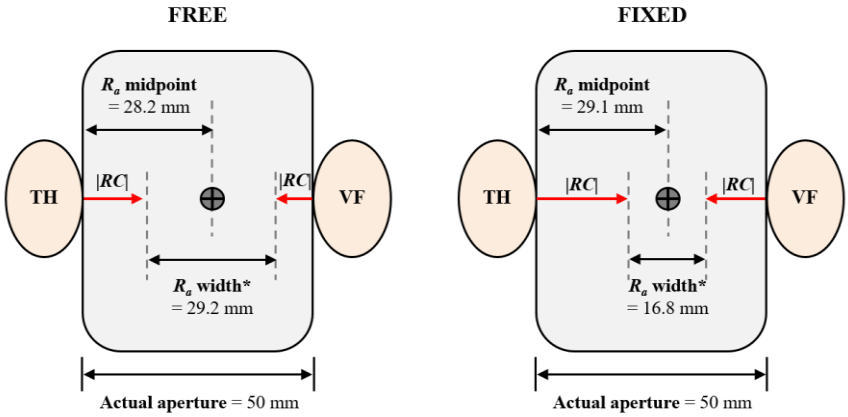


**Figure 3.5.** An illustration for width ($R_a^w$) and midpoint ($R_a^m$) of referent aperture obtained in FREE (left) and FIXED (right). The $R_a$ is determined by magnitudes of the *RC* of the thumb (TH) and virtual finger (VF). The grey circle inside the rectangular object is the location of $R_a^m$, which is skewed towards the VF.

The width of referent aperture ($R_a^w$) in the FREE and FIXED condition were 29.17 ± 1.43 and 16.79 ± 3.07 mm, respectively (Figure 3.5); the paired *t*-test found that $R_a^w$ was significantly larger in the FREE condition ($t_{[9]}$=4.63, $p$=0.001, Cohen's $d$=1.46). The midpoint of referent aperture ($R_a^m$) was significantly skewed toward VF from the center of the actual aperture (Figure 3.5). The average $R_a^m$ was 28.24 ± 1.77 mm from the TH in the FREE condition, and 29.14 ± 0.69 mm in the FIXED condition. These unbalanced locations of $R_a^m$ were confirmed by the single-sample *t*-tests, which showed that the $R_a^m$ were significantly larger than the value of 25 (i.e., midpoint of the grip width) (FREE: $t_{[9]}$=5.79, $p$<0.001, Cohen's $d$=1.83; FIXED: $t_{[9]}$=5.99, $p$<0.001, Cohen's $d$=1.89).

### 3.3.2. Permutation-based Analyses to Quantify Synergies in {*RC*, *k*}

## Spaces

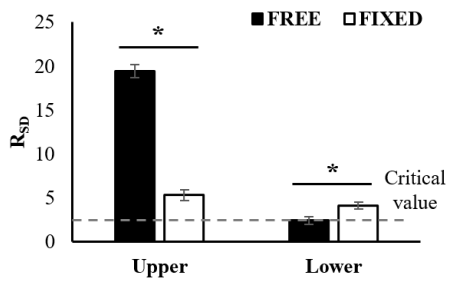


**Figure 3.6.** Across-subject mean and standard errors of $R_{SD}$ for each hierarchy and prehension condition. The upper level $R_{SD}$ are determined using the 4-dimensional $\{RC_i, k_i\}$ values ($i$ = TH and VF), and the lower level using 8-dimensional $\{RC_i, k_i\}$ ($i$ = I, M, R, and L). The solid bars and open bars indicate the FREE and FIXED, respectively. The dashed line represents the critical $R_{SD}$ value. The asterisks indicate significant differences between prehension conditions.

Single sample *t*-test for comparing $R_{SD}$ with the critical value of 2 revealed $\{RC, k\}$ synergies in all cases except for the lower-level FREE condition (upper-level FREE: $t_{[9]}$=23.60, $p$<0.000, Cohen's $d$=7.46; upper-level FIXED: $t_{[9]}$=5.25, $p$=0.001, Cohen's $d$=1.66; lower-level FIXED: $t_{[9]}$=5.69, $p$<0.001, Cohen's $d$=1.79). The upper-level $R_{SD}$ values, which quantified the covariation in the 4-dimensional $\{RC, k\}$ space of the TH and VF for stabilizing $F^N_{TOT}$, were significantly larger in the FREE than the FIXED condition (Figure 3.6). In contrast, the lower-level $R_{SD}$ quantifying synergies within the 8-dimensional space of $\{RC_i, k_i\}$ was smaller in the FREE condition. These findings were confirmed by *Hierarchy* × *Type* RM ANOVA, which showed significant interaction ($F_{[1,9]}$=667.93, $p$<0.001, $\eta p^2$=0.99).

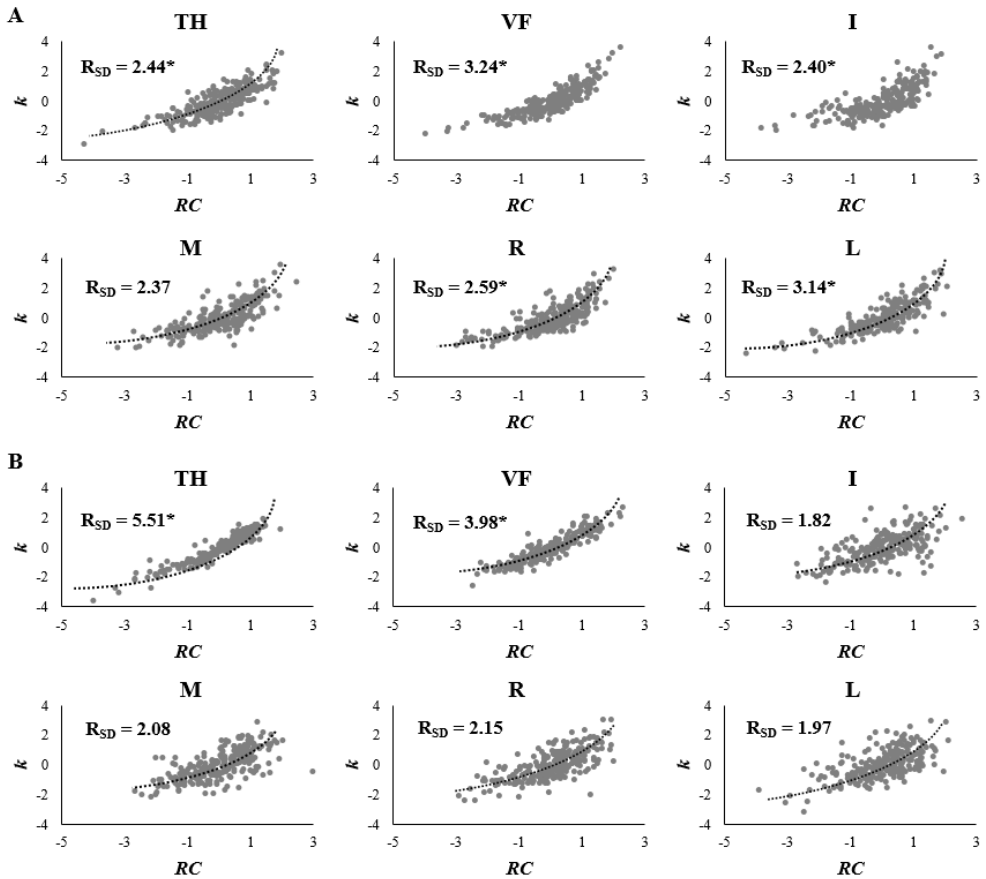


**Figure 3.7.** The scatter plots of *RC* and *k* for individual digit in the (A) FREE and (B) FIXED conditions. The {*RC*, *k*} pairs of corresponding digit are pooled across trials and subjects by transforming values to z-score. Average $R_{SD}$ for across subjects is presented with hyperbola regression line for each digit. The asterisks indicate the presence of significant synergy effects above critical value 2.

We further quantified {*RC*, *k*} synergies for the individual digits. The across-trial *RC* and *k* data for individual digits and conditions pooled across subjects and the across-subject average of the $R_{SD}$ values are presented in Figure 3.7. The single-sample *t*-tests showed significant synergies within the {*RC*, *k*} space in all digits except the middle finger in the FREE condition (Figure 3.7A; TH: $t_{[9]}$=3.64, $p$=0.005, Cohen's $d$=1.15; VF: $t_{[9]}$=6.94, $p$<0.001, Cohen's $d$=2.19; I: $t_{[9]}$=2.37,

$p$=0.042, Cohen's $d$=0.74; R: $t_{[9]}$=2.81, $p$=0.021, Cohen's $d$=0.88; L: $t_{[9]}$=3.86, $p$=0.004, Cohen's $d$=1.22). For the FIXED condition, however, there were synergies only in the upper-level digits (Figure 3.7B; TH: $t_{[9]}$=7.17, $p$<0.001, Cohen's $d$=2.26; VF: $t_{[9]}$=4.68, $p$=0.001, Cohen's $d$=1.47).

The individual digit $R_{SD}$ were different between control hierarchy depending on the FREE and FIXED conditions. For the upper level, the $R_{SD}$ was larger in the FIXED than in FREE condition for both TH and VF. In contrast, the $R_{SD}$ of the four fingers (i.e., lower-level I, M, R, and L) were larger in the FREE than in FIXED condition. These results were supported by *Digit* × *Type* RM ANOVA performed separately for each hierarchy. Both analyses showed significant main effect of *Type* (upper-level: $F_{[1,9]}$=10.74, $p$=0.01, $\eta p^2$=0.54; lower-level: $F_{[1,9]}$=6.36, $p$=0.03, $\eta p^2$=0.41).

### 3.3.3. UCM-based Synergy Indices of Digit Forces

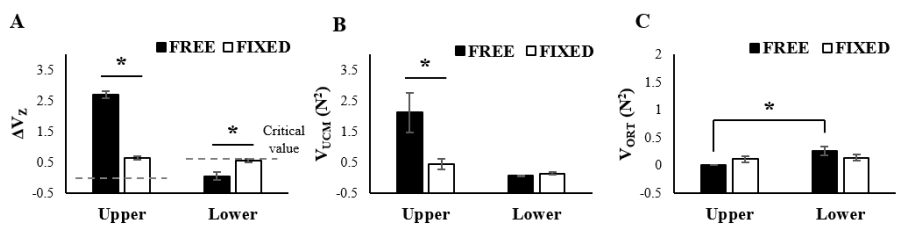


**Figure 3.8.** (A) Across-subject mean and standard errors of $\Delta V_Z$ stabilizing upper and lower-level digit normal forces in the FREE and FIXED condition. (B) and (C) show variance in the space of UCM ($V_{UCM}$) and orthogonal to the UCM ($V_{ORT}$), respectively. The solid and open bars indicate the FREE and FIXED, respectively. Horizontal dashed lines represent critical $\Delta V_Z$ values (= 0 for upper-level, and ≈ 0.55 for lower-level). The asterisks indicate significant differences between condition and hierarchy.

The synergy indices for the stabilization of net grip force were higher than the critical value only at the upper level (FREE: $t_{[9]}$=22.88, $p$<0.001, Cohen's $d$=7.23; FIXED: $t_{[9]}$=10.99, $p$<0.001, Cohen's $d$=3.47). In particular, $\Delta V_Z$ stabilizing $F^N_{TOT}$ at the upper level was greater in the FREE than in the FIXED condition (Figure 3.8A). In contrast, at the lower level, the finger normal forces that yield $F^N_{VF}$ showed the opposite pattern (Figure 3.8A). This was supported by a *Type* × *Hierarchy* interaction ($F_{[1,9]}$=119.93, $p$<0.001, $\eta p^2$=0.93). The $V_{UCM}$ for the FREE condition was greater than FIXED condition at the upper-level, and there was no significant difference at the lower-level (Figure 3.8B). Significant difference in $V_{UCM}$ between hierarchy was observed only in the FREE condition. In the case of $V_{ORT}$, there were no significant differences of two levels of Type in both hierarchies, and in the FREE condition, the lower-level was significantly larger than the upper-level (Figure 3.8C). These finding were confirmed by significant *Type* × *Hierarchy* interactions ($V_{UCM}$: $F_{[1,9]}$=10.65, $p$=0.01, $\eta p^2$=0.54; $V_{ORT}$: $F_{[1,9]}$=7.42, $p$=0.023, $\eta p^2$=0.45).

### 3.3.4. Relationship Between the Synergy Indices Obtained from the Permutation and UCM Analyses

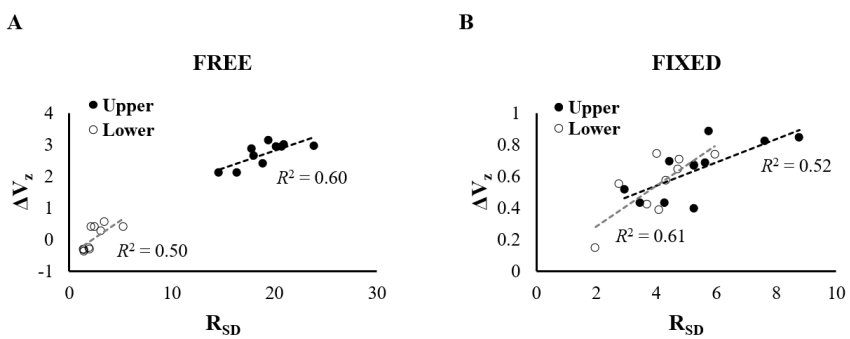

**Figure 3.9.** Relationship between $R_{SD}$ and $\Delta V_Z$ in the (A) FREE and (B) FIXED condition. Linear regression was performed separately for each hierarchy using data pooled across subjects. Black circle and open circle represent upper and lower-level, respectively. The best-fit regression line with $R^2$ values are presented for each hierarchy.

The $R_{SD}$ values (obtained from permutation analysis) were compatible with the $\Delta V_Z$ values (obtained from UCM analysis). For the regression analysis, the pooled data across all subjects were used separately for the two conditions and hierarchies (Figure 3.9). These data were well approximated in the least-squared sense by a linear function (upper-level FREE: $R^2$=0.60, $p$=0.009; lower-level FREE: $R^2$=0.50, $p$=0.023; upper-level FIXED: $R^2$=0.52, $p$=0.019; lower-level FIXED: $R^2$=0.61, $p$=0.008).

## 3.4. Discussion

In this study, we quantified the referent aperture ($R_a$) and the synergistic organization of mechanical and control variables involved in the static grasp of a fixed and a free object. The data supported the four hypotheses formulated in the *Introduction*. We found that the apparent digit stiffness ($k$) and width of the $R_a$ were larger in free- than in fixed-object prehension (hypothesis H1). We also confirmed that the midpoint of $R_a$ was skewed toward the virtual finger (hypothesis H2). Further, synergic organization for the stabilization of total force on the object was observed in the space of the control variables $\{RC, k\}$ as well as in the space of the digit forces (hypothesis H3). Lastly, we observed relatively large strength of synergies at the higher level of the hierarchy in the free condition than in fixed condition (hypothesis

H4). These results add to the current literature by demonstrating that grasp control involves modulation of digit apparent stiffness in addition to the referent coordinate and by identifying the synergistic organization of the control variables during static grasp.

### 3.4.1. Effect of Mechanical Constraints on the Formation of the Referent Aperture for Grip Force Production

Comparing the hypothetical control variables $\{RC, k\}$ across the two tasks – the static grasp of the free and the fixed handle – allowed us to identify the functional roles of the variables in managing grasp stability. We note that the *RC* and *k* are measurable surrogates for two neural control signals (Ambike, Mattos, Zatsiorsky, & Latash, 2018) that form a hierarchy (Feldman, 2015). Specifically, the R-command defines the spatial coordinate (*RC*), and the C-command (associated with *k*) is associated with a co-activation zone about the spatial coordinate defined by the R-command. The R-command influences the position and/or the contact forces, and the C-command is associated with the stiffness of the effector. Therefore, the changes in *RC* and *k* can be interpreted as arising from the underlying R- and C-commands.

The passive mechanical stiffness (i.e., with no spinal reflexes) of the virtual finger is over twice that of the thumb (1.17 N/mm vs 0.46 N/mm) (Park, Pazin, Friedman, Zatsiorsky, & Latash, 2014). While grasping, however, this passive stiffnesses will be modulated via the tonic stretch reflex, thus yielding the apparent stiffness, and the apparent stiffness increases with the magnitude of the generated digit force (Feldman & Orlovsky, 1972). Therefore, we controlled the digit force

across grasping conditions. Indeed, the thumb and the virtual finger forces between the two conditions w ere not significantly different (Figure 3.4A).

Despite the consistent force, $k$ was higher for the TH and VF in the FREE compared to the FIXED condition (Figure 3.4C). Correspondingly, the aperture width ($R_a^{w}$) was smaller by 73% (about 12 mm) for the FREE condition. One interpretation of this finding is that the muscle co-activation (C-command) of the hand/finger system was larger in the free object prehension, likely to maintain the stability of the grasp. In contrast, when the stability of the handle was ensured by the surrounding support structure, the human control system responded by reducing the digit stiffnesses and using a smaller referent aperture instead. Thus, a possible strategy to set the two control variables is the increment of $k$, and a decrement of $RC$; this may be a way to prevent the slip and enlarge safety margin (Singh & Ambike, 2017) without the changes in the force magnitude.

The midpoint of $R_a$ ($R_a^m$) was located within 3~4 mm of the center of the handle along the horizontal axis (i.e., $z$ axis) regardless of whether the handle was externally constrained or not. In particular, $R_a^m$ was closer to the virtual finger (Figure 3.5), which was associated with the larger apparent stiffness ($k$). Note that the difference in the apparent stiffnesses of the thumb and the virtual finger during grasping mirrored the difference in their passive stiffnesses (Park et al., 2014). This may be explained in part by the fact that the virtual finger is comprised of four fingers, and its apparent stiffness is the addition of four spring stiffnesses, one per finger, arranged in parallel. It is unclear whether this TH-VF asymmetry in terms of the $RC$ and $k$ (and the corresponding shift in $R_a^m$) is functional, or whether it is a characteristic arising from the structure of the human hand (4 fingers in opposition

with one thumb). This point needs to be clarified in the future studies.

However, our results of the two control variables in the free object prehension task point to the functional roles of individual fingers. Notably, there were no significant differences in the magnitudes of individual finger forces in the FREE condition (Figure 3.4A), while {*RC*, *k*} showed significant main effect of *Finger* (Figures 3.4B, 3.4C). Previous studies showed that the central fingers, M and R, are responsible primarily for resultant force production, whereas the lateral fingers, I and L, are specialized for rotational action, i.e., moment of force production (Zatsiorsky & Latash, 2008). This interpretation was further supported by the coefficients of the quadratic objective function that explained the across-finger force distribution when the four fingers produce pressing forces (Park, Singh, et al., 2012). Here, we observed larger *k* value for the lateral index finger, which may be helpful to maintain the rotational equilibrium.

A recent study suggested a more complete set of referent variables for describing the grasp of a free object in a gravity field and in the presence of external torques (Ambike et al., 2014; Latash et al., 2010). There was not only $R_a$, but also a *referent orientation (angle)* and *referent vertical coordinate* reflecting the rotational equilibrium constraint and load forces, respectively. We observed that the *k* of the index finger was greater than the other fingers in both prehension conditions (Figure 3.4C). This difference in *k* between fingers was consistent with the previous finding (Park et al., 2014). A large *k* value implies a more rapid change in the corresponding digit normal force when the handle is expanded, and this change results in a manipulation moment that can change the orientation of the handle. In the current study, the high *k* of the index finger changed the direction of the moment of normal

force during the handle expansion phase, but the resultant moment was kept constant and the change in handle orientation was minimized due to the compensatory behavior of the moment of tangential force. Note that the "do not intervene" paradigm employed in our experiment did not dictate either the digit forces or orientation of the handle. Therefore, the fact that the produced moment during aperture expansion caused by the unbalanced *k* among four fingers while not reacting to the handle expansion was naturally canceled by another moment component, partially supports the existence of the referent orientation as an independent control variable to produce a required net moment on the object. This result is similar to the *principle of superposition* which states that the control for translational and rotational stability could be decoupled in the grasping task (Shim et al., 2005b; Shim & Park, 2007).

Although we measured both normal and tangential forces during multi-digit prehension, our analyses were restricted to the horizontal axis. Grasp stability would be influenced by normal and tangential forces, and any interaction between these forces would influence our interpretations. However, the PCA showed that the normal and tangential digit forces were decoupled (indicated by the loading factors for the first 2 PCs; Table 3.1). The decoupling implies that the fine tuning (i.e., synergic action) of two groups of forces is organized independently. Therefore, the estimation and interpretation of the control variables along the direction of the normal forces without the consideration of tangential forces is reasonable. Nevertheless, we admit that the current study could estimate only $R_a$ because our device changed the position of the digits along the direction of normal forces only. Quantification of other referent variables (i.e., referent angle and referent vertical

coordinate) is required, and we aim to accomplish this reconstruction in our future study.

### 3.4.2. Hierarchical Organization of Control Variables for Grip Stability

We observed synergies for the stabilization of the net grasping force ($F^N_{TOT}$) around zero in the space of the thumb and virtual finger forces as well as the space of $\{RC, k\}$. In addition, stronger synergies were observed when the digits were responsible for ensuring adherence to the mechanical constraints of static prehension, i.e., in the FREE condition. The two types of synergies – one between the digit forces (obtained via the UCM analysis) and one between the control variables (obtained with the permutation analysis) provide consistent results, as shown by the positive correlations in Figure 3.9; thus, the permutation analysis of $\{RC, k\}$ can be used to assess the stability of the grasp.

Recent studies based on the framework of referent configuration provide ample evidence that the referent configuration is possibly a control variable at a higher level of a control hierarchy. In other words, the reference configuration defines a set of thresholds values of all involved muscles for the given task (i.e., the threshold of the tonic stretch reflex). In the present case, the referent variables $\{RC, k\}$ at the Hand level (Figure 3.1B) are the salient performance variables that are specified at the higher level of the hierarchy, which yield grasp force and stability as a consequence of the interactions between the body effectors and the object. A series of few-to-many transformations yield variables at the lower levels of the control hierarchy. This idea, which originated from the equilibrium-point hypothesis (Feldman, 1986), is compatible with the concept of the hierarchy of motor synergies

(Gorniak et al., 2009); hierarchical organization of motor synergies has been observed in finger force or force-mode spaces (Latash et al., 2007). That is, the controller governs only task level variables of motor actions, and the features such as the activation and covariation of individual finger forces seem to be a secondary consideration within the scope of control by the CNS. Indeed, the pattern of covariation between the variables at a higher level does not specify the unique combination of the lower-level variables in a redundant biological system (Latash, 2020a). Previous theoretical studies (Cutkosky & Howe, 1990; Iberall, 1997) and experimental studies on hand and finger actions (Baud-Bovy & Soechting, 2001; Santello & Soechting, 1997; Shim et al., 2003) have suggested a hierarchical control of multi-digit prehension based on the notions of the virtual finger (VF) and individual finger (IF), i.e., at the higher level (VF level) the thumb and VF are coordinated to satisfy task mechanics whereas at the lower level (IF level) the individual fingers are coordinated to generate a desired task-specific outcome of the virtual finger. In other words, the higher-level variables are coordinated to stabilize salient performance variables, whereas at the lower-level are coordinated to generate a desired task-specific outcome that has a mechanical link to the higher-level variables. Indeed, it has been reported that the net normal forces were stabilized only at the task level during multi-finger pressing and prehensile tasks with the thumb and fingers (Gorniak et al., 2009; Kang, Shinohara, Zatsiorsky, & Latash, 2004; Park et al., 2015; Shim et al., 2003).

Our results here are in line with the previous findings. We observed synergies in both the spaces of force and control variable in the upper level of the hierarchy for the FREE condition, but the synergies vanished at the lower level

(Figures 3.6, 3.8A, 3.9A). This indicates that the covariation between the fingers functioned to *destabilize* the VF normal force; this may assist the VF to respond to changes in the thumb normal force so that the total force on the handle is stabilized (Gorniak et al., 2009). Further, when the constraints on the digit behavior were removed by externally fixing the object, the synergies in both spaces at the upper hierarchical level declined (Figures 3.6A, 3.8A). However, the synergy indices were still greater than the corresponding critical values, indicating that the subjects were able to coordinate the thumb and VF forces and $\{RC, k\}$ values to maintain close to zero value of total normal force. In contrast, the synergy indices at the lower hierarchical level were higher for the FIXED relative to the FREE condition. The magnitudes of these synergy indices were low, however, and this effect may be a byproduct of the changes in synergistic organization at the upper level. Since the VF normal force does not need to change in response to the thumb normal force, the fingers are not as coordinated to destabilize the VF normal force.

## 3.5. Conclusion

This study quantified the referent aperture location and width – the postulated control variables within the referent control hypothesis – for the control of multi-finger grasping by reconstructing the digit referent positions (*RC*s) and apparent stiffnesses ($k$). We found large $k$ and referent aperture when holding a free object compared to holding an object that is externally constrained; the larger digit stiffness is important when the digits are responsible for grip stability. The referent aperture was located closer to the virtual finger than the thumb, and it was not the centered within the actual aperture. More work is required to identify whether this

asymmetry has functional origins, or whether it is a characteristic of the structure of the grasp, with 4 fingers in opposition with one thumb. We also demonstrated the stabilization of critical task variables via synergistic covariation in the control variables *RC* and *k* as well as in the digit forces at two different levels of the control hierarchy. Furthermore, we demonstrated that the synergistic organization of the variables is sensitive to the presence/absence of external constraints on the object. These findings extend the ideas on grasp control with referent configurations by demonstrating that the digit apparent stiffness is modulated in addition to the digit referent coordinate for grip control, and by quantifying the synergistic organization of various control variables in the control hierarchy.

# Chapter 4. Rotational Equilibrium Control:
## *Hierarchical and Synergistic Organization of Control Variables for Magnitude and Direction of Multi-digit Moment Production*

## 4.1. Introduction

In the previous study (*Chapter 3*), we quantified the referent aperture ($R_a$), as a task-level control variable for grip force production, and the digit referent coordinate (*RC*) and the apparent stiffness (*k*) that related digit normal force production during static prehension. We found that the patterns of the specifying the digit *RC* and *k* varied depending on given mechanical constraints. Specifically, the width of $R_a$ and the digit *k* was relatively higher when the digit forces are responsible for static constraints (i.e., free object prehension) compare to an externally fixed object. We interpreted these results as a strategy to increment grip stability with the possible effect of maintaining rotational equilibrium (Ambike et al., 2014). According to the referent control hypothesis, movement is produced by changing referent position of the relevant effectors, and as a result of changes in these variables and the interaction of the effector with an external force field, measurable mechanical variables appear (Hasanbarani, Batalla, Feldman, & Levin, 2021). Latash and his colleagues (2010) proposed referent orientation (angle) as a threshold hand position to describe the net moment production that occurs to satisfy the rotational equilibrium of the object against the external torque (Figure 2.9). When the CNS specifies the referent orientation at the hand level, the net moment of force is generated due to the difference between the referent orientation and the actual

orientation of the grasped object. This process can simplify the control of moment of force production involving a set of redundant elements, similar to the process of the grip force control by specifying the referent aperture as a single united parameter at the task-specific level. Studies to estimate the control parameters determining the normal finger forces (i.e., *RC* and *k*) and to characterize their stability properties have been continuously conducted (Ambike et al., 2016; Cuadra, Gilmore, et al., 2020; Cuadra, Wojnicz, et al., 2020; de Freitas et al., 2018; Martin et al., 2011; Mattos et al., 2015; Reschechtko & Latash, 2017, 2018), but quantification of the referent orientation as well as the pairs of digit referent angle ($R_\theta$) and apparent rotational stiffness ($k_\theta$) have not yet been made. Therefore, in this study, we quantified these variables related to the digit moment production to control the rotation of the grasping objects.

The hierarchical organization scheme (i.e., the few-to-many mapping) for control with designating the pair of $R_\theta$ and $k_\theta$ involves the same redundancy problem as shown in the previous chapter (Figure 3.1B). In the previous chapter dealing with the *RC* and *k*, we found the typical trade-off synergies between the control layer that the significant synergies were present only in the upper hierarchy, not the lower hierarchy. However, different results may be confirmed in the current study since we are interested in hierarchical synergies of control variables for stabilizing digit moments, not digit forces. Earlier studies that addressed multi-finger synergy have reported that stabilization of rotational equilibrium action (i.e., stabilization of net moment) is a default control strategy (Latash, Scholz, Danion, & Schoner, 2001; Zhang, Zatsiorsky, & Latash, 2006) that emerges, even if not given as a salient task variable (Scholz, Danion, Latash, & Schoner, 2002). It has been also proposed that

in the case of static prehension, the CNS may be more concerned in the rotational equilibrium control than the grip stability control when a mechanical perturbation is given to the hand-held object (Shim, Park, Zatsiorsky, & Latash, 2006). Indeed, we previously found that the synergies in the $\{RC, k\}$ space within the lower level individual finger, especially lateral finger (i.e., index and little fingers), were relatively higher under the free object prehension in which rotational equilibrium was to be satisfied (Figure 3.7). Therefore, we expected that the synergies stabilizing the digit moment would appear in the upper hierarchy as well as the lower hierarchy. This is a plausible prediction because, unlike digit normal forces, moment stabilization can occur in both control hierarchies in the static multi-digit prehension (Park et al., 2015). Nevertheless, it has not yet been tested whether this hierarchical stabilization aspect is valid even at the level of the control variables.

It has been known that the translation and rotation stability are independently controlled by the CNS. This idea, the principle of superposition, was first proposed by Arimoto and Nguyen (2001) to control robotic hand motion, and it includes separating the motor task into two subtasks controlled by independent controllers. A series of studies have provided evidence supporting the principle of superposition, that is the mechanical outcomes, grip forces and moments, are decoupled in the human prehension (Shim et al., 2003, 2005a, 2005b; Zatsiorsky et al., 2004). In follow-up studies, this principle was preserved in circular objects (Shim & Park, 2007) and even when two-finger moments were created on a small fixed lever that was not a prehensile action (Song, Kim, et al., 2021). It naturally led to a current research problem that identifying the validity of the principle of superposition and extending it into the space of control variables even in the

externally fixed object prehension in which the digit force and moment are not mechanically constrained. We observed that the digit normal forces were independent to tangential forces in both free and fixed object condition in the previous chapter (Table 3.1). Further, the unbalanced net moment was naturally canceled by another moment component while the subject did not voluntarily intervene, and it partially supported the existence of a control variable for rotational equilibrium independent of the translational constraint.

We devised an experimental handle in which an external actuator could induce an angular displacement about the fixed axis of rotation of the handle. As if holding the doorknob and turning it, we employed an experimental task to produce digit moments on the externally fixed handle with different moment magnitudes in both direction (i.e., pronation and supination direction), which was a typical experimental protocol used in previous studies that explored the superposition principle in the human prehension. A set of hypotheses was formulated as follows. Firstly, we expected that the designation of the control variables $R_{\theta}$, and $k_{\theta}$ for multi-digit moment production would depend on the moment magnitudes and directions (H1). Second hypotheses were associated with synergic behavior for stabilization of digit moment. Hierarchical stabilization of digit moment by covariation of mechanical variables would exist at both upper and lower hierarchies, and it would be consistent with synergies in the space of $\{R_{\theta}, k_{\theta}\}$ (H2-1). Since the lateral fingers are more responsible for moment production than the medial finger (Zatsiorsky et al., 2003b), it was also expected that the $\{R_{\theta}, k_{\theta}\}$ synergies contributing to rotational stability would be higher within the lateral fingers than the medial fingers (H2-2). The third hypothesis was related to the decouple control strategy of objet translation

and rotation. Thumb and virtual finger normal forces would be decoupled from the moment components. Thus, the task-specific covariation of $R_\theta$ and $k_\theta$ would be independent of the grip force stabilization (H3).

## 4.2. Methods

### 4.2.1 Subjects

Twelve healthy male subjects, age 29.1 ± 3.75 (mean ± SD) years, mass 76 ± 6.39 kg, and height 1.75 ± 0.05 m, voluntarily participated in the current experiment. All participants were right-handed, which was confirmed by the Edinburgh handedness test (Oldfield, 1971). They had no history of neurological or musculoskeletal disorder that could affect the completion of the experimental tasks (by self-report). All experiments proceeded after all participants were asked to fill out an informed consent in accordance with the recommendations of the Seoul National University Institutional Review Board (IRB No. 2007/002-023).

### 4.2.2. Apparatus

We devised an experimental handle that can change the orientation (angle) of the handle with electrical actuators while grasping the handle. Five 6-component force transducers (Nano-17, ATI Industrial Automation, Garner, NC, USA) were attached to the handle to measure the individual digit forces. A detailed description of this handle is presented in Figure 4.1. The force transducers were aligned in the handle-fixed *x-z* plane. The distance between the centers of adjacent transducers

placed vertically corresponding to four fingers was 30 mm, and the transducer corresponding to the thumb (TH) was located in the center of the middle and ring finger transducers along the *x*-axis. The grip width, defined as the horizontal distance between the contact surfaces of the TH and fingers' transducers along the *z*-axis, was set to 50 mm (Figure 4.1B). 100-grit Sandpapers were attached to the contact surface of each transducer to increase the friction with digit tips. The static friction coefficient of digit tip-sandpaper was about 1.4-1.5 (Savescu et al., 2008).

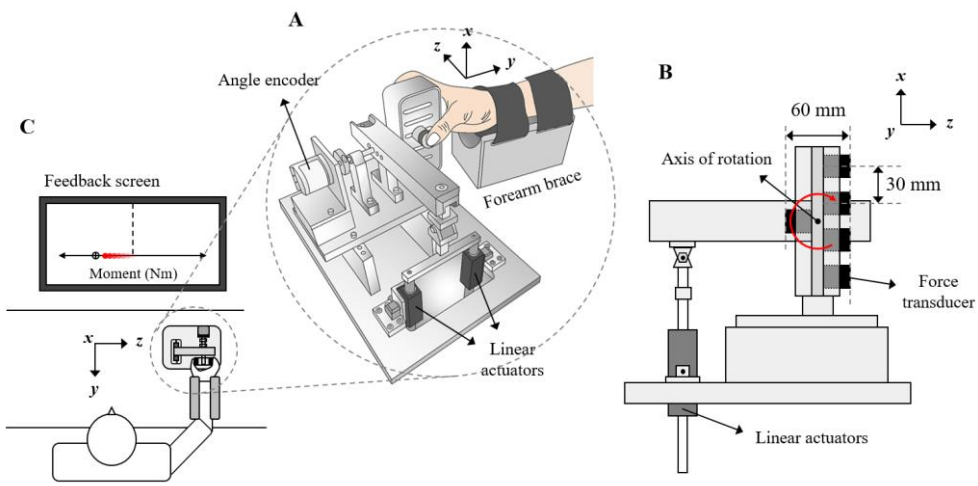

**Figure 4.1.** An illustration of the customized handle fame and experimental setup. (A) Experimental handle frame located on the table. Two linear DC-servo actuators were connected to the end of the lever arm, and the handle and lever were fixed by the same axis of rotation. Therefore, the forces from the actuators could change the orientation (angle) of the handle. An angle encoder was attached the behind of the rotation axis and recorded the angular displacement of the handle. (B) Five 6-component force transducers were aligned in the handle-fixed *x*-*z* plane to measure the individual digit forces. The distance between the transducers corresponding to the four fingers was 30 mm, and the width of the thumb to four fingers transducers was 50 mm. (C) Subjects positioned their right forearm on the rigid forearm brace on the table. Target total moment was presented as a horizontal line on the feedback screen. For pronation direction (counterclockwise direction) corresponding to positive moment on *y*-axis, the cursor moved to the left, and for supination direction (clockwise direction), the cursor moved to the right.

The rotation axis of the handle located at the point of intersection on the vertical midline of the grip width and on a horizontal line passing through the center of the TH transducer was securely fixed to the axis of the lever arm. Thus, rotation of the lever necessarily caused rotation of the handle. At one end of the lever, two linear DC-servo motors (LM 2070, Faulhaber SA, Germany) were connected in parallel to generate the angular displacement of the lever and the handle by driving the actuators (Figure 4.1A). Further, an angle transducer (absolute encoder AHS36A, SICK AG, Germany) was mounted on the shaft of the axis to measure the changes in the angle of the handle at a rate of 100 Hz. A 24-inch monitor, placed at 0.8 m in front of the participants, was used to provide visual feedback on produced digit moments on the handle (Figure 4.1C). All force signals were set to zero before each trial begin and sampled at a rate of 200 Hz and digitized with an analog-to-digital converter (Gen5, AMTI, Watertown, MA, USA). We used a customized LabVIEW program (National Instruments) for the force and angle data acquisition, control the

servo actuators, and provide real-time visual feedback.

### 4.2.3. Experimental Procedure

The subjects positioned their right forearm on the rigid brace in a natural grasping configuration (Figure 4.1C). A height-adjustable chair was used to keep the posture of the right upper extremity of each subject constant. The subjects were instructed to hold a vertically aligned handle with the center of each fingertip coincident with the center of each transducer. The main experimental task was to hold the handle with five digits and to produce prescribed target moment of force in isometric condition. The target moment was defined as the sum of the individual digit moments (i.e., total moment, $M^{TOT}$) required by the subject and consisted of three moment magnitudes in the two moment direction: 0.2, 0.4, and 0.6 Nm in the pronation direction (counterclockwise direction); -0.2, -0.4, and -0.6 Nm in the supination direction (clockwise direction). Therefore, each subject performed an experiment for a total of six moment conditions.

Each trial lasted 15 s. The subjects were given 3 s after the start of each trial to match the target moment as accurately as possible and maintain the value while watching the real-time visual feedback on the $M^{TOT}$. Note that the $M^{TOT}$ about the rotation axis of the handle was not measured but computed by Equation 4.1. The magnitude of the target moment and computed $M^{TOT}$ were displayed along the horizontal line (Figure 4.1C). The cursor ($M^{TOT}$) moved to the left when the subjects produce moments in the pronation direction and moved to the right for the supination direction. At a random time between 5 and 10 s after upon the trial onset, the two linear servo actuators were driven to tilt the handle by 5° and then return to its

original vertical orientation (0°) over 2 s (i.e., 5°/s). The direction in which the handle was tilted by the actuator was opposite to the generated digit moment. Thus, it led to an increase and decrease of the $M^{TOT}$ as a spring-like reaction. While the angle of the handle was changing, the "do not voluntarily intervene" paradigm was used. The subjects were requested “do not react to the tilting of the handle”, “do not adjust your commands to the hand” and to continue producing the target moment on the handle until the end of the trial (Feldman, 1966; Latash, 1994). The real-time visual feedback was removed at the onset of the actuator since the feedback while changing the angle of the handle might interfere with the instruction not to react voluntarily intervene.

The experiment was conducted over three days. On the first day, subjects had practice sessions to familiarize experimental setup and tasks. On the second and third days, the experiment was conducted by dividing three of the six moment conditions in random order. The subjects performed 20 trials in each moment condition, for a total of 150 trials (25 trials × 6 moment conditions) over two days. We gave the subjects a mandatory 45 s rest after each of the trial, and subjects were required to ask for additional rest if they felt fatigue. None of the subject reported any fatigue. The total duration of the experiment per day was ~ 60 min.

### 4.2.4. Data Analysis

Customized code written in MATLAB (MathWorks Inc., Natick, MA) was used for data analysis. The force and angular displacement data were digitally low-pass filtered with a fourth-order, zero-lag Butterworth filter with a cutoff of 10 Hz. The analysis in this study was limited to the grasping plane defined as the handle-

fixed *x*-*z* plane (Figure 4.1B) (Zatsiorsky et al., 2002a). In this plane, the normal forces ($F^N$) to the contact surface of the transducer corresponded to the *z*-axis, and the *x*-axis corresponded to the tangential forces ($F^T$).

The time-series digit $F^N$ and $F^T$ were used to compute the $M^{TOT}$ about the fixed axis of rotation as follows.

$$M^{TOT} = \sum_i \left(F_i^N \cdot d_i + F_i^T \cdot r_i\right), \qquad i = \{TH, I, M, R, L\} \qquad (4.1)$$

where the subscripts *TH*, *I*, *M*, *R*, *L* stand for the thumb, index, middle, ring, and little finger, respectively; the superscripts *N* and *T* refer to the digit normal and tangential forces, respectively; the coefficients *d* and *r* stand for the moment arms of the normal and tangential forces, respectively. We computed the positions of the digit force application points along with the *x*-axis respect to the center of transducers by dividing the moments on *y*-axis of the transducer by the corresponding normal forces. The *d* of each digit normal force was determined as the coordinate of the force application point of each transducer with respect to the axis of rotation (Figure 4.1B) along the *x*-axis. The moment arms of the $F^T$ (*r*) along the *z*-axis were the same for all the digits as half of the grip width (i.e., -25 mm for the TH and 25 mm for the fingers).

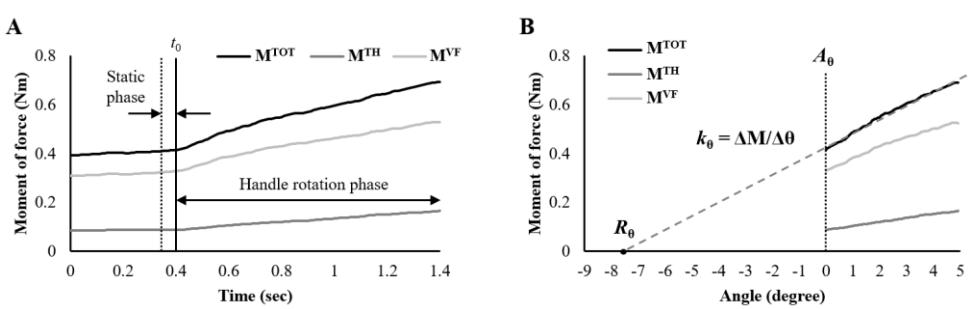

**Figure 4.2.** (A) An example of time-series digit moments for the thumb ($M^{TH}$), virtual finger ($M^{VF}$), and total moment ($M^{TOT}$). The representative trial data are acquired under the 0.4 Nm target moment condition. The vertical solid line indicates the time of the onset of the actuator ($t_0$). From the dashed vertical line to $t_0$ corresponds to the static phase. The section in which the moments increase after $t_0$ corresponds to the handle rotation phase. (B) Representative angular displacement versus digit moment data in handle rotation phase. The net change in the digit moment ($\Delta M$) and angular displacement ($\Delta\theta$) were determined by subtracting the initial steady-state value from its final value. The $k_\theta$ is defined as the ratio of $\Delta M$ to $\Delta\theta$ according to Hooke's law. The $R_\theta$ is the threshold angle the digit is trying to reach and corresponds to the intercept of the slope $k_\theta$.

We subsequently obtained the time-series moment of each digit for each trial, including virtual finger (VF). The moment data were aligned with respect to $t_0$, the point at which the actuator was operated (Figure 4.2A). Two analysis phases were defined as follows: static phase for 50 ms before the point of $t_0$ and handle rotation phase until the peak angular displacement (5°) were observed. All dependent variables were analyzed involving two levels of the control hierarchy; in the following sections, we used the term "Upper-level" to refer to the hierarchically higher level created between the TH and VF, and "Lower-level" to indicate the hierarchy produced by each finger individually (i.e., I, M, R, and L). Since the rotation axis where the digit moment is formed is located at the center of the four fingers (i.e., between M and R fingers), antagonist moments corresponding to the direction opposite to the desired net moment inevitably occur (Zatsiorsky & Latash, 2008). In generating a moment in the pronation direction, the I and M fingers serve as moment agonist fingers, while the R and L act as moment antagonist fingers. In the supination direction, the R and L fingers are defined as moment agonists and the I and M fingers are defined as moment antagonists.

#### *4.2.4.1. Reconstruction of $R_\theta$ and $k_\theta$ at Two Hierarchical Levels*

The set of data for the moment of each digit and angular displacement of the handle were used to compute the control variables, referent angle ($R_\theta$) and apparent rotational stiffness ($k_\theta$). We formulated the equation 4.2 in which the two control variables determine the moment (M) of the effector as follows.

$$M^i = k_\theta^i \times \left(A_\theta^i - R_\theta^i\right), \qquad (4.2)$$

where $i$ stands for individual digit; $A_\theta$ refers the actual angle of the handle (Figure 4.2B); Since the above formula was based on the linear approximation, we first verified whether each digit moment changes linearly with changing angular displacement. For this purpose, several linear regressions were performed separately on each digit using changes in digit moment and angular displacement in a handle rotation phase. We only included the trials in which the absolute $R$-values of the involved digits are above 0.9 for further analyses (Reschechtko & Latash, 2017). This process yielded between 17 and 23 trials for all moment condition, with average of 20.3 trials across subjects.

The net change in the moment of force (ΔM) and angular displacement (Δθ) while tilting the handle (i.e., the period in which the digit moments increase) were calculated. The ΔM and Δθ were computed by subtracting the initial value from its final value; the initial values were obtained from the average moment and angle in the static phase, and the final values were obtained as the average values over the final 10 ms of the handle rotation phase. Note that the ΔM was varied for the individual digit, but the Δθ was identical. The $k_\theta$ and $R_\theta$ were then calculated using

equation 4.3 and 4.4, respectively.

$$k_\theta^i = \frac{\Delta M^i}{\Delta \theta^i}, \qquad (4.3)$$

$$R_\theta^i = \frac{M_{static}^i}{k_\theta^i}, \qquad (4.4)$$

where the $M_{static}$ is the average digit moment in static phase. Thus, the calculated $R_\theta$ represented the threshold angle where the digit moment was stationary prior to the handle was rotated. The unit of the $k_\theta$ was Nm/degree, and the $R_\theta$ was yielded in the dimension of degrees. We consequently obtained pairs of $\{R_\theta, k_\theta\}$ for all digits and moment conditions.

#### *4.2.4.2. Permutation Analysis of $R_\theta$ and $k_\theta$*

One of purpose of current study was to identify the task-specific covariation of control variables for stabilization of digit moment in two hierarchies. Because typical clouds of data points in $\{R_\theta, k_\theta\}$ space appeared in nonlinear hyperbolic shapes, we used random permutation analysis (Muller & Sternad, 2003) to quantify synergistic covariation of the $R_\theta$ and $k_\theta$. The permutation analysis is the technique that creates a set of random surrogate data, which is expected to remove the effect of task-specific covariation among the involved variables. After permutation, indices of performance variability ($R_{SD}$) across trials are compared between the actual and surrogate data sets to determine whether or not the covariation of actual data contributed to reduce performance variability. If the $R_{SD}$ is greater than 1, theoretically, it means that the two parameters purposefully co-vary to stabilize the outcome performance variable (i.e., digit moment in the current analysis). However,

we conservatively set a critical value to 2, indicating the presence of the synergy within the space of the control variable.

The permutation analysis was conducted at each hierarchy and digit, separately for each moment condition. For the upper hierarchy, the $M^{TOT}$ can be expressed as the sum of the moment of the TH and VF. For the lower hierarchy, the moment of VF ($M^{VF}$) arises from the individual finger moment (Equation 4.5).

$$M^{TOT} = R_\theta^{TH} \times k_\theta^{TH} + R_\theta^{VF} \times k_\theta^{VF},$$

$$M^{VF} = \sum_i RC_\theta^i \times k_\theta^i, \qquad (4.5)$$

Thus, the synergy for the upper hierarchy was quantified in the 4-dimensional $\{R_\theta, k_\theta\}$ space, and the lower hierarchy was in the 8-dimensional space. In addition, to investigate the functional roles of the lateral and medial fingers, we quantified the synergies stabilizing lateral and medial finger moments, respectively, in four-dimensional space (lateral finger: $\{R_\theta^I, k_\theta^I, R_\theta^L, k_\theta^L\}$; medial finger: $\{R_\theta^M, k_\theta^M, R_\theta^R, k_\theta^R\}$). Finally, synergies in the space of 2-dimensional $\{R_\theta, k_\theta\}$ space within individual digits were also quantified.

#### *4.2.4.3. UCM-based Analysis of Variance on Digit Moment and Normal Forces*

The UCM approach was employed to analyze the hierarchical organization of mechanical variables stabilizing grip force and moment (Scholz & Schoner, 1999). Thus, it was performed separately with set to digit normal forces and total moment as performance variables (PVs). For the upper hierarchy, total normal force ($F^N_{TOT}$) and $M^{TOT}$ were PV, and for the lower hierarchy, virtual finger's normal force ($F^N_{VF}$)

and moment ($M^{VF}$) were set to PV. The UCM analysis is to partition the inter-trial variance in space of redundant elemental variables (EV) into two components. One functions to keep the task-level PV, and it has been referred to as UCM. Whereas the other component orthogonal to UCM leads to a change in the value of the PV across trials (ORT). The changes in the PV can be written as a function of the changes in EV, ΔEV as follows.

$$\Delta PV = J \cdot \Delta EV^T, \qquad (4.6)$$

where *J* is the Jacobian that links infinitesimal changes in EV with changes in the PV, the superscript *T* refers a sign of transpose. In the moment-related analysis, EV was the moment of the TH and VF ($M^{TH}$ and $M^{VF}$) in the upper hierarchy, and the moment of four fingers ($M^I$, $M^M$, $M^R$, and $M^L$) in the lower hierarchy. Similarly, $F^N$ of the corresponding digit was set as EV for normal force-related analysis ($F^N_{TH}$ and $F^N_{VF}$ in upper hierarchy; $F^N_I$, $F^N_M$, $F^N_R$, and $F^N_L$ in lower hierarchy). The UCM space was estimated as the null space of the Jacobian matrix that was set to [1, 1] and [1, -1] for the moment- and force-related analysis in the upper hierarchy, respectively. The positive or negative sign in Jacobian matrix is determined by the typical co-variation pattern of the corresponding elemental variables. The Jacobian was configured as [1, 1, 1, 1] in both moment- and force-related analysis for the lower hierarchy.

The two component of variances within two separated UCM and ORT manifold ($V_{UCM}$ and $V_{ORT}$, respectively) were computed across trials for each subject and moment conditions. The synergy index (ΔV) was calculated as the difference between $V_{UCM}$ and $V_{ORT}$, which was normalized by the total variance ($V_{TOT}$) as follows.

$$\Delta V = \frac{V_{UCM}/DOF_{UCM} - V_{ORT}/DOF_{ORT}}{V_{TOT}/DOF_{TOT}}, \qquad (4.7)$$

where $V_{UCM}$, $V_{ORT}$, and $V_{TOT}$ are further normalized by the degrees of freedom (DOF) of their respective subspaces, allowing comparison of the indices across two subspaces that were observed in different dimensions. Subsequently, ΔVs were log-transformed using the Fischer transformation applied for the computational boundaries such that -2 to 2 for upper-level analyses, -4 to 1.33 for the lower-level analyses.

### 4.2.5. Statistics

A standard description of parametric statistics was used, and data are presented as means and standard errors (SE). Repeated-measures (RM) ANOVAs with the factors of *Direction* (two levels: pronation and supination), *Magnitude* (three levels: ±0.2, ±0.4, and ±0.6 Nm), *hierarchy* (two levels: upper and lower hierarchies), and *Digit* (two levels in the upper hierarchy: TH and VF; four levels in the lower hierarchy: I, M, R, and L) were performed to investigate the differences of dependent variables between experimental conditions and digits at different hierarchical levels. The factors were selected for particular comparisons to test the hypotheses. Note that since the digit moments and the $R_\theta$ were opposite signs depending on the moment direction, absolute values were used when testing the differences according to moment direction. All $R_{SD}$, the synergy index in the space of control variables, were compared with the critical value of 2 using single-sample *t*-test, separately for each hierarchy and digit. Similarly, $\Delta V_Z$ values determined from the UCM analysis were compared with the relevant critical values using single-

sample *t*-tests. The critical value of $\Delta V_Z$ was set to 0 for the upper hierarchy, and 0.55 for the lower hierarchy. Further, linear regression was performed to identify the patterns of the significant changes in dependent variables according to increasing magnitude of moment, separately for each direction. Pearson coefficients of correlation were computed to characterize the relation of variables. This analysis was used to investigate the relationship between the normal force ($F^N$), their moment arm ($d^N$), and moment of normal force ($M^N$) at the virtual finger level in relation to decouple strategy of grip force and moment production (principle of superposition). In addition, correlation analyses were also performed on the $R_{SD}$ with the two $\Delta V_Z$ (i.e., moment and normal force stabilization) separately to confirm the relationship of the synergistic effect between the $\{R_\theta, k_\theta\}$ and the mechanical variables spaces.

Mauchly's sphericity test was used to confirm the assumptions of sphericity, and their violations were corrected by the Greenhouse-Geisser estimation. All pairwise comparisons with Bonferroni corrections were performed to explore significant interaction effects. The effect size was quantified using partial eta-squared ($\eta p^2$) for the ANOVAs and Cohen's *d* for the *t*-tests. We conducted all statistical analyses using SPSS 24.0 (IBM, Armonk, NY), and the level of significance was set at $p<.05$.

## 4.3. Results

### 4.3.1. Values of Digit Moment and Control Variables According to the Magnitudes and Directions of Moment

The total moment ($M^{TOT}$) changed systematically with the magnitude of

moment condition, and this finding was expected since the target moment was given as the magnitude of the $M^{TOT}$. The absolute magnitude of virtual finger moment ($|M^{VF}|$) was always larger than the thumb ($|M^{TH}|$) in the all moment conditions, and the $M^{TH}$ and $M^{VF}$ were significantly increased with increasing moment condition (Figure 4.3). These results were supported by two-way RM ANOVA with factors *Digit* and *Magnitude* performed separately on each direction. It showed the significant main effects of *Digit* (pronation: $F_{[1,11]}$=386.18, $p$<0.001, $\eta p^2$=0.97; supination: $F_{[1,11]}$=234.6, $p$<0.001, $\eta p^2$=0.96) and *Magnitude* (pronation: $F_{[2,22]}$=133013.29, $p$<0.001, $\eta p^2$=0.99; supination: $F_{[2,22]}$=150199.45, $p$<0.001, $\eta p^2$=0.99) and factor interactions (pronation: $F_{[2,22]}$=420.57, $p$<0.001, $\eta p^2$=0.97; supination: $F_{[2,22]}$=265.09, $p$<0.001, $\eta p^2$=0.96). Further, the magnitudes of $|M^{TH}|$ were larger in supination than pronation, whereas opposite patterns were observed for $|M^{VF}|$ (Figure 4.3). These results were supported by *Direction* × *Magnitude* RM ANOVA performed separately on each digit, which showed the significant main effects of *Direction* (TH: $F_{[1,11]}$=123.791, $p$<0.001, $\eta p^2$=0.92; VF: $F_{[1,11]}$=140.74, $p$<0.001, $\eta p^2$=0.93) and *Magnitude* (TH: $F_{[2,22]}$=647.31, $p$<0.001, $\eta p^2$=0.98; VF: $F_{[2,22]}$=7013.49, $p$<0.001, $\eta p^2$=0.99) and significant factor interactions (TH: $F_{[2,22]}$=26.19, $p$<0.001, $\eta p^2$=0.70; VF: $F_{[2,22]}$=28.07, $p$<0.001, $\eta p^2$=0.72).

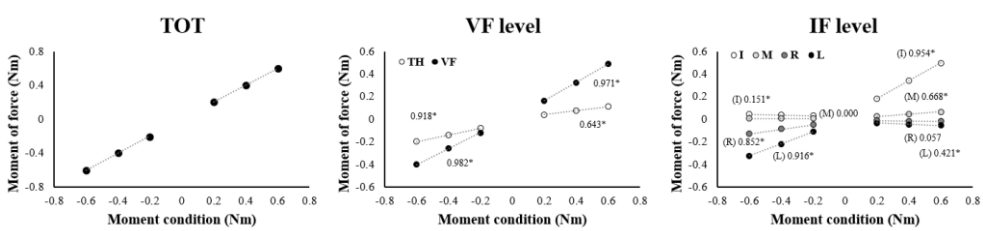

**Figure 4.3.** Average magnitudes of digit moment under different moment conditions are presented with standard error bars. The total digit moment and moment of TH and VF are presented in left and middle panel, respectively. The right panel corresponds to the moment of individual fingers (I, M, R, and L). Regression lines are shown with the coefficients of determination ($R^2$). The asterisks (*) are presented for significant $R^2$.

For the individual finger level (IF level), the absolute magnitudes of individual finger moments were different each other in all moment condition. Specifically, $|M^I| > |M^M| > |M^L| > |M^R|$ in the pronation direction, and $|M^L| > |M^R| > |M^I| > |M^M|$ in the supination direction. Individual finger moments were systematically changed with changing moment condition, except for medial antagonist finger. That is, the $M^R$ and $M^M$ did not significantly change in the pronation and supination direction, respectively. These findings were supported *Digit* × *Magnitude* RM ANOVA, which showed the significant main effects of *Digit* (pronation: $F_{[1.52,16.73]}$=1259.62, $p$<0.001, $\eta p^2$=0.99; supination: $F_{[1.41,15.48]}$=534.4, $p$<0.001, $\eta p^2$=0.98) and *Magnitude* (pronation: $F_{[2,22]}$=2872.48, $p$<0.001, $\eta p^2$=0.99; supination: $F_{[2,22]}$=3077.67, $p$<0.001, $\eta p^2$=0.99) and factor interactions (pronation: $F_{[2.15,23.66]}$=954.22, $p$<0.001, $\eta p^2$=0.99; supination: $F_{[1.5,16.54]}$=252.52, $p$<0.001, $\eta p^2$=0.96). The $|M^I|$ and $|M^M|$ were significantly larger in the pronation direction than the supination, while the $|M^L|$ and $|M^R|$ were significantly larger in the supination than the pronation direction. There were significant main effects of *Direction* (I: $F_{[1,11]}$=1499.03, $p$<0.001, $\eta p^2$=0.99; M: $F_{[1,11]}$=109.25, $p$<0.001, $\eta p^2$=0.91; R: $F_{[1,11]}$=347.63, $p$<0.001, $\eta p^2$=0.97; L: $F_{[1,11]}$=678.12, $p$<0.001, $\eta p^2$=0.98) and *Magnitude* (I: $F_{[2,22]}$=1994.98, $p$<0.001, $\eta p^2$=0.99; M: $F_{[1.23,13.57]}$=55.35, $p$<0.001, $\eta p^2$=0.83; R: $F_{[1.34,14.72]}$=231.66, $p$<0.001, $\eta p^2$=0.96; L: $F_{[2,22]}$=521.91, $p$<0.001,

$\eta p^2$=0.98) and significant factor interactions (I: $F_{[2,22]}$=1099.75, $p$<0.001, $\eta p^2$=0.99; M: $F_{[1.44,15.85]}$=115.43, $p$<0.001, $\eta p^2$=0.91; R: $F_{[1.09,11.96]}$=156.19, $p$<0.001, $\eta p^2$=0.93; L: $F_{[2,22]}$=405.97, $p$<0.001, $\eta p^2$=0.97) on *Direction* × *Magnitude* RM ANOVAs.

The linear regression performed separately on each digit and moment direction revealed that all digit moment, including VF and IF level, linearly changed with moment condition ($p$<0.05), except for the $M^R$ in the pronation and the $M^M$ in the supination direction (i.e., medial finger in role of the moment antagonist) (Figure 4.3).

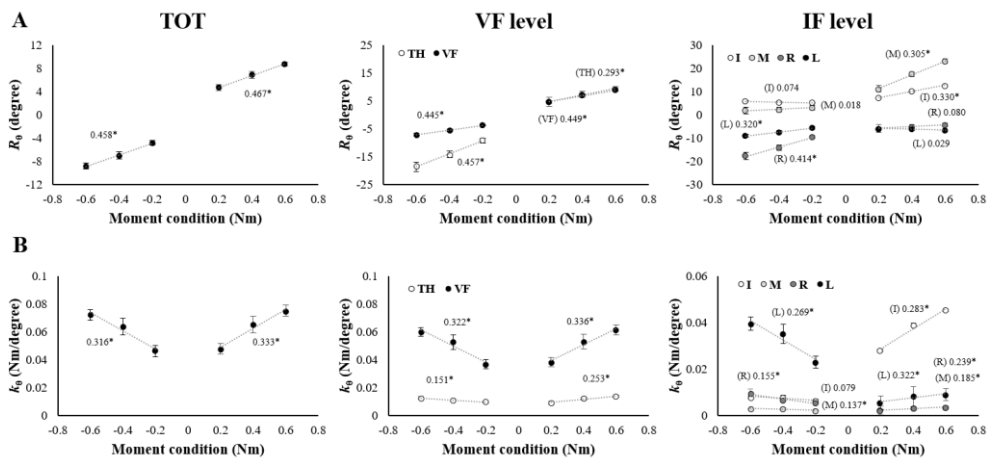


**Figure 4.4.** Average magnitudes of (A) $R_\theta$ and (B) $k_\theta$ under different moment conditions are presented with standard error bars. The left panel corresponds to the total level (TOT), and the middle panel corresponds to the VF level, including TH and VF. The right panel shows the IF level corresponding to individual fingers (I, M, R, and L). Regression lines are shown with the coefficients of determination ($R^2$). The asterisks (*) are presented for significant $R^2$.

The absolute magnitude of the total $R_\theta$ and $k_\theta$ ($|R_\theta^{TOT}|$ and $k_\theta^{TOT}$) were significantly different according to magnitudes of moment conditions, but

directional differences were not found (Figure 4.4A and B). These results were supported by *Direction* × *Magnitude* RM ANOVA performed separately on each $R_\theta$ and $k_\theta$, which showed the significant main effects of *Magnitude* ($R_\theta$: $F_{[2,22]}$=110.3, $p$<0.001, $\eta p^2$=0.91; $k_\theta$: $F_{[2,22]}$=78.44, $p$<0.001, $\eta p^2$=0.88) without factor interaction.

For the VF level, the $R_\theta^{TH}$ was significantly smaller than the $R_\theta^{VF}$ in the supination direction, whereas $R_\theta$ of TH and VF were not different each other in the pronation direction (Figure 4.4A). Further, the $|R_\theta^{TH}|$ in the supination was larger than in the pronation, and opposite pattern was observed for the $|R_\theta^{VF}|$. These findings were supported by *Digit* × *Magnitude* RM ANOVA, which showed the significant main effects of *Digit* (supination: $F_{[1,11]}$=92.15, $p$<0.001, $\eta p^2$=0.89) and *Magnitude* (pronation: $F_{[2,22]}$=66.76, $p$<0.001, $\eta p^2$=0.86; supination: $F_{[1.3,14.3]}$=45.96, $p$<0.001, $\eta p^2$=0.81) and factor interactions (supination: $F_{[1.12,12.37]}$=15.1, $p$=0.002, $\eta p^2$=0.58). The *Direction* × *Magnitude* RM ANOVA on the $R_\theta^{TH}$ and $R_\theta^{VF}$ resulted in the significant main effects of *Direction* (TH: $F_{[1,11]}$=138.1, $p$<0.001, $\eta p^2$=0.93; VF: $F_{[1,11]}$=47.95, $p$<0.001, $\eta p^2$=0.81) and *Magnitude* (TH: $F_{[2,22]}$=56.97, $p$<0.001, $\eta p^2$=0.84; VF: $F_{[2,22]}$=96.15, $p$<0.001, $\eta p^2$=0.9) and significant factor interactions (TH: $F_{[1.17,12.86]}$=6.63, $p$=0.02, $\eta p^2$=0.38). The $k_\theta$ of VF ($k_\theta^{VF}$) was significantly higher than the $k_\theta$ of TH ($k_\theta^{TH}$) in all moment magnitudes and directions. Note that unlike the $R_\theta^{TH}$ and $R_\theta^{VF}$, there was no directional difference of moment production in the both $k_\theta^{TH}$ and $k_\theta^{VF}$ (Figure 4.4B). These findings were supported by RM ANOVA with factors *Digit* and *Magnitude*, which showed the significant main effects of *Digit* (pronation: $F_{[1,11]}$=169.98, $p$<0.001, $\eta p^2$=0.94; supination: $F_{[1,11]}$=132.94, $p$<0.001, $\eta p^2$=0.92) and *Magnitude* (pronation: $F_{[2,22]}$=61.35, $p$<0.001, $\eta p^2$=0.85; supination: $F_{[2,22]}$=40.02, $p$<0.001, $\eta p^2$=0.78) and factor interactions (pronation: $F_{[2,22]}$=41.51,

$p$<0.001, $\eta p^2$=0.79; supination: $F_{[2,22]}$=44.56, $p$<0.001, $\eta p^2$=0.8). The *Direction* × *Magnitude* RM ANOVA on the $k_\theta^{TH}$ and $k_\theta^{VF}$ showed that there was only present the main effect of *Magnitude*, no *Direction* (TH: $F_{[1.35,14.83]}$=21.6, $p$<0.001, $\eta p^2$=0.66; VF: $F_{[2,22]}$=82, $p$<0.001, $\eta p^2$=0.88).

For the IF level, the differences in the magnitude of the $R_\theta$ for individual fingers depended on the role of the moment agonist and antagonist (Figure 4.4A). The $R_\theta^I$ and $R_\theta^M$ were significantly different in pronation direction, whereas they were not significantly different in supination direction. Similarly, the $R_\theta^R$ and $R_\theta^L$ were significantly different each other in supination direction, but not in the pronation direction. Further, only moment agonist finger (i.e., $R_\theta^I$ and $R_\theta^M$ for the pronation direction, and $R_\theta^R$ and $R_\theta^L$ for the supination direction) significantly increased with increasing magnitudes of moment. These results were supported by the significant main effects of *Digit* (pronation: $F_{[1.54,16.92]}$=132.22, $p$<0.001, $\eta p^2$=0.68; supination: $F_{[1.29,14.15]}$=130.51, $p$<0.001, $\eta p^2$=0.92) and *Magnitude* (pronation: $F_{[2,22]}$=23.48, $p$<0.001, $\eta p^2$=0.68; supination: $F_{[2,22]}$=27.94, $p$<0.001, $\eta p^2$=0.72) and factor interactions (pronation: $F_{[2.43,26.77]}$=10.66, $p$<0.001, $\eta p^2$=0.49; supination: $F_{[2.03,22.34]}$=13.02, $p$<0.001, $\eta p^2$=0.54). The $|R_\theta^I|$ and $|R_\theta^M|$ were significantly lager in pronation direction than supination, and $|R_\theta^R|$ was larger in supination than pronation direction. In the case of $R_\theta^L$, the directional difference was present only in the 0.6 and -0.6 Nm. These results supported by the significant main effects of *Direction* (I: $F_{[1,11]}$=25.01, $p$<0.001, $\eta p^2$=0.69; M: $F_{[1,11]}$=42.3, $p$<0.001, $\eta p^2$=0.79; R: $F_{[1,11]}$=136.62, $p$<0.001, $\eta p^2$=0.93) and *Magnitude* (I: $F_{[1.28,14.08]}$=30.63, $p$<0.001, $\eta p^2$=0.74; M: $F_{[222]}$=8.272, $p$=0.002, $\eta p^2$=0.43; R: $F_{[2,22]}$=14.77, $p$<0.001, $\eta p^2$=0.57; L: $F_{[2,22]}$=25.55, $p$<0.001, $\eta p^2$=0.7) and significant factor interactions (I:

$F_{[1.18,13.02]}$=19.73, $p$<0.001, $\eta p^2$=0.64; M: $F_{[2,22]}$=17.65, $p$<0.001, $\eta p^2$=0.62; R: $F_{[2,22]}$=28.1, $p$<0.001, $\eta p^2$=0.72; L: $F_{[2,22]}$=7.89, $p$=0.003, $\eta p^2$=0.42) on *Direction* × *Magnitude* RM ANOVAs. The $k_\theta^I$ and $k_\theta^L$ were significantly larger than the $k_\theta^M$ and $k_\theta^R$ in the pronation moment conditions. In the supination moment condition, the magnitudes of the individual finger $k_\theta$ were $k_\theta^L > k_\theta^I$ and $k_\theta^R > k_\theta^M$ (Figure 4.4B). All the finger $k_\theta$ were significantly increased with increasing magnitude of the moment, while the $k_\theta^I$ did not change in the supination moments. Further, the $k_\theta^I$ and $k_\theta^M$ in the pronation moments were significantly larger than those of supination, while the $k_\theta^R$ and $k_\theta^L$ in the supination moments were larger than pronation. These results were supported by the significant main effects of *Digit* (pronation: $F_{[1.03,11.35]}$=117.34, $p$<0.001, $\eta p^2$=0.91; supination: $F_{[1.14,12.58]}$=73.24, $p$<0.001, $\eta p^2$=0.87) and *Magnitude* (pronation: $F_{[2,22]}$=55.24, $p$<0.001, $\eta p^2$=0.83; supination: $F_{[2,22]}$=45.16, $p$<0.001, $\eta p^2$=0.8) and factor interactions (pronation: $F_{[1.9,20.88]}$=36.88, $p$<0.001, $\eta p^2$=0.77; supination: $F_{[2.31,25.31]}$=24.77, $p$<0.001, $\eta p^2$=0.69). The *Direction* × *Magnitude* RM ANOVA performed separately for individual finger showed that there were main effects of *Direction* (I: $F_{[1,11]}$=118.95, $p$<0.001, $\eta p^2$=0.91; M: $F_{[1,11]}$=8.13, $p$=0.016, $\eta p^2$=0.43; R: $F_{[1,11]}$=18.4, $p$=0.001, $\eta p^2$=0.63; L: $F_{[1,11]}$=67.87, $p$<0.001, $\eta p^2$=0.86) and *Magnitude* (I: $F_{[2,22]}$=49.47, $p$<0.001, $\eta p^2$=0.82; M: $F_{[2,22]}$=20.97, $p$<0.001, $\eta p^2$=0.66; R: $F_{[1.13,12.44]}$=10.87, $p$=0.005, $\eta p^2$=0.5; L: $F_{[2,22]}$=50.7, $p$<0.001, $\eta p^2$=0.82) and factor interactions (I: $F_{[2,22]}$=35.68, $p$<0.001, $\eta p^2$=0.76; L: $F_{[2,22]}$=30.69, $p$<0.001, $\eta p^2$=0.74).

The linear regression performed separately on each digit and moment direction confirmed that changes of the $R_\theta^{TOT}$ and $k_\theta^{TOT}$, as well as the $R_\theta$ and $k_\theta$ for the TH and VF, according to magnitudes of the moment were well described by a

linear model ($p$<0.05) (Figure 4.4A and B). For the IF level, the moment agonist finger $R_\theta$ (i.e., $R_\theta^I$ and $R_\theta^M$ in the pronation, and $R_\theta^R$ and $R_\theta^L$ in the supination) were linearly changed with moment conditions ($p$<0.05). For the $k_\theta$, all fingers $k_\theta$ were the best fit by the linear equations except for the $k_\theta^I$ of supination direction ($p$<0.05).

### 4.3.2. Synergies and Hierarchical Organization in the Space of {$R_\theta$, $k_\theta$} and Mechanical Variables

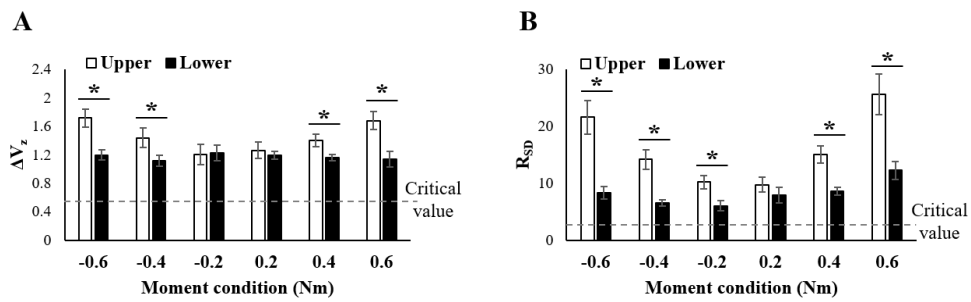


**Figure 4.5.** Across-subject mean and standard errors of (A) moment stabilizing $\Delta V_Z$ and (B) $R_{SD}$ under the different moment conditions. The solid bars and the open bars indicate the upper and lower hierarchy, respectively. The dashed line represents the critical values implying a significant synergic effect. For the $\Delta V_Z$, the critical values are 0 for the upper hierarchy and ≈ 0.55 for the lower hierarchy. The critical value of $R_{SD}$ is set to 0 in both hierarchies. The asterisks (*) indicate significant differences between hierarchies.

The synergy indices ($\Delta V_Z$) stabilizing digit moment were significantly larger in the upper hierarchy than lower hierarchy for 0.4, 0.6, -0.4, and -0.6 Nm conditions (Figure 4.5A). the $\Delta V_Z$ for upper hierarchy significantly increased with moment magnitudes, whereas the lower hierarchy $\Delta V_Z$ did not changed. These findings were supported by RM ANOVA with factors *Hierarchy* and *Magnitude*, which showed the significant main effects of *Hierarchy* (pronation: $F_{[1,11]}$=11.66,

$p$=0.006, $\eta p^2$=0.52; supination: $F_{[1,11]}$=5.06, $p$=0.046, $\eta p^2$=0.31) without factor interactions. The *Direction* × *Magnitude* RM ANOVA performed separately on each hierarchy resulted in that the main effect of *Direction* existed only in the upper hierarchy ($F_{[2,22]}$=7.43, $p$=0.003, $\eta p^2$=0.4). The single-sample $t$-test with critical $\Delta V_Z$ values revealed that the purposeful covariation across trials to stabilize digit moment was present both upper (0.2 Nm: $t_{[12]}$=10.85, $p$<0.001, Cohen's $d$=3.13; 0.4 Nm: $t_{[12]}$=15.95, $p$<0.001, Cohen's $d$=4.6; 0.6 Nm: $t_{[12]}$=13.05, $p$<0.001, Cohen's $d$=3.77; -0.2 Nm: $t_{[12]}$=8.35, $p$<0.001, Cohen's $d$=2.41; -0.4 Nm: $t_{[12]}$=10.35, $p$<0.001, Cohen's $d$=2.98; -0.6 Nm: $t_{[12]}$=13.84, $p$<0.001, Cohen's $d$=3.99) and lower hierarchies (0.2 Nm: $t_{[12]}$=12.39, $p$<0.001, Cohen's $d$=3.58; 0.4 Nm: $t_{[12]}$=14.38, $p$<0.001, Cohen's $d$=4.15; 0.6 Nm: $t_{[12]}$=5.43, $p$<0.001, Cohen's $d$=1.57; -0.2 Nm: $t_{[12]}$=7.28, $p$<0.001, Cohen's $d$=2.1; -0.4 Nm: $t_{[12]}$=7.28, $p$<0.001, Cohen's $d$=2.1; -0.6 Nm: $t_{[12]}$=9.27, $p$<0.001, Cohen's $d$=2.68) under the all moment conditions.

The upper and lower hierarchy $R_{SD}$ determined from the 4- and 8-dimensional $\{R_\theta, k_\theta\}$ space, respectively, showed a similar hierarchical difference to the $\Delta V_Z$. The $R_{SD}$ in the upper hierarchy was significantly higher than that in the lower hierarchy, except for the 0.2 Nm. Significant changes in $R_{SD}$ according to the magnitude of moment were present in both hierarchies. Further, $R_{SD}$ in the lower hierarchy was significantly larger in the pronation moment than the supination moment (Figure 4.5B). These findings were supported by RM ANOVA with factors *Hierarchy* and *Magnitude*, which showed the significant main effects of *Hierarchy* (pronation: $F_{[1,11]}$=48.51, $p$<0.001, $\eta p^2$=0.82; supination: $F_{[1,11]}$=67.83, $p$<0.001, $\eta p^2$=0.86) and *Magnitude* (pronation: $F_{[2,22]}$=12.71, $p$<0.001, $\eta p^2$=0.54; supination: $F_{[2,22]}$=6.85, $p$=0.005, $\eta p^2$=0.38) with factor interactions (pronation: $F_{[1.23,13.55]}$=8.74,

$p$=0.008, $\eta p^2$=0.44; supination: $F_{[2,22]}$=5.89, $p$=0.009, $\eta p^2$=0.35). The *Direction* × *Magnitude* RM ANOVA performed separately on each hierarchy resulted in the significant main effect of *Direction* (lower: $F_{[1,11]}$=7.42, $p$=0.02, $\eta p^2$=0.41) and *Magnitude* (upper: $F_{[2,22]}$=21.92, $p$<0.001, $\eta p^2$=0.67; lower: $F_{[2,22]}$=7.29, $p$=0.004, $\eta p^2$=0.4). Strong $\{R_\theta, k_\theta\}$ synergies stabilizing moment of each hierarchy were present in all moment conditions. The single-sample $t$-tests confirmed these results, the all $R_{SD}$ significantly exceeded the critical value in the upper (0.2 Nm: $t_{[12]}$=5.74, $p$<0.001, Cohen's $d$=1.66; 0.4 Nm: $t_{[12]}$=8.58, $p$<0.001, Cohen's $d$=2.48; 0.6 Nm: $t_{[12]}$=6.69, $p$<0.001, Cohen's $d$=1.93; -0.2 Nm: $t_{[12]}$=6.82, $p$<0.001, Cohen's $d$=1.97; -0.4 Nm: $t_{[12]}$=6.91, $p$<0.001, Cohen's $d$=1.99; -0.6 Nm: $t_{[12]=}$6.58, $p$<0.001, Cohen's $d$=1.9) and lower hierarchies (0.2 Nm: $t_{[12]}$=4.21, $p$=0.001, Cohen's $d$=1.21; 0.4 Nm: $t_{[12]}$=9.54, $p$<0.001, Cohen's $d$=2.75; 0.6 Nm: $t_{[12]}$=6.29, $p$<0.001, Cohen's $d$=1.82; -0.2 Nm: $t_{[12]}$=4.63, $p$<0.001, Cohen's $d$=1.34; -0.4 Nm: $t_{[12]}$=8.3, $p$<0.001, Cohen's $d$=2.4; -0.6 Nm: $t_{[12]}$=5.56, $p$<0.001, Cohen's $d$=1.61).

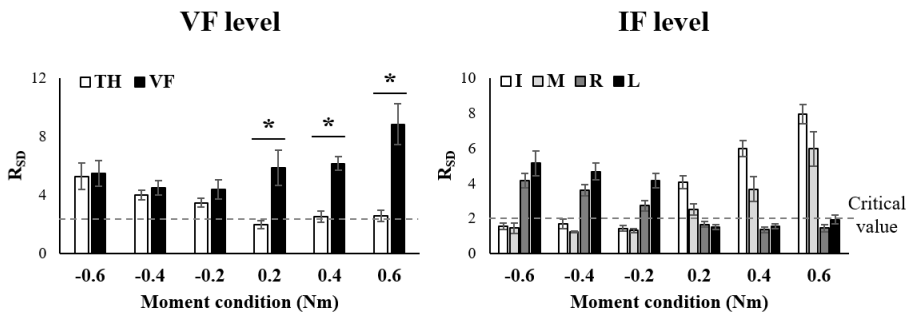


**Figure 4.6.** Across-subject mean and standard errors of the $R_{SD}$ under the different moment conditions. These $R_{SD}$ values were computed from 2-dimensional $\{R_\theta, k_\theta\}$ space within individual digit. The left and right panel corresponds to VF and IF level, respectively. The dashed line represents the critical value of 2 implying a significant synergic effect. The asterisks (*) indicate significant differences between digits.

For the VF level $R_{SD}$ stabilizing individual TH and VF moment, the $R_{SD}$ of VF ($R_{SD}^{VF}$) was significantly larger than the $R_{SD}$ of TH ($R_{SD}^{TH}$) in the pronation moment conditions. The $R_{SD}^{TH}$ and $R_{SD}^{VF}$ were significantly increased with increasing magnitudes of moment. Further, $R_{SD}^{TH}$ was larger in supination than pronation, while $R_{SD}^{VF}$ showed opposite pattern (Figure 4.6). These findings were supported by The *Digit* × *Magnitude* RM ANOVA, which showed the significant main effects of *Digit* (pronation: $F_{[1,11]}$=41.31, $p$<0.001, $\eta p^2$=0.79) without factor interactions. The *Direction* × *Magnitude* RM ANOVA performed separately on each digit resulted in the significant main effect of *Direction* (TH: $F_{[1,11]}$=29.67, $p$<0.001, $\eta p^2$=0.73; VF: $F_{[1,11]}$=13.7, $p$=0.003, $\eta p^2$=0.56) and *Magnitude* (TH: $F_{[2,22]}$=5.1, $p$=0.015, $\eta p^2$=0.32; VF: $F_{[2,22]}$=4.71, $p$=0.02, $\eta p^2$=0.3) without factor interactions. Significant synergies within the individual digit $\{R_\theta, k_\theta\}$ space were present for TH in supination moment (-0.2 Nm: $t_{[12]}$=4.66, $p$=0.001, Cohen's $d$=1.34; -0.4 Nm: $t_{[12]}$=6.29, $p$<0.001, Cohen's $d$=1.82; -0.6 Nm: $t_{[12]}$=3.68, $p$=0.004, Cohen's $d$=1.06) and for VF in all moment conditions (0.2 Nm: $t_{[12]}$=3.17, $p$=0.009, Cohen's $d$=0.92; 0.4 Nm: $t_{[12]}$=8.85, $p$<0.001, Cohen's $d$=2.55; 0.6 Nm: $t_{[12]}$=4.94, $p$<0.001, Cohen's $d$=1.42; -0.2 Nm: $t_{[12]}$=3.58, $p$=0.004, Cohen's $d$=1.03; -0.4 Nm: $t_{[12]}$=5, $p$<0.001, Cohen's $d$=1.44; -0.6 Nm: $t_{[12]}$=3.91, $p$=0.002, Cohen's $d$=1.13).

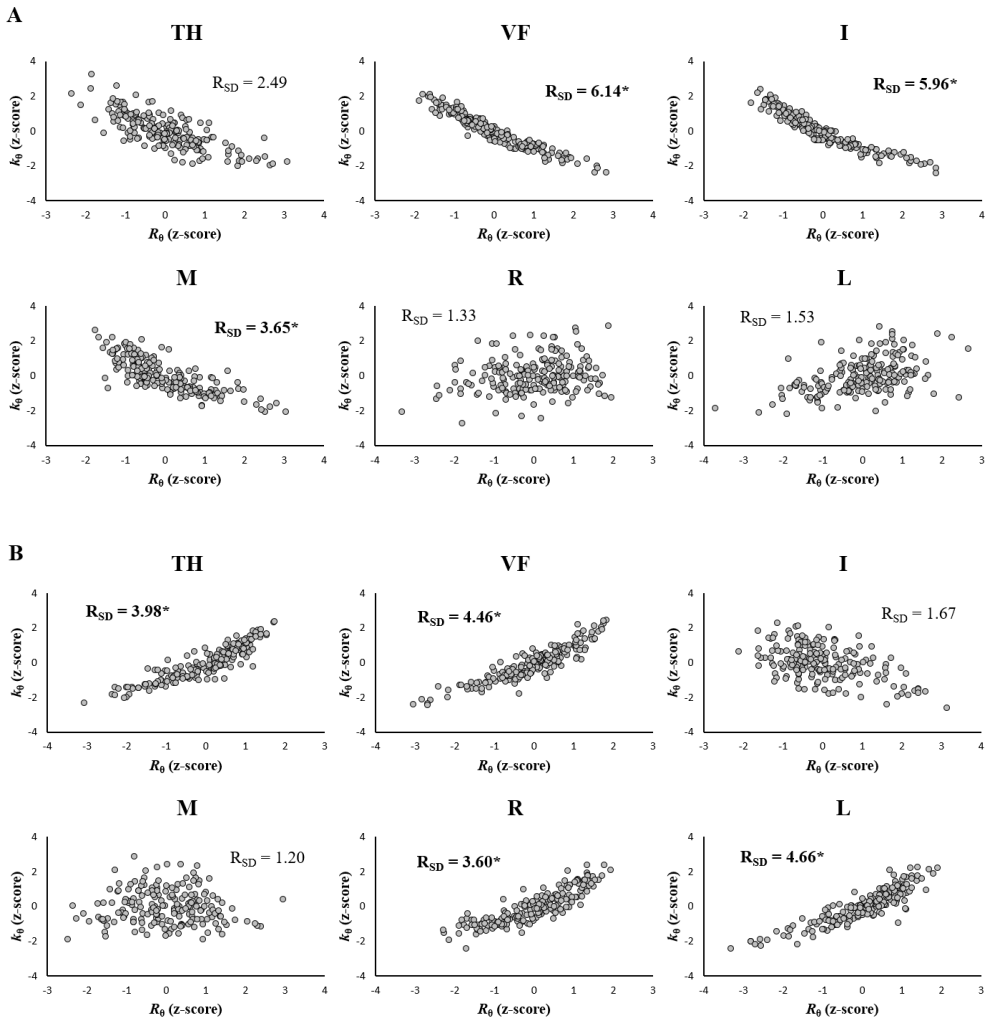


**Figure 4.7.** The scatter plots for covariation of $R_\theta$ and $k_\theta$ within the individual digit. Data are presented with 0.4 and -0.4 Nm conditions as representative moment conditions for (A) pronation and (B) supination moment, respectively. The $\{R_\theta, k_\theta\}$ pairs of corresponding digit are pooled across trials and subjects by transforming values to z-score. Average $R_{SD}$ for across subjects is presented for each digit, and the asterisks (*) indicate significant $R_{SD}$ above critical value 2.

For the IF level $R_{SD}$ stabilizing individual finger moment, the $R_{SD}$ of moment agonist finger were significantly larger than that of the moment antagonist finger. The $R_{SD}^{I}$ and $R_{SD}^{M}$ were larger than the $R_{SD}^{R}$ and $R_{SD}^{L}$ in the pronation

moment, and opposite pattern was observed in the supination moment (Figure 4.6). The $R_{SD}^{I}$ and $R_{SD}^{M}$ significantly increased with increasing magnitude of the moment only in the pronation, while the $R_{SD}^{R}$ significantly increased only in the supination. Further, $R_{SD}^{I}$ and $R_{SD}^{M}$ were significantly larger in the pronation direction than the supination direction, whereas opposite pattern was present for $R_{SD}^{R}$ and $R_{SD}^{L}$. These results were supported by The *Digit* × *Magnitude* RM ANOVA, which showed the significant main effects of *Digit* (pronation: $F_{[1.92,21.08]}$=40.97, $p$<0.001, $\eta p^2$=0.79; supination: $F_{[1.62,17.79]}$=49.19, $p$<0.001, $\eta p^2$=0.81) and *Magnitude* (pronation: $F_{[2,22]}$=20.3, $p$<0.001, $\eta p^2$=0.65; supination: $F_{[2,22]}$=4.02, $p$=0.033, $\eta p^2$=0.27) with factor interaction (pronation: $F_{[2.648,29.12]}$=8.73, $p$<0.001, $\eta p^2$=0.44). The *Direction* × *Magnitude* RM ANOVA performed separately on each finger resulted in the significant main effect of *Direction* (I: $F_{[1,11]}$=170.08, $p$<0.001, $\eta p^2$=0.94; M: $F_{[1,11]}$=22.32, $p$=0.001, $\eta p^2$=0.67; R: $F_{[1,11]}$=49.66, $p$<0.001, $\eta p^2$=0.82; L: $F_{[1,11]}$=44.85, $p$<0.001, $\eta p^2$=0.8) and *Magnitude* (I: $F_{[2,22]}$=20.76, $p$<0.001, $\eta p^2$=0.65; M: $F_{[2,22]}$=9.97, $p$=0.001, $\eta p^2$=0.48) with factor interactions (I: $F_{[2,22]}$=24.46, $p$<0.001, $\eta p^2$=0.69; M: $F_{[2,22]}$=6.26, $p$=0.007, $\eta p^2$=0.36; R: $F_{[2,22]}$=6.58, $p$=0.006, $\eta p^2$=0.37). Significant synergistic effects within the individual finger $\{R_\theta, k_\theta\}$ space appeared only when that finger acted as a moment agonist (Figure 4.7). $R_{SD}^{I}$ (0.2 Nm: $t_{[12]}$=5.67, $p$<0.001, Cohen's $d$=1.64; 0.4 Nm: $t_{[12]}$=8.69, $p$<0.001, Cohen's $d$=2.51; 0.6 Nm: $t_{[12]}$=10.61, $p$<0.001, Cohen's $d$=3.06) and $R_{SD}^{M}$ (0.4 Nm: $t_{[12]}$=2.3, $p$=0.042, Cohen's $d$=0.66; 0.6 Nm: $t_{[12]}$=4.07, $p$=0.002, Cohen's $d$=1.18) were significantly higher than the critical value in the pronation moments (Figure 4.7A), whereas the $R_{SD}^{R}$ (-0.2 Nm: $t_{[12]}$=2.4, $p$=0.035, Cohen's $d$=0.70; -0.4 Nm: $t_{[12]}$=4.85, $p$=0.001, Cohen's $d$=1.4; -0.6 Nm: $t_{[12]}$=5.14, $p$<0.001, Cohen's $d$=1.48) and $R_{SD}^{L}$ (-0.2 Nm: $t_{[12]}$=5.21, $p$<0.001, Cohen's $d$=1.5; -0.4 Nm: $t_{[12]}$=5.61, $p$<0.001, Cohen's $d$=1.62; -0.6 Nm:

$t_{[12]}$=4.46, $p$=0.001, Cohen's $d$=1.29) exceeded the critical value in the supination moments (Figure 4.7B).

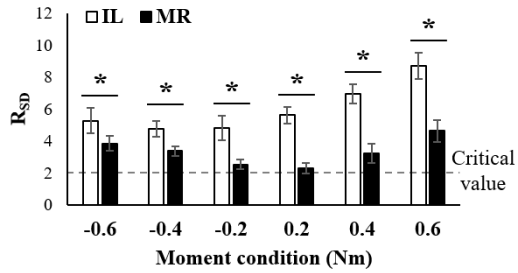


**Figure 4.8.** Average $R_{SD}$ of medial (MR) and lateral (IL) finger under different moment conditions were presented with standard errors. These $R_{SD}$ were computed from 4-dimensional $\{R_\theta, k_\theta\}$ space within medial and lateral finger. The dashed line represents the critical value of 2 implying a significant synergic effect. The asterisks (*) indicate significant differences between digits.

We additionally quantified and compared the moment stabilization synergies of the medial (MR) and lateral (IL) fingers in a 4-dimensional $\{R_\theta, k_\theta\}$ space (Figure 4.8). As results, lateral finger showed higher $R_{SD}$ than medial finger in all moment conditions. The medial and lateral finger $R_{SD}$ significantly increased with increasing magnitude of moment condition. Further, the lateral finger's $R_{SD}$ was significantly larger in the pronation than supination direction, while directional difference was not found in medial finger. These findings were supported by RM ANOVA with factors *M-L* (two levels: medial and lateral finger) and *Magnitude*, which showed the significant main effects of *M-L* (pronation: $F_{[1,11]}$=37.1, $p$<0.001, $\eta p^2$=0.77; supination: $F_{[1,11]}$=11.5, $p$=0.006, $\eta p^2$=0.51) and *Magnitude* (pronation: $F_{[2,22]}$=12.83, $p$<0.001, $\eta p^2$=0.54) without factor interactions. The *Direction* ×

*Magnitude* RM ANOVA performed separately on each medial and lateral finger showed that there were main effects of *Direction* (lateral: $F_{[1,11]}$=11.12, $p$=0.007, $\eta p^2$=0.5) and *Magnitude* (medial: $F_{[2,22]}$=8.88, $p$=0.001, $\eta p^2$=0.45; lateral: $F_{[2,22]}$=7.67, $p$=0.003, $\eta p^2$=0.41) without factor interactions. The significant synergies within the lateral fingers' $\{R_\theta, k_\theta\}$ space were present in all moment conditions (0.2 Nm: $t_{[12]}$=7.16, $p$<0.001, Cohen's $d$=2.07; 0.4 Nm: $t_{[12]}$=8.36, $p$<0.001, Cohen's $d$=2.41; 0.6 Nm: $t_{[12]}$=8.06, $p$<0.001, Cohen's $d$=2.33; -0.2 Nm: $t_{[12]}$=3.67, $p$=0.004, Cohen's $d$=1.06; -0.4 Nm: $t_{[12]}$=5.66, $p$<0.001, Cohen's $d$=1.63; -0.6 Nm: $t_{[12]}$=4.11, $p$=0.002, Cohen's $d$=1.19), while the medial finger's $R_{SD}$ exceeded the critical value only in the relatively higher moment condition (0.6 Nm: $t_{[12]}$=3.8, $p$=0.003, Cohen's $d$=1.1; -0.4 Nm: $t_{[12]}$=4.51, $p$=0.001, Cohen's $d$=1.3; -0.6 Nm: $t_{[12]}$=3.83, $p$=0.003, Cohen's $d$=1.11).

### 4.3.3. Relationship Between Grip Force and Digit Moment Stabilization

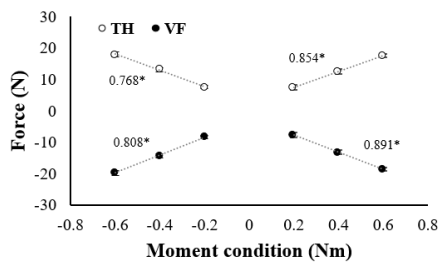


**Figure 4.9.** Average magnitudes of digit normal forces ($F^N$) for TH and VF under different moment conditions are presented with standard error bars. The open and filled circle indicate the $F^N$ of the TH and VF, respectively. Regression lines are shown with the coefficients of determination ($R^2$). The asterisks (*) are presented for significant $R^2$.

The absolute magnitudes of digit normal forces for the VF ($|F^N_{VF}|$) were larger than the those of the TH ($|F^N_{TH}|$) in the all moment conditions (Figure 4.9). Across subjects' average unbalanced $F^N$ between TH and VF was -0.95 N. The $|F^N_{TH}|$ and $|F^N_{VF}|$ significantly increased with increasing magnitudes of moment condition. These findings were supported *Digit* × *Magnitude* RM ANOVA that performed separately on each direction. It showed the significant main effects of *Digit* (pronation: $F_{[1,11]}$=8.91, $p$=0.012, $\eta p^2$=0.45; supination: $F_{[1,11]}$=63.71, $p$<0.001, $\eta p^2$=0.85) and *Magnitude* (pronation: $F_{[2,22]}$=729.14, $p$<0.001, $\eta p^2$=0.8; supination: $F_{[1.17,12.91]}$=506.87, $p$<0.001, $\eta p^2$=0.98) and factor interactions (pronation: $F_{[2,22]}$=4.08, $p$=0.031, $\eta p^2$=0.27; supination: $F_{[2,22]}$=10.1, $p$=0.001, $\eta p^2$=0.48). Further, the changes of $F^N_{TH}$ and $F^N_{VF}$ according to moment magnitudes were well described by the linear equations in both pronation and supination directions ($p$<0.05) (Figure 4.9).

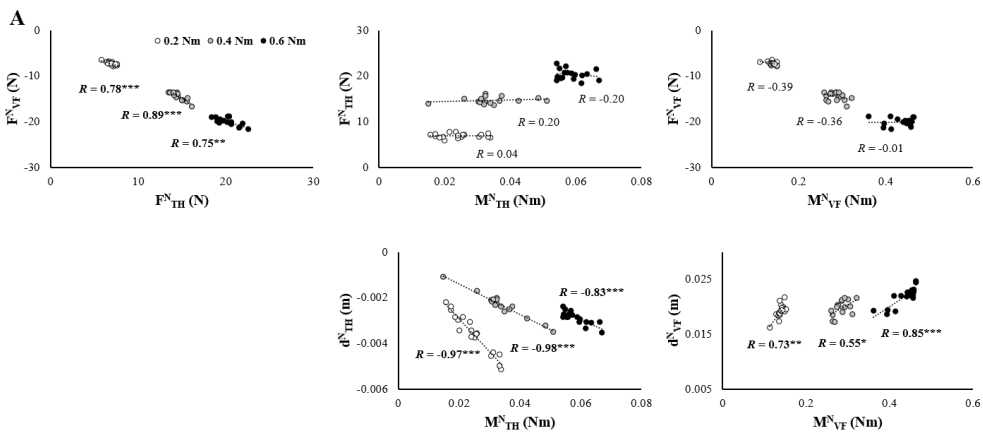

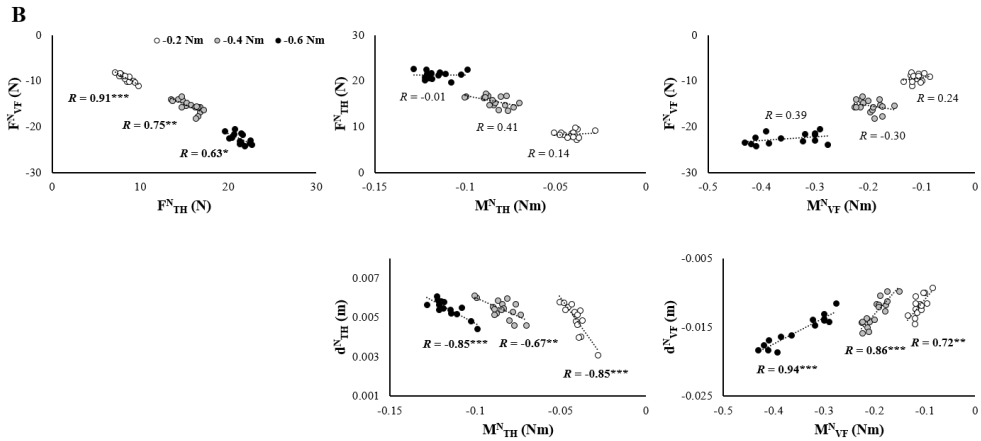


**Figure 4.10.** Interrelations among the TH and VF normal forces ($F^N$), moment arms of the normal force ($d^N$), and moments of normal force ($M^N$). These data are pooled across-trials for representative subject in the (A) pronation moment and (B) supination moment conditions. The open, gray, and black dot correspond to the ± 0.2, ± 0.4, and ± 0.6 Nm moment conditions, respectively. The best-fit linear regression line with coefficients of correlation are presented in each moment condition. Triple asterisks (***) indicate $p<0.001$; double asterisks (**) indicate $p<0.01$; single asterisks (*) indicate $p<0.05$.

Separate correlation analyses were performed to identify the relationship of trial-to-trial changes of variables contributing to grip force and moment production within each moment condition (Figure 4.10). In both directions of moment production, the $F^N_{TH}$ was correlated closely with the $F^N_{VF}$ in all moment conditions. Note that the inter-trial changes of each $F^N_{TH}$ and $F^N_{VF}$ did not correlated with the changes of the moment of normal forces (i.e., $M^N_{TH}$ and $M^N_{VF}$). On the other hand, the moment arm of the normal force of the two digits (i.e., $d^N_{TH}$ and $d^N_{VF}$) showed significant correlations with each $M^N_{TH}$ and $M^N_{VF}$ in all moment magnitudes.

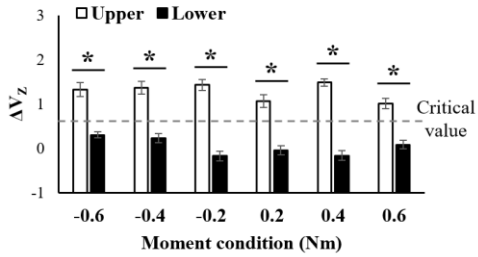


**Figure 4.11.** Across-subject's average $\Delta V_Z$ for stabilization of digit normal forces were presented under different moment condition with standard error bars. The solid bars and the open bars indicate the upper and lower hierarchy, respectively. The dashed line represents the critical values corresponding to lower hierarchy (= 0 for upper, and ≈ 0.55 for lower hierarchy) implying a significant synergic effect. The asterisks (*) indicate significant differences between hierarchies.

The $\Delta V_Z$ stabilizing digit normal force were significantly larger in the upper hierarchy than the lower hierarchy in the all moment conditions (Figure 4.11). The $\Delta V_Z$ for both hierarchies did not systematically change with the magnitudes of moment conditions, while the upper level $\Delta V_Z$ in the 0.4 Nm were significantly larger than those of 0.2 and 0.6 Nm. These findings were supported by RM ANOVA with factors *Hierarchy* and *Magnitude*, which showed the significant main effects of *Hierarchy* (pronation: $F_{[1,11]}$=27.23, $p$<0.001, $\eta p^2$=0.83; supination: $F_{[1,11]}$=54.81, $p$<0.001, $\eta p^2$=0.83) with factor interactions (pronation: $F_{[2,22]}$=7.07, $p$=0.004, $\eta p^2$=0.39). The single-sample $t$-test with critical $\Delta V_Z$ values revealed that the purposeful covariation across trials to stabilize digit normal force was present only in the upper hierarchy (0.2 Nm: $t_{[12]}$=7.55, $p$<0.001, Cohen's $d$=2.18; 0.4 Nm: $t_{[12]}$=17.99, $p$<0.001, Cohen's $d$=5.19; 0.6 Nm: $t_{[12]}$=8.42, $p$<0.001, Cohen's $d$=2.43; -0.2 Nm: $t_{[12]}$=11.44, $p$<0.001, Cohen's $d$=3.3; -0.4 Nm: $t_{[12]}$=9.22, $p$<0.001, Cohen's $d$=2.66; -0.6 Nm: $t_{[12]}$=8.4, $p$<0.001, Cohen's $d$=2.42).

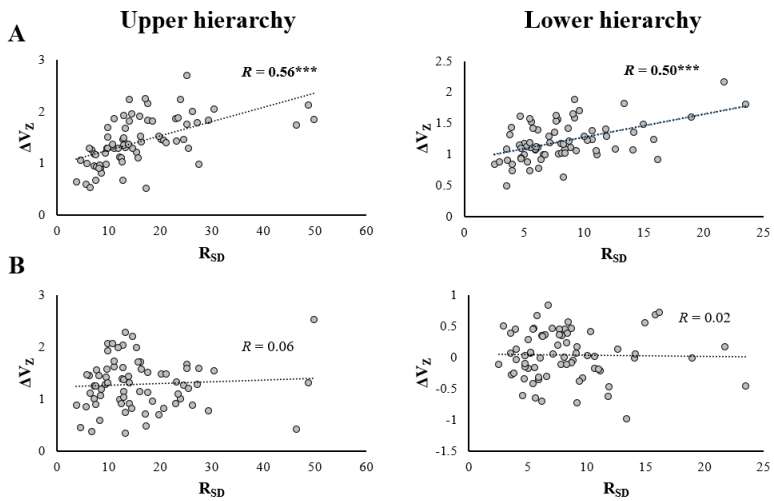


**Figure 4.12.** Relationship of the $R_{SD}$ determined in the space of control variables $\{R_\theta, k_\theta\}$ to the $\Delta V_Z$ for digit (A) moment and (B) normal force stabilization. Correlation analysis was performed separately for each hierarchy using data pooled across subjects. The left and right panel correspond to upper and lower hierarchy, respectively. The best-fit linear regression line with coefficients of correlation are presented. Triple asterisks (***) indicate $p<0.001$.

We further identified the relationship between synergies within the $\{R_\theta, k_\theta\}$ space and within the mechanical variable space. This analysis was conducted separately on each hierarchy and $\Delta V_Z$ for digit moment and force stabilization. Correlations between the $R_{SD}$ vs. $\Delta V_Z$ stabilizing digit moment and between $R_{SD}$ vs. $\Delta V_Z$ stabilizing digit normal force were presented in Figure 4.12A and 4.12B, respectively. There was a strong linear relationship between the $R_{SD}$ and moment stabilizing $\Delta V_Z$ in both hierarchies (upper hierarchy: $R$=0.56, $p$<0.001; lower hierarchy: $R$=0.5, $p$<0.001). However, the $\Delta V_Z$ for normal force stabilization did not correlate to the $R_{SD}$ in both hierarchies.

## 4.4. Discussion

In this study, the hypothetical control variables (i.e., $R_\theta$ and $k_\theta$) for digit moment production were quantified during multi-digit moment production with an experimental task employing different magnitudes and directions of the moment. We were able to confirm all three hypotheses formulated in the *Introduction*. At the virtual finger level, the thumb and virtual finger's $k_\theta$ did not differ depending on the direction of moment generation, but the $R_\theta$ of the thumb and virtual finger were assigned differently depending on the moment direction. Further, we found the $R_\theta$ and $k_\theta$ with different properties according to the change in moment magnitudes at the individual finger level. These results supported our first hypothesis (H1). It was confirmed that the moments and the $\{R_\theta, k_\theta\}$ pairs for individual digits were organized in synergistic ways across two control hierarchies, and the covariation of control variables stabilizing the moment of lateral fingers was more prominent than that of the medial fingers (H2). Lastly, the covariation of $R_\theta$ and $k_\theta$ were strongly correlated to synergies in digit moment space, but it was independent of synergies for grip force stabilization (H3). The following sections addressed these results with strategies to achieve rotational equilibrium in the static prehension based on the referent control hypothesis.

### 4.4.1. Possible Functional Roles of Parameters $R_\theta$ and $k_\theta$ in Stable Moment Production

In terms of the referent control, the reciprocal (R) command specifies a threshold position (referent variables, i.e., *RC* or $R_\theta$) where the activity of all muscles

related to movement is disappeared if the external load is zero, and the co-activation (C) command controls the apparent stiffness ($k$) of effectors by defining the range in which agonist-antagonist muscles that cross the involved joints are co-activated (Feldman, 2015). In isometric conditions where the movement of the effector is restricted by the environment, both the referent position and the apparent stiffness can be attributed to the magnitude of the isometric force generation (Latash, 2020a). Studies using an inverse piano apparatus that can vertically change the fingertip position during the four finger pressing task helped understand the characteristics of normal finger force production with variables $RC$ and $k$ (Ambike et al., 2016; Cuadra, Gilmore, et al., 2020; Cuadra, Wojnicz, et al., 2020; Martin et al., 2011; Reschechtko & Latash, 2017, 2018), but the possible effects of the mechanical consequences (e.g., magnitudes of force or moment) on the designation patterns of two control variables have not yet been elucidated. In the previous chapter, we dealt with the control variables $RC$ and $k$ to explain the grip force production during static prehension. In this chapter, we quantified $R_\theta$ and $k_\theta$, which induce the digit moments while the subjects produced moments of various directions and magnitudes. This approach was essential to understanding rotational equilibrium control in static multi-digit prehension and was currently the first attempt.

It is well known that the co-activation of agonist and antagonist muscles increases after a quick movement, then slowly subsides without change in effector position (Gottlieb, Corcos, & Agarwal, 1989; Yamazaki et al., 1994). This phenomenon has been interpreted that the R-command is primarily responsible for the control of action, whereas the C-command is subordinate to the change in the R-command (Feldman, 2015). Similarly, we easily perform the co-contraction of the

elbow flexor and extensor muscles without moving the upper limb in the absence of an external stop, and it suggests that the C-command can be changed naturally without a change in the R-command. Cuadra, Wojnicz, et al. (2020) reported the hierarchical relations and different neural mechanisms between R- and C-command. Specifically, they suggested that the sense of effort to finger force production reflects the magnitude of *RC* specified by the R-command independently of the C-command. This view was in line with our observation that the functional roles of the $R_\theta$ for moment production depend on the magnitude and direction of the moment. It was found that the magnitude of digit moments produced by the thumb were increased in the supination direction compared to the pronation direction although the sum of thumb and virtual finger moments were not different (Figure 4.3). This disparity was preserved in the $R_\theta$ but not in the $k_\theta$ — the $k_\theta$ of the thumb and virtual finger did not differ depending on the direction of moment production, whereas the magnitude of thumb $R_\theta$ was relatively larger in the supination direction, similar to the outcome digit moments (Figure 4.4). In other words, although both control variables can affect the digit moment production under the isometric condition, the direction and magnitude of digit moment can be interpreted as being affected by the magnitude of $R_\theta$ rather than $k_\theta$. Thus, the designation of $R_\theta$ could be related to the desired magnitude and direction of the moment, which might be a functional feature of the R-command in the isometric digit moment production.

We described in the previous chapter that the apparent stiffness was larger when holding a free object than in the fixed object prehension condition as a strategy to improve the grip stability. Similarly, the designation patterns of the $k_\theta$ for ensuring the stability of mechanical effects were also observed in the current results. As the

required magnitude of the digit moment increased in both directions, the magnitude of the individual finger $R_\theta$ significantly increased in moment agonist fingers that coincided with the net moment direction, whereas the $R_\theta$ of the moment antagonist fingers did not change with the moment magnitudes. On the other hand, the $k_\theta$ changed significantly with the changes in the moment magnitude for not only the moment agonist but also the antagonist fingers. An inevitable antagonist moment occurs in the task of grasping a handle using five digits and applying a moment on a centrally located rotation axis. The antagonist moment, which is opposite to the direction of the desired net moment generated by the activation of moment antagonist fingers, has been explained to be partially due to the enslaving effects of fingers (Kilbreath & Gandevia, 1994; Kilbreath, Gorman, Raymond, & Gandevia, 2002; Z. N. Li et al., 1998; Zatsiorsky et al., 2002b; Zatsiorsky, Li, & Latash, 2000). However, the functional implications of antagonist moments in the digit moment generation have not yet been reported. The antagonist moment seems to be mechanically not efficient because it should be compensated by the effort of moment agonist fingers. Nevertheless, the mechanical effect of the moment antagonist finger increased with the increase of net moment in the current results (Figure 4.3), and it originated from an increase in the $k_\theta$ rather than $R_\theta$. This suggested that a functional role of the antagonist moments might be related to the stability of digit moment production. In the current experimental task, the subjects were provided visual feedback about the target net moment and were instructed to match the moment magnitude as accurately as possible and keep it constant. Thus, the designation patterns of the two control variables could be interpreted as reflecting the strategy to keep the digit moment accurate and constant. Increasing the apparent stiffness by C-command increases the spatial range (safety zone) where unpredictable changes in

effector position are less (Latash, 2018). Further, it is well known that the muscle co-activation improves the mechanical stability of the joint and does not significantly affect the change in the net torque since the paired antagonistic muscles are scaled in parallel (Heitmann, Ferns, & Breakspear, 2011). Therefore, the patterns of $k_\theta$ observed at the moment antagonist finger might be a strategy to stabilize the digit moment for satisfying the given task instruction. Since the increased $k_\theta$ by co-activation lead to an unintentional increase in the mechanical effect of the digit (Cuadra, Gilmore, et al., 2020; Cuadra, Wojnicz, et al., 2020; Latash, 2018, 2020a), it would inevitably induce an increase in the moment of the antagonist fingers. Overall, the moment produced in the opposite direction of the desired net moment was due to the $k_\theta$ of the moment antagonist fingers, which was considered to reflect the rotational stability of the grasped objects.

### 4.4.2. Hierarchical Organization of Control Variables for Decoupled Control of Translational and Rotational Equilibrium

When holding an object and applying digit forces and moments, it is possible to generate the identical mechanical effect through an infinite combination of two control variables, referent digit position and apparent stiffness (Ambike et al., 2018; Ambike et al., 2016; Latash, 2017). The referent orientation and apparent rotational stiffness can be utilized to define the threshold lengths (λ) of redundant agonist and antagonist muscles for multi-finger moment production (Parsa, O'Shea, Zatsiorsky, & Latash, 2016). It is essential to figure out the functional implications for the neural controller to choose a particular pair of $R_\theta$ and $k_\theta$ in the particular trial among the numerous combinations of two control variables. In the UCM hypothesis

proposed to solve the problem of motor redundancy, the neural controller generates families of solutions that can equally solve the task rather than finding the unique optimal solution based on certain cost functions. In the current results, the variance of $R_\theta$ and $k_\theta$ that appeared in repeated trials was formed along the hyperbolic UCM line that ensures the invariance of the digit moment (Figure 4.7). Of course, their organizing patterns were somewhat different depending on the control hierarchies and digits. Further, the permutation analysis was to compare the actual $\{R_\theta, k_\theta\}$ data set with the surrogate data set, which removed intentional covariation of two control variables. The synergy index (i.e., $R_{SD}$) derived from this analysis also confirmed that the $R_\theta$ and $k_\theta$ quantified in the current study were purposefully organized to stabilize the outcome moments. Therefore, it could be suggested that the particular combination of the $R_\theta$ and $k_\theta$ selected by the neural controller in a particular trial has functional meaning to reduce the error and enhance the consistency of the outcome mechanical effect.

The difference in the hierarchical organization of control variables between translation and rotation equilibrium control was observed in the lower hierarchy. As described in Chapter 3, the synergistic behavior of *RC* and *k* for stabilizing digit force appeared only in the upper hierarchy. On the other hand, the synergies in the $R_\theta$ and $k_\theta$ spaces related to the generation of digit moment were prominent in the both upper and lower hierarchies, and this result was consistent with our hypothesis. Since the hierarchical organization of individual digit moments stabilizing net moment of both upper and lower hierarchies in static prehension has been observed in earlier studies (Gorniak et al., 2009; Park et al., 2015), it was expected that this tendency would be extended and applied to the level of $\{R_\theta, k_\theta\}$ space. This finding indirectly supports

the idea that stabilization of rotational equilibrium during human prehension may be an inherent control strategy, rather than an action made compulsory by the mechanics (Latash et al., 2001; Zhang et al., 2006). According to the referent control hypothesis, the task-specific level of the control hierarchy defines the time profiles of control variables in high dimensional lower levels of the hierarchy. The sequence of few-to-many mappings ensures the synergistic covariation of redundant elemental effectors at lower levels such as limbs, digits, and joints. Similarly, we could observe the synergistic organization of control variables over the two control hierarchies to stabilize the variable at a task-specific level, which were the referent aperture (Chapter 3) and referent orientation (Chapter 4), affecting the translational and rotational equilibrium, respectively. This feature is applicable to training and learning in various types of sports activities, as well as static prehension control. For learning racket sports, which is similar to prehensile action that includes multiple joints and the body interacts with external objects, providing feedback on the motion of the racket as an effector at task-specific level rather than the configuration of individual segments would be an effective strategy to improve the skill. In addition, it is appropriate to provide feedback on the motion of the effector for an external reference frame rather than an internal body reference frame, as the way the common referent configuration is specified at the task-specific level. This approach is in line with the well-known strategy of the *Constrained action hypothesis*, suggests that internal attentional feedback could be negative on an athlete, causing them to interfere with their body's natural movements (Kal, van der Kamp, & Houdijk, 2013; Vidal, Wu, Nakajima, & Becker, 2018).

What should be noted was the relationship of the two synergies determined

from different spaces. Principle of superposition prescribes the relationship between digit forces and moments for multi-digit static prehension (Arimoto & Nguyen, 2001; Shim & Park, 2007; Zatsiorsky et al., 2004). The thumb and virtual fingers' normal forces were strongly correlated with each other independently of moment of normal forces (Figure 4.10), it meant that the decoupled control strategy of object's translation and rotation were preserved in the current experimental task that was similar to generating a moment for a fixed doorknob. The relationship between organization of control variables for translation and rotation could not be directly confirmed in the present experiment since it was difficult to simultaneously reconstruct both $\{RC, k\}$ and $\{R_\theta, k_\theta\}$ during generating digit forces and moments. Nevertheless, our findings provided indirect evidence that the principle of superposition might be valid even in the space of control variables. We already identified in the previous chapter that the two synergies of $\{RC, k\}$ and digit force spaces have a strong relationship regardless of the mechanical constraints (i.e., free and fixed object prehension). Further, the synergies within space of $\{R_\theta, k_\theta\}$ showed a strong linear relationship with the synergies in digit moment space in both hierarchies (Figure 4.12A), whereas it did not correlate with synergies related to the grip force production (i.e., digit normal forces) (Figure 4.12B). Therefore, it was possible that the $\{RC, k\}$ and $\{R_\theta, k_\theta\}$ determining the magnitude of digit force and moment, respectively, could be organized independently for decoupled control of translational and rotational equilibrium.

Individual fingers are specialized differently in generating forces and moments. When applying the moment on the holding objects, fingers located farther away from the axis of rotation (i.e., lateral fingers) generate larger force. It has been

generalized to the *mechanical advantage hypothesis* (Devlin & Wastell, 1986; Frey & Carlson, 1994; Gielen et al., 1988), which implies the effects of the lateral finger having a larger moment arm depends mainly on the moment magnitude, whereas the effect of the central fingers (i.e., medial fingers) depends on grip force production (Park, Baum, et al., 2012; Shim et al., 2004; Song, Kim, et al., 2021). Indeed, the lateral fingers more contributed to the net moment production regardless of the direction and magnitude of the moment, and the synergistic effects for stabilizing the digit moment in the $\{R_\theta, k_\theta\}$ space were also pronounced (Figure 4.8). This result suggests that the mechanical advantage hypothesis not just the level of mechanical effect on the lateral fingers but also might explain the consideration of task-specific stability at the control level. Another interesting finding was that the moment stabilization synergies between the thumb and virtual finger were not different in generating a moment for the supination direction, whereas in the pronation direction, only synergies within the virtual finger showed a significant effect exceeding the critical value (Figure 4.6). This result meant that the effect of digits that ensure the stable moment production might differ depending on the direction of the moment—both thumb and virtual finger contributed to moment stability equally in the supination direction, while the virtual finger solely affected that in the pronation direction. For the moment agonist fingers, the $R_\theta$ and $k_\theta$ covaried in a synergistic manner to stabilize the digit moment, but there was no synergistic effect on the organizational pattern of the two control variables within the moment antagonist fingers (Figure 4.7). Note that the moment stabilization by agonist fingers in the supination direction (i.e., little and ring fingers) was relatively lower than that in the pronation direction (i.e., index and middle fingers). Moreover, the little and ring fingers have relatively large interdependence (i.e., enslaving effect) compared to

other fingers (Zatsiorsky et al., 2000), suggesting that it is difficult for the two fingers to compensate for each other's errors. Therefore, considering the relatively small capacity of moment production (Figure 4.3) and stability properties for the little and ring fingers in the supination direction, it was possible that the thumb actively made an effort to satisfy a certain level of moment magnitude and stability. This result has a room that can be utilized to design objects that need to manipulate the moment by hand. In the case of manufacturing an object that requires rotational manipulation, such as a doorknob, especially if repeated moment generation to supination direction is required, a symmetrical shape may be inefficient. Rather, designing a large moment arm of the thumb in the supination direction to compensate for the little finger would be a way to reduce muscle fatigue and increase the efficiency of moment manipulation.

There was an important limitation in the current methodology. The issue of limitation was related to the measurement of the invariant characteristics (i.e., force-length properties at an invariant value of the threshold position), which requires to be done under a constant state in central command. To ensure this end, the task instruction of the "do not voluntarily intervene" paradigm was applied as used in the previous studies (Ambike et al., 2018; Ambike et al., 2016; Ambike, Paclet, Latash, & Zatsiorsky, 2013; Ambike et al., 2014; Ambike et al., 2015; Cuadra, Gilmore, et al., 2020; Cuadra, Wojnicz, et al., 2020; de Freitas et al., 2018; Feldman, 1966, 1986, 2011; Feldman et al., 2007; Feldman & Orlovsky, 1972; Frenkel-Toledo et al., 2019; Martin et al., 2011; Pilon et al., 2007; Reschechtko & Latash, 2017, 2018; Zatsiorsky et al., 2006). This instruction required that the subjects behave in a natural way without trying to intentionally modify their effort on handle motion, but it might or

might not be effective in preventing voluntary response. Current measurement techniques, including brain imaging, cannot directly quantify the changes in human motor command generated in the central nervous system, so it was bound to be a limitation inherent in this experiment. Nevertheless, the mechanical variables (i.e., digit forces and moments) determined in the current experiment suggested that the subjects adequately complied with the requirement not to react to the handle movement within the individual measurement. The force-length characteristics of a single muscle are typically nonlinear, despite the action of the stretch reflex is linearly well fitted (Nichols & Houk, 1976). However, the overall digit-force characteristics become closer to linear in the condition that the equilibrium-point is situated within the co-activation zone formed by agonist and antagonist muscles (see overall torque-angle characteristic in Figure 2.5). Although the current study did not directly measure the muscular electrical activities (i.e., electromyogram), it was expected that the nonzero antagonist activities could be present because the necessity of extensor muscles to ensure the fingers do not collapse (i.e. finger extensor mechanism) during isometric force production (Li, Zatsiorsky, & Latash, 2000, 2001). Indeed, we observed strong linear relationships between digit force/moment and handle motion over the two experiments for translation and rotation of the handle— the number of trials with $R$ values exceeding 0.9 was found to be the average of 24.2 out of 30 trials and 20.3 among 25 trials in Chapters 3 and 4, respectively. These trial data were used to compute the control variables; thus, the linear approximation was justified.

Another points that could be controversial in the current analysis for reconstructing the control variables were the possible effects induced by the

movement of the handle (i.e., expansion and rotation of the handle). At present, there is no way of directly measuring the referent position of the effector in isometric force production. Thus, the apparent stiffness was obtained by passively inducing the displacement of the digit-tip, and the referent position could be then calculated indirectly. Note that the force applied to the subjects' digit-tip due to the motion of the handle could trigger the excitation of several sensory afferents, such as cutaneous receptors, and inevitably affects the patterns in which the control variables are defined. In fact, the equilibrium point hypothesis has addressed this point, which is a common misconception of this framework that the R-command alone directly specifies the threshold length (λ) of involved muscles (Feldman & Latash, 2005; Sainburg, 2015). There are non-central components, such as dependence of the stretch velocity (i.e., damping properties), heteronymous proprioceptive and cutaneous afferent, and history-dependent intrinsic properties of the motoneuron, can influence the setting of the λ (Asatryan & Feldman, 1965; Feldman, 1966). Therefore, it is more appropriate to say that quantified control variables in the present study were designated by reflecting all experimentally manipulated conditions as well as the effect of the central command. The characteristics of the contact surface of the sensors and the speed at which the handle moves can cause the natural variability in the steady-state properties of the components described above. In particular, it was necessary to make soft perturbations to restore the invariant behavior because the neuromotor system is not tolerate strong and destabilizing perturbations (Dizio & Lackner, 1995; Hinder & Milner, 2003; Lackner & Dizio, 1994). Accordingly, we set the conditions for the contact surface and driving speed of the handle to be constant across all experimental conditions and subjects (Ambike et al., 2016; Reschechtko & Latash, 2017, 2018), and this regulation made it possible to identify

the effects of the independent variables that were the mechanical constraints (Chapter 3) and the magnitude/direction of digit moments (Chapter 4). In addition, one may be concerned that the apparent stiffness could change while the handle was moving since the changes in the co-activation by the C-command are independent of the R-command. Previous studies that addressed the perceptual and motor effects of the co-activation reported that an increase in the co-activation during isometric finger pressing leads to an unintentional increase in finger force not perceived by the subjects (Cuadra, Gilmore, et al., 2020; Cuadra, Wojnicz, et al., 2020). If there was a change in digit apparent stiffness that the participants were not aware of during the handle movement, it would inevitably be observed as a change in the mechanical outcomes. Thus, it is reasonable to assume that the observed smooth changes of digit force/moment and their linearity with handle movement did not present significant changes in the extent of co-activation and apparent stiffness.

Nevertheless, the arguments we have mentioned so far cannot completely rule out the limitations inherent in this experiment. There is also unresolved limitation to the referent control of action that have been debated in the literature for many years, including violations in the equifinality predictions (Lackner & Dizio, 1994; Popescu & Rymer, 2000; Sainburg, Lateiner, Latash, & Bagesteiro, 2003). Unfortunately, those studies assuming the equifinality are based on non-biological "mass-spring" systems, and should not be considered for all cases of biological action, as the force-length properties of muscle and sensorimotor behavior are largely nonlinear (Feldman & Latash, 2005). The spring analogy has been introduced in the equilibrium-point hypothesis helped to understand the position-dependent properties of muscle forces, whereas the spring analogy within the λ-model represents to the

entire neuromuscular system, not to the muscles per se. The integration of various afferent inputs in the spinal circuitry (i.e., non-central components) may lead to disparities between the final threshold values and common referent configuration, and these differences also be the causes of violation in the equifinality (Feldman, 2015).

## 4.5. Conclusion

For the first time, the current study empirically quantified the control variables, digit referent orientation/angle ($R_\theta$) and apparent rotational stiffness ($k_\theta$), for describing control of rotational equilibrium in the static prehension. The $k_\theta$ of the thumb and virtual finger were not different depending on the direction of moment production, while the disparity was present on the $R_\theta$. At the individual finger level, the effects of the moment antagonist finger increased with increasing net moment demand, which was manifestly attributed to the $k_\theta$ rather than $R_\theta$. These results suggested functional implications of the two control variables in static digit moment production. The designation pattern of the $R_\theta$ might reflect the desired magnitude and direction of the net moment, while the $k_\theta$ could be considered to reflect the rotational stability of the holding objects. We found indirect evidence that the principle of superposition might be valid even in the space of control variables by the fact that two sets of the control variables $\{RC, k\}$ and $\{R_\theta, k_\theta\}$ could be organized independently for decoupled control of translational and rotational equilibrium. We also observed that the functional specialization of the fingers, which affects the organization of forces and moments, could be reflected in the covariation pattern of control variables among fingers. Overall, current results suggest that the neural

controller specifies the control variables required for static prehension by reflecting the desired magnitude and direction of mechanical effects and stability properties for effectors, and the designated control variables at multiple control hierarchies are organized synergistically for stabilization of task-specific level.

# Chapter 5. General Conclusion

This dissertation aimed to extend the understanding of human prehension mechanisms, known mainly as mechanical variables such as digit forces and moments, to a control level based on the referent control hypothesis. We devised two types of motorized handle apparatus that could induce the handle displacement for translation and rotation to quantify two sets of the control variables; individual digits' referent coordinate ($RC$) and apparent stiffness ($k$) related to digit force production, and the referent angle ($R_\theta$) and apparent rotational stiffness ($k_\theta$) for describing digit moment generation. The referent aperture and the referent orientation, which are control variables reflecting the task-specific level that ensure the translational and rotational equilibrium of the holding objects, were further determined. The overall results obtained from the two experiments lead to the following conclusions.

1) The neural controller specifies a set of control variables to produce desired mechanical outcomes by reflecting the mechanical constraints of the performing tasks. This proposition was derived from Chapter 3, and the control variables were organized differently depending on given external constraints, the free and fixed object prehension.

2) There could be different functional implications for the designation of two control variables for digit force or moment production in the isometric condition; the referent position (i.e., $RC$ and $R_\theta$) is related to direction and magnitude of net force/moment, while the apparent stiffness (i.e., $k$ and $k_\theta$) reflects the stability properties for the corresponding effectors and given tasks.

3) The hierarchical organization of control variables was valid in multi-digit prehension involving two levels of control hierarchies. In the upper hierarchy, all the control variables for digit force and moment are organized synergistically. In the lower hierarchy, it is organized in a way that only the effects of digit moment are stabilized.

4) The decoupled control of grasp and rotation might be valid not only in the space of mechanical variables but also at the control level. In Chapter 4, it was confirmed that the $\{RC, k\}$ and $\{R_{\theta}, k_{\theta}\}$ could be organized independently, consistent with the principle of superposition in human prehension.

5) The mechanical advantage hypothesis, which dictates the specialization of the individual fingers in moment production, not just the level of mechanical effect but also can explain the consideration of task-specific stability at the control level. We observed the higher synergistic action of the control variables within the lateral fingers than in the medial fingers, as well as the finger acting as a moment agonist.

The referent control hypothesis is the neurophysiological based model that approaches identifying the laws of physics that explain the neural control of biological action and perception. Moreover, it is currently the only hypothesis that resolves the posture-movement paradox by integrating the postural control and movement into a single control scheme. However, this hypothesis remains unexplained in several aspects of human motor control, and it may be an explicit limitation of the current dissertation based on the hypothesis. Our future study will explore the control mechanisms of various human movements, including sports situations, by supplementing the current literature on human motor control.

# Bibliography


Adamovich, S., Burlachkova, N. I., & Feldman, A. G. (1984). Wave nature of the central process of formation of the trajectories of change in the joint angle in man. *Biophysics, 29*(1), 130-134.

Ambike, S., Mattos, D., Zatsiorsky, V., & Latash, M. (2018). Systematic, Unintended Drifts in the Cyclic Force Produced with the Fingertips. *Motor Control, 22*(1), 82-99.

Ambike, S., Mattos, D., Zatsiorsky, V. M., & Latash, M. L. (2016). Synergies in the Space of Control Variables within the Equilibrium-Point Hypothesis. *Neuroscience, 315*, 150-161.

Ambike, S., Paclet, F., Latash, M. L., & Zatsiorsky, V. M. (2013). Grip-force modulation in multi-finger prehension during wrist flexion and extension. *Experimental Brain Research, 227*(4), 509-522.

Ambike, S., Paclet, F., Zatsiorsky, V. M., & Latash, M. L. (2014). Factors affecting grip force: anatomy, mechanics, and referent configurations. *Experimental Brain Research, 232*(4), 1219-1231.

Ambike, S., Zhou, T., Zatsiorsky, V. M., & Latash, M. L. (2015). Moving a Hand-Held Object: Reconstruction of Referent Coordinate and Apparent Stiffness Trajectories. *Neuroscience, 298*, 336-356.

Arbib, M. A., Iberall, T., & Lyons, D. (1985). Coordinated control programs for movements of the hand. *Experimental Brain Research*, 111-129.

Archambault, P. S., Mihaltchev, P., Levin, M. F., & Feldman, A. G. (2005). Basic elements of arm postural control analyzed by unloading. *Experimental Brain Research, 164*(2), 225-241.

Arimoto, S., & Nguyen, P. T. A. (2001). Principle of superposition for realising dexterous pinching motions of a pair of robot fingers with soft-tips. *Ieice Transactions on Fundamentals of Electronics Communications and Computer Sciences, E84a*(1), 39-47.

Asatryan, D. G., & Feldman, A. G. (1965). Functional tuning of the nervous system with control of movement or maintenance of a steady posture. 1. Mechanographic

analysis of the work of the joint on execution of a postural task. *Biophysics, 10*, 925-935.

Baud-Bovy, G., & Soechting, J. F. (2001). Two virtual fingers in the control of the tripod grasp. *Journal of neurophysiology, 86*(2), 604-615.

Bernstein, N. A. (1930). A new method of mirror cyclographie and its application towards the study of labor movements during work on a workbench. *Hygiene, Safety and Pathology of labor, 5*, 3-9.

Bernstein, N. A. (1947). On the Construction of Movements. Moscow: Medgiz. *1947./HA BepHurreihi, O Hocrpoelmn gB14> KeH14ii. Mocxsa: Meztras*.

Bernstein, N. A. (1966). The co-ordination and regulation of movements. *The co-ordination and regulation of movements*.

Cole, K. J., & Abbs, J. H. (1987). Kinematic and Electromyographic Responses to Perturbation of a Rapid Grasp. *Journal of neurophysiology, 57*(5), 1498-1510.

Corcos, D. M., Agarwal, G. C., Flaherty, B. P., & Gottlieb, G. L. (1990). Organizing Principles for Single-Joint Movements .4. Implications for Isometric Contractions. *Journal of neurophysiology, 64*(3), 1033-1042.

Cuadra, C., Gilmore, R., & Latash, M. L. (2020). Finger Force Matching and Verbal Reports: Testing Predictions of the Iso-Perceptual Manifold Concept. *Journal of motor behavior*.

Cuadra, C., Wojnicz, W., Kozinc, Z., & Latash, M. L. (2020). Perceptual and Motor Effects of Muscle Co-activation in a Force Production Task. *Neuroscience, 437*, 34-44.

Cutkosky, M. R., & Howe, R. D. (1990). Human Grasp Choice and Robotic Grasp Analysis. *Dextrous Robot Hands*, 5-31.

Danion, F., Schoner, G., Latash, M. L., Li, S., Scholz, J. P., & Zatsiorsky, V. M. (2003). A mode hypothesis for finger interaction during multi-finger force-production tasks. *Biological cybernetics, 88*(2), 91-98.

de Freitas, P. B., Freitas, S. M. S. F., Lewis, M. M., Huang, X. M., & Latash, M. L. (2018). Stability of steady hand force production explored across spaces and methods of analysis. *Experimental Brain Research, 236*(6), 1545-1562.

Devlin, H., & Wastell, D. G. (1986). The Mechanical Advantage of Biting with the Posterior Teeth. *Journal of Oral Rehabilitation, 13*(6), 607-610.

Dizio, P., & Lackner, J. R. (1995). Motor Adaptation to Coriolis-Force Perturbations of

Reaching Movements - End-Point but Not Trajectory Adaptation Transfers to the Nonexposed Arm. *Journal of neurophysiology, 74*(4), 1787-1792.

Fedirchuk, B., & Dai, Y. (2004). Monoamines increase the excitability of spinal neurones in the neonatal rat by hyperpolarizing the threshold for action potential production. *Journal of Physiology-London, 557*(2), 355-361.

Feldman, A. G. (1966). Functional Tuning of Nervous System during Control of Movement or Maintenance of a Steady Posture .3. Mechanographic Analysis of Execution by Man of Simplest Motor Tasks. *Biophysics-Ussr, 11*(4), 766-&.

Feldman, A. G. (1980). Superposition of motor programs--I. Rhythmic forearm movements in man. *Neuroscience, 5*(1), 81-90.

Feldman, A. G. (1986). Once More on the Equilibrium-Point Hypothesis Lambda-Model) for Motor Control. *Journal of motor behavior, 18*(1), 17-54.

Feldman, A. G. (2011). Space and time in the context of equilibrium-point theory. *Wiley Interdisciplinary Reviews-Cognitive Science, 2*(3), 287-304.

Feldman, A. G. (2015). Referent control of action and perception. *Challenging Conventional Theories in Behavioral Neuroscience*.

Feldman, A. G. (2019). Indirect, referent control of motor actions underlies directional tuning of neurons. *Journal of neurophysiology, 121*(3), 823-841.

Feldman, A. G., Goussev, V., Sangole, A., & Levin, M. F. (2007). Threshold position control and the principle of minimal interaction in motor actions. *Computational Neuroscience: Theoretical Insights into Brain Function, 165*, 267-281.

Feldman, A. G., & Latash, M. L. (2005). Testing hypotheses and the advancement of science: recent attempts to falsify the equilibrium point hypothesis. *Experimental Brain Research, 161*(1), 91-103.

Feldman, A. G., & Orlovsky, G. N. (1972). The influence of different descending systems on the tonic stretch reflex in the cat. *Experimental neurology, 37*(3), 481-494.

Flash, T., & Hogan, N. (1985). The Coordination of Arm Movements - an Experimentally Confirmed Mathematical-Model. *Journal of Neuroscience, 5*(7), 1688-1703.

Foisy, M., & Feldman, A. G. (2006). Threshold control of arm posture and movement adaptation to load. *Experimental Brain Research, 175*(4), 726-744.

Freitas, S. M. S. F., & Scholz, J. P. (2009). Does hand dominance affect the use of motor abundance when reaching to uncertain targets? *Human Movement Science, 28*(2),

169-190.

Frenkel-Toledo, S., Yamanaka, J., Friedman, J., Feldman, A. G., & Levin, M. F. (2019). Referent control of anticipatory grip force during reaching in stroke: an experimental and modeling study. *Experimental Brain Research, 237*(7), 1655-1672.

Frey, D. D., & Carlson, L. E. (1994). A Body Powered Prehensor with Variable Mechanical Advantage. *Prosthetics and Orthotics International, 18*(2), 118-123.

Gao, F., Latash, M. L., & Zatsiorsky, V. M. (2005a). Control of finger force direction in the flexion-extension plane. *Experimental Brain Research, 161*(3), 307-315.

Gao, F., Latash, M. L., & Zatsiorsky, V. M. (2005b). Internal forces during object manipulation. *Experimental Brain Research, 165*(1), 69-83.

Gao, F., Latash, M. L., & Zatsiorsky, V. M. (2006). Maintaining rotational equilibrium during object manipulation: linear behavior of a highly non-linear system. *Experimental Brain Research, 169*(4), 519-531.

Gelfand, I. M., & Latash, M. L. (1998). On the problem of adequate language in movement science. *Motor Control, 2*, 306-313.

Gelfand, I. M., & Tsetlin, M. L. (1966). On mathematical modeling of the mechanisms of the center nervous system. *Models of the structural-functional organization of certain biological systems*, 9-26.

Gelfand, I. M., & Tsetlin, M. L. (1971). Some methods of controlling complex systems. *Models of structural-functional organization of certain biological systems. MIT Press, Cambridge*, 329-345.

Ghez, C., & Gordon, J. (1987). Trajectory Control in Targeted Force Impulses .1. Role of Opposing Muscles. *Experimental Brain Research, 67*(2), 225-240.

Gielen, C., van Zuylen, E., & Denier van der Gon, J. (1988). Coordination of arm muscles in simple motor tasks. *International series on biomechanics, 7*, 155-166.

Gorniak, S. L., Zatsiorsky, V. M., & Latash, M. L. (2009). Hierarchical control of static prehension: II. Multi-digit synergies. *Experimental Brain Research, 194*(1), 1-15.

Gottlieb, G. L., Corcos, D. M., & Agarwal, G. C. (1989). Strategies for the Control of Voluntary Movements with One Degree of Freedom. *Behavioral and brain sciences, 12*(2), 189-210.

Gottlieb, G. L., Corcos, D. M., & Agarwal, G. C. (1991). Strategies for the Control of Voluntary Movements with One Mechanical Degree of Freedom. *Behavioral and*

*brain sciences, 14*(2), 352-352.

Hager-Ross, C., & Schieber, M. H. (2000). Quantifying the independence of human finger movements: Comparisons of digits, hands, and movement frequencies. *Journal of Neuroscience, 20*(22), 8542-8550.

Hasanbarani, F., Batalla, M. A. P., Feldman, A. G., & Levin, M. F. (2021). Mild Stroke Affects Pointing Movements Made in Different Frames of Reference. *Neurorehabilitation and Neural Repair, 35*(3), 207-219.

Heckman, C. J., Johnson, M., Mottram, C., & Schuster, J. (2008). Persistent inward currents in spinal motoneurons and their influence on human motoneuron firing patterns. *Neuroscientist, 14*(3), 264-275.

Heitmann, S., Ferns, N., & Breakspear, M. (2011). Muscle co-contraction modulates damping and joint stability in a three-link biomechanical limb. *Frontiers in Neurorobotics, 5*, 5.

Hinder, M. R., & Milner, T. E. (2003). The case for an internal dynamics model versus equilibrium point control in human movement. *Journal of Physiology-London, 549*(3), 953-963.

Hughlings Jackson, J. (1889). On the comparative study of disease of the nervous system. *British Medical Journal, 355*, 362.

Iberall, T. (1997). Human prehension and dexterous robot hands. *International Journal of Robotics Research, 16*(3), 285-299.

Ilmane, N., Sangani, S., & Feldman, A. G. (2013). Corticospinal control strategies underlying voluntary and involuntary wrist movements. *Behavioural Brain Research, 236*, 350-358.

Ivanenko, Y. P., Cappellini, G., Dominici, N., Poppele, R. E., & Lacquaniti, F. (2005). Coordination of locomotion with voluntary movements in humans. *Journal of Neuroscience, 25*(31), 7238-7253.

Ivanenko, Y. P., Poppele, R. E., & Lacquaniti, F. (2004). Five basic muscle activation patterns account for muscle activity during human locomotion. *Journal of Physiology-London, 556*(1), 267-282.

Jo, H. J., Maenza, C., Good, D. C., Huang, X., Park, J., Sainburg, R. L., & Latash, M. L. (2016). Effects of Unilateral Stroke on Multi-Finger Synergies and Their Feed-Forward Adjustments. *Neuroscience, 319*, 194-205.

Kaiser, H. F. (1960). The Application of Electronic-Computers to Factor-Analysis.

*Educational and Psychological Measurement, 20*(1), 141-151.

Kal, E. C., van der Kamp, J., & Houdijk, H. (2013). External attentional focus enhances movement automatization: A comprehensive test of the constrained action hypothesis. *Human Movement Science*, 32(4), 527-539.

Kang, N., Shinohara, M., Zatsiorsky, V. M., & Latash, M. L. (2004). Learning multi-finger synergies: an uncontrolled manifold analysis. *Experimental Brain Research, 157*(3), 336-350.

Karol, S., Kim, Y. S., Huang, J. F., Kim, Y. H., Koh, K., Yoon, B. C., & Shim, J. K. (2011). Multi-finger pressing synergies change with the level of extra degrees of freedom. *Experimental Brain Research, 208*(3), 359-367.

Kilbreath, S. L., & Gandevia, S. C. (1994). Limited Independent Flexion of the Thumb and Fingers in Human-Subjects. *Journal of Physiology-London, 479*(3), 487-497.

Kilbreath, S. L., Gorman, R. B., Raymond, J., & Gandevia, S. C. (2002). Distribution of the forces produced by motor unit activity in the human flexor digitorum profundus. *Journal of Physiology-London, 543*(1), 289-296.

Kong, J., Kim, K., Joung, H. J., Chung, C. Y., & Park, J. (2019). Effects of spastic cerebral palsy on multi-finger coordination during isometric force production tasks. *Experimental Brain Research, 237*(12), 3281-3295.

Krawitz, S., Fedirchuk, B., Dai, Y., Jordan, L. M., & McCrea, D. A. (2001). State-dependent hyperpolarization of voltage threshold enhances motoneurone excitability during fictive locomotion in the cat. *Journal of Physiology, 532*(Pt 1), 271-281.

Lackner, J. R., & Dizio, P. (1994). Rapid Adaptation to Coriolis-Force Perturbations of Arm Trajectory. *Journal of neurophysiology, 72*(1), 299-313.

Latash, M. L. (1994). Reconstruction of Equilibrium Trajectories and Joint Stiffness Patterns during Single-Joint Voluntary Movements under Different Instructions. *Biological cybernetics, 71*(5), 441-450.

Latash, M. L. (2008). *Synergy*: Oxford University Press.

Latash, M. L. (2010). Motor Synergies and the Equilibrium-Point Hypothesis. *Motor Control, 14*(3), 294-322.

Latash, M. L. (2012). The bliss (not the problem) of motor abundance (not redundancy). *Experimental Brain Research, 217*(1), 1-5.

Latash, M. L. (2017). Biological Movement and Laws of Physics. *Motor Control, 21*(3), 327-

344.

Latash, M. L. (2018). Muscle coactivation: definitions, mechanisms, and functions. *Journal of neurophysiology, 120*(1), 88-104.

Latash, M. L. (2020a). Laws of nature that define biological action and perception. *Physics of Life Reviews*.

Latash, M. L. (2020b). On Primitives in Motor Control. *Motor Control, 24*(2), 318-346.

Latash, M. L. (2021). Efference copy in kinesthetic perception: A copy of what is it? *Journal of neurophysiology, 125*(4), 1079-1094.

Latash, M. L., Friedman, J., Kim, S. W., Feldman, A. G., & Zatsiorsky, V. M. (2010). Prehension synergies and control with referent hand configurations. *Experimental Brain Research, 202*(1), 213-229.

Latash, M. L., & Gottlieb, G. L. (1991). Reconstruction of Shifting Elbow Joint Compliant Characteristics during Fast and Slow Movements. *Neuroscience, 43*(2-3), 697-712.

Latash, M. L., & Huang, X. (2015). Neural Control of Movement Stability: Lessons from Studies of Neurological Patients. *Neuroscience, 301*, 39-48.

Latash, M. L., Scholz, J. F., Danion, F., & Schoner, G. (2001). Structure of motor variability in marginally redundant multifinger force production tasks. *Experimental Brain Research, 141*(2), 153-165.

Latash, M. L., Scholz, J. P., & Schoner, G. (2007). Toward a new theory of motor synergies. *Motor Control, 11*(3), 276-308.

Latash, M. L., Shim, J. K., Smilga, A. V., & Zatsiorsky, V. M. (2005). A central back-coupling hypothesis on the organization of motor synergies: a physical metaphor and a neural model. *Biological cybernetics, 92*(3), 186-191.

Leijnse, J. N. A. L., Snijders, C. J., Bonte, J. E., Landsmeer, J. M. F., Kalker, J. J., Vandermeulen, J. C., . . . Hovius, S. E. R. (1993). The Hand of the Musician - the Kinematics of the Bidigital Finger System with Anatomical Restrictions. *Journal of biomechanics, 26*(10), 1169-1179.

Li, Z. M., Latash, M. L., & Zatsiorsky, V. M. (1998). Force sharing among fingers as a model of the redundancy problem. *Experimental Brain Research, 119*(3), 276-286.

Li, Z. M., Zatsiorsky, V. M., & Latash, M. L. (2000). Contribution of the extrinsic and intrinsic hand muscles to the moments in finger joints. *Clinical biomechanics, 15*(3), 203-211.

Li, Z. M., Zatsiorsky, V. M., & Latash, M. L. (2001). The effect of finger extensor mechanism on the flexor force during isometric tasks. *Journal of biomechanics, 34*(8), 1097-1102.

Li, Z. M., Latash, M. L., Newell, K. M., & Zatsiorsky, V. M. (1998). Motor redundancy during maximal voluntary contraction in four-finger tasks. *Experimental Brain Research, 122*(1), 71-78.

Liddell, E. G. T., & Sherrington, C. (1924). Reflexes in response to stretch (myotatic reflexes). *Proceedings of the Royal Society of London Series B-Containing Papers of a Biological Character, 96*(675), 212-242.

MacKenzie, C. L., & Iberall, T. (1994). *The grasping hand*: Elsevier.

Martin, J. R., Budgeon, M. K., Zatsiorsky, V. M., & Latash, M. L. (2011). Stabilization of the total force in multi-finger pressing tasks studied with the 'inverse piano' technique. *Human Movement Science, 30*(3), 446-458.

Martin, V., Scholz, J. P., & Schoner, G. (2009). Redundancy, Self-Motion, and Motor Control. *Neural Computation, 21*(5), 1371-1414.

Mason, M. T., Salisbury, J. K., & Parker, J. K. (1989). Robot hands and the mechanics of manipulation.

Matthews, P. B. (1959). A study of certain factors influencing the stretch reflex of the decerebrate cat. *The Journal of physiology, 147*(3), 547-564.

Matthews, P. B. (1972). Mammalian muscle receptors and their central actions.

Mattos, D., Schoner, G., Zatsiorsky, V. M., & Latash, M. L. (2015). Motor equivalence during multi-finger accurate force production. *Experimental Brain Research, 233*(2), 487-502.

Muller, H., & Sternad, D. (2003). A randomization method for the calculation of covariation in multiple nonlinear relations: illustrated with the example of goal-directed movements. *Biological cybernetics, 89*(1), 22-33.

Mullick, A. A., Turpin, N. A., Hsu, S. C., Subramanian, S. K., Feldman, A. G., & Levin, M. F. (2018). Referent control of the orientation of posture and movement in the gravitational field. *Experimental Brain Research, 236*(2), 381-398.

Murray, R. M., Li, Z., & Sastry, S. S. (2017). *A mathematical introduction to robotic manipulation*: CRC press.

Mussaivaldi, F. A., & Hogan, N. (1991). Integrable Solutions of Kinematic Redundancy Via

Impedance Control. *International Journal of Robotics Research, 10*(5), 481-491.

Nichols, T. R., & Houk, J. C. (1976). Improvement in Linearity and Regulation of Stiffness That Results from Actions of Stretch Reflex. *Journal of neurophysiology, 39*(1), 119-142.

Oldfield, R. C. (1971). The Assessment and Analysis of Handedness: The Edinburgh Inventory. *Neuropsychologia, 9*(1), 97-113.

Park, J., Baum, B. S., Kim, Y. S., Kim, Y. H., & Shim, J. K. (2012). Prehension Synergy: Use of Mechanical Advantage During Multifinger Torque Production on Mechanically Fixed and Free Objects. *Journal of applied biomechanics, 28*(3), 284-290.

Park, J., Han, D. W., & Shim, J. K. (2015). Effect of Resistance Training of the Wrist Joint Muscles on Multi-Digit Coordination. *Perceptual and Motor Skills, 120*(3), 816-840.

Park, J., Kim, Y. S., & Shim, J. K. (2010). Prehension synergy: Effects of static constraints on multi-finger prehension. *Human Movement Science, 29*(1), 19-34.

Park, J., Lewis, M. M., Huang, X. M., & Latash, M. L. (2013). Effects of olivo-ponto-cerebellar atrophy (OPCA) on finger interaction and coordination. *Clinical Neurophysiology, 124*(5), 991-998.

Park, J., Pazin, N., Friedman, J., Zatsiorsky, V. M., & Latash, M. L. (2014). Mechanical properties of the human hand digits: Age-related differences. *Clinical biomechanics, 29*(2), 129-137.

Park, J., Singh, T., Zatsiorsky, V. M., & Latash, M. L. (2012). Optimality versus variability: effect of fatigue in multi-finger redundant tasks. *Experimental Brain Research, 216*(4), 591-607.

Park, J., Wu, Y. H., Lewis, M. M., Huang, X. M., & Latash, M. L. (2012). Changes in multifinger interaction and coordination in Parkinson's disease. *Journal of neurophysiology, 108*(3), 915-924.

Park, J., Zatsiorsky, V. M., & Latash, M. L. (2010). Optimality vs. variability: an example of multi-finger redundant tasks. *Experimental Brain Research, 207*(1-2), 119-132.

Parsa, B., O'Shea, D. J., Zatsiorsky, V. M., & Latash, M. L. (2016). On the nature of unintentional action: a study of force/moment drifts during multifinger tasks. *Journal of neurophysiology, 116*(2), 698-708.

Pataky, T. C., Latash, M. L., & Zatsiorsky, V. M. (2004a). Prehension synergies during nonvertical grasping, I: experimental observations. *Biological cybernetics, 91*(3), 148-158.

Pataky, T. C., Latash, M. L., & Zatsiorsky, V. M. (2004b). Tangential load sharing among fingers during prehension. *Ergonomics, 47*(8), 876-889.

Pataky, T. C., Latash, M. L., & Zatsiorsky, V. M. (2008). Multifinger Ab- and Adduction Strength and Coordination. *Journal of Hand Therapy, 21*(4), 377-385.

Pilon, J. F., De Serres, S. J., & Feldman, A. G. (2007). Threshold position control of arm movement with anticipatory increase in grip force. *Experimental Brain Research, 181*(1), 49-67.

Pilon, J. F., & Feldman, A. G. (2006). Threshold control of motor actions prevents destabilizing effects of proprioceptive delays. *Experimental Brain Research, 174*(2), 229-239.

Popescu, F. C., & Rymer, W. Z. (2000). End points of planar reaching movements are disrupted by small force pulses: An evaluation of the hypothesis of equifinality. *Journal of neurophysiology, 84*(5), 2670-2679.

Raptis, H., Burtet, L., Forget, R., & Feldman, A. G. (2010). Control of wrist position and muscle relaxation by shifting spatial frames of reference for motoneuronal recruitment: possible involvement of corticospinal pathways. *Journal of Physiology-London, 588*(9), 1551-1570.

Reschechtko, S., & Latash, M. L. (2017). Stability of hand force production. I. Hand level control variables and multifinger synergies. *Journal of neurophysiology, 118*(6), 3152-3164.

Reschechtko, S., & Latash, M. L. (2018). Stability of hand force production. II. Ascending and descending synergies. *Journal of neurophysiology, 120*(3), 1045-1060.

Rosenbaum, D. A., Loukopoulos, L. D., Meulenbroek, R. G. J., Vaughan, J., & Engelbrecht, S. E. (1995). Planning Reaches by Evaluating Stored Postures. *Psychological Review, 102*(1), 28-67.

Sainburg, R. L. (2015). Should the equilibrium point hypothesis (eph) be considered a scientific theory? *Motor Control, 19*(2), 142.

Sainburg, R. L., Lateiner, J. E., Latash, M. L., & Bagesteiro, L. B. (2003). Effects of altering initial position on movement direction and extent. *Journal of neurophysiology, 89*(1), 401-415.

Sangani, S. G., Raptis, H. A., & Feldman, A. G. (2011). Subthreshold corticospinal control of anticipatory actions in humans. *Behavioural Brain Research, 224*(1), 145-154.

Santello, M., & Soechting, J. F. (1997). Matching object size by controlling finger span and

hand shape. *Somatosensory and Motor Research, 14*(3), 203-212.

Santello, M., & Soechting, J. F. (2000). Force synergies for multifingered grasping. *Experimental Brain Research, 133*(4), 457-467.

Savescu, A. V., Latash, M. L., & Zatsiorsky, V. M. (2008). A technique to determine friction at the fingertips. *Journal of applied biomechanics, 24*(1), 43-50.

Schieber, M. H., & Santello, M. (2004). Hand function: peripheral and central constraints on performance. *Journal of applied physiology, 96*(6), 2293-2300.

Scholz, J. P., Danion, F., Latash, M. L., & Schoner, G. (2002). Understanding finger coordination through analysis of the structure of force variability. *Biological cybernetics, 86*(1), 29-39.

Scholz, J. P., & Schoner, G. (1999). The uncontrolled manifold concept: identifying control variables for a functional task. *Experimental Brain Research, 126*(3), 289-306.

Schoner, G. (1995). Recent developments and problems in human movement science and their conceptual implications. *Ecological Psychology, 7*(4), 291-314.

Seif-Naraghi, A. H., & Winters, J. M. (1990). Optimized strategies for scaling goal-directed dynamic limb movements. In *Multiple muscle systems* (pp. 312-334): Springer.

Shim, J. K., Huang, J., Hooke, A. W., latash, M. L., & Zatsiorsky, V. M. (2007). Multi-digit maximum voluntary torque production on a circular object. *Ergonomics, 50*(5), 660-675.

Shim, J. K., Latash, M. L., & Zatsiorsky, V. M. (2003). Prehension synergies: trial-to-trial variability and hierarchical organization of stable performance. *Experimental Brain Research, 152*(2), 173-184.

Shim, J. K., Latash, M. L., & Zatsiorsky, V. M. (2004). Finger coordination during moment production on a mechanically fixed object. *Experimental Brain Research, 157*(4), 457-467.

Shim, J. K., Latash, M. L., & Zatsiorsky, V. M. (2005a). Prehension synergies in three dimensions. *Journal of neurophysiology, 93*(2), 766-776.

Shim, J. K., Latash, M. L., & Zatsiorsky, V. M. (2005b). Prehension synergies: Trial-to-trial variability and principle of superposition during static prehension in three dimensions. *Journal of neurophysiology, 93*(6), 3649-3658.

Shim, J. K., Park, J., Zatsiorsky, V. M., & Latash, M. L. (2006). Adjustments of prehension synergies in response to self-triggered and experimenter-triggered load and torque

perturbations. *Experimental Brain Research, 175*(4), 641-653.

Shim, J. K., & Park, J. B. (2007). Prehension synergies: principle of superposition and hierarchical organization in circular object prehension. *Experimental Brain Research, 180*(3), 541-556.

Singh, T., & Ambike, S. (2017). A soft-contact model for computing safety margins in human prehension. *Human Movement Science, 55*, 307-314.

Song, J., Kim, K., & Park, J. (2021). Do Tangential Finger Forces Utilize Mechanical Advantage During Moment of Force production? *Journal of motor behavior, 53*(5), 558-574.

Song, J., Shin, N., Kim, K., & Park, J. (2021). Changes in intersegmental stability during gait in patients with spastic cerebral palsy. *Gait and Posture, 88*, 264-271.

StOnge, N., Adamovich, S. V., & Feldman, A. G. (1997). Control processes underlying elbow flexion movements may be independent of kinematic and electromyographic patterns: Experimental study and modelling. *Neuroscience, 79*(1), 295-316.

Todorov, E. (2004). Optimality principles in sensorimotor control. *Nature Neuroscience, 7*(9), 907-915.

Vidal, A., Wu, W., Nakajima, M., & Becker, J. (2018). Investigating the Constrained Action Hypothesis: A Movement Coordination and Coordination Variability Approach. *Journal of motor behavior*, 50(5), 528-537.

Westling, G., & Johansson, R. S. (1984). Factors Influencing the Force Control during Precision Grip. *Experimental Brain Research, 53*(2), 277-284.

Wu, Y. H., Zatsiorsky, V. M., & Latash, M. L. (2012). Static prehension of a horizontally oriented object in three dimensions. *Experimental Brain Research, 216*(2), 249-261.

Yamazaki, Y., Ohkuwa, T., Itoh, H., & Suzuki, M. (1994). Reciprocal Activation and Coactivation in Antagonistic Muscles during Rapid Goal-Directed Movements. *Brain Research Bulletin, 34*(6), 587-593.

Yang, J. F., Scholz, J. P., & Latash, M. L. (2007). The role of kinematic redundancy in adaptation of reaching. *Experimental Brain Research, 176*(1), 54-69.

Zatsiorsky, V. M. (2002). *Kinetics of human motion*: Human kinetics.

Zatsiorsky, V. M., Gao, F., & Latash, M. L. (2003a). Finger force vectors in multi-finger prehension. *Journal of biomechanics, 36*(11), 1745-1749.

Zatsiorsky, V. M., Gao, F., & Latash, M. L. (2003b). Prehension synergies: Effects of object

geometry and prescribed torques. *Experimental Brain Research, 148*(1), 77-87.

Zatsiorsky, V. M., Gao, F., & Latash, M. L. (2006). Prehension stability: Experiments with expanding and contracting handle. *Journal of neurophysiology, 95*(4), 2513-2529.

Zatsiorsky, V. M., Gregory, R. W., & Latash, M. L. (2002a). Force and torque production in static multifinger prehension: biomechanics and control. I. Biomechanics. *Biological cybernetics, 87*(1), 50-57.

Zatsiorsky, V. M., Gregory, R. W., & Latash, M. L. (2002b). Force and torque production in static multifinger prehension: biomechanics and control. II. Control. *Biological cybernetics, 87*(1), 40-49.

Zatsiorsky, V. M., & Latash, M. L. (2008). Multifinger prehension: An overview. *Journal of motor behavior, 40*(5), 446-475.

Zatsiorsky, V. M., Latash, M. L., Gao, F., & Shim, J. K. (2004). The principle of superposition in human prehension. *Robotica, 22*, 231-234.

Zatsiorsky, V. M., Li, Z. M., & Latash, M. L. (2000). Enslaving effects in multi-finger force production. *Experimental Brain Research, 131*(2), 187-195.

Zhang, L., Feldman, A. G., & Levin, M. F. (2018). Vestibular and corticospinal control of human body orientation in the gravitational field. *Journal of neurophysiology, 120*(6), 3026-3041.

Zhang, W., Zatsiorsky, V. M., & Latash, M. L. (2006). Accurate production of time-varying patterns of the moment of force in multi-finger tasks. *Experimental Brain Research, 175*(1), 68-82.

# 국문 초록

다중 손가락을 이용한 쥐기(multi-digit prehension)는 다양한 손가락의 힘과 모멘트 조합을 통해 정적 평형을 달성할 수 있는 전형적인 운동요소과잉(motor redundancy)이 내제된 인간의 기능적 움직임이다. 본 연구는 골격근의 제어 원리를 설명하기 위한 평형점 가설(equilibrium-point hypothesis)에서 일반화된 레퍼런트 제어(referent control) 모델을 기반으로 하여 다섯 손가락을 이용한 정적인 쥐기(static prehension) 과제에서 나타나는 역학적 및 제어적 특징을 살펴보기 위해 수행되었다. 이를 위해 모터의 외력에 의해 핸들의 변위가 발생하는 실험용 핸들을 고안하였으며, 정적 쥐기에서 병진(translation) 및 회전 평형의 제어를 설명하기 위해 손가락의 힘과 모멘트 생성을 제어하는 매개변수를 정량화 하였다. 다중 손가락 쥐기 과제는 두 제어 계층, 즉 네 손가락이 형성하는 하위 계층과 엄지와 손가락들의 효과가 더해지는 상위계층으로 구성된다. 연구결과, 손가락의 기계적 효과를 유발하는 제어 매개변수는 과제 수준(task-specific level)에서 요구되는 힘과 모멘트를 안정화하하기 위해 협응적으로(synergistic) 조직화 됨을 확인하였다. 기계적 제약조건을 다르게 설정한 실험을 통해 병진 운동의 평형을 보장하는 제어 매개변수의 계층적 안정화 정도는 기계적 제약조건에 따라 변할 수 있음을 확인하였으며, 손가락 모멘트의 크기와 방향을 달리한 실험을 통해 제어 매개변수 간 기능적 차이를 확인하였다. 또한 정적인 쥐기에서 물체의 병진과 회전의 제어가 독립적으로 이루어짐을 시사하는 중첩의 원리(principle of superposition)가 기계적 변수와 제어 매개변수의 수준 모두에서 유효하게 적용 될 수 있다는 근거를 확인하였다. 본 연구에서 도출된 이 결과들은 과잉된 운동요소를 통해 정적인 평형을 유지해야 하는 다중 손가락 쥐기 과제에서 신경운동시스템(neuromotor system)은 주어진 외부제약조건과 기계적 효과, 그리고 손가락의 구조적 특성과 안정성을 반영하여 손가락의 힘과 모멘트를 발생시키는 운동 명령을 생성 한다는 것을 시사한다.

**주요어:** 다중 손가락 쥐기, 평형점 가설, 레퍼런트 제어, 인간 운동 제어, 운동 요소 과잉, 시너지

**학 번:** 2017-31990

# Acknowledgements

For several years, I taught exercise experts about the functional anatomy of the human musculoskeletal system and effective rehabilitation strategies for movement impairment. Not long after that, I was faced with an inherent unanswerable problem regarding the mechanism of human motor control; *how does the central nervous system control the complex physical body system?* This question started to create small loopholes in my lectures and was the reason that brought me back as a student so belatedly.

Dr. Jaebum Park, my advisor in the Human Biomechanics Lab, instructed me on the mechanical and physiological aspects of the neuromotor system and how to quantify the various human movements for the doctoral program. He has overseen all my research, including this dissertation over five and a half years. I express my heartfelt appreciation to him, and he is definitely the person who has had the most significant impact on my life. I also express appreciation to my committee members, Dr. Seonjin Kim, Dr. Jae Kun Shim, Dr. Jooeun Ahn, and Dr. Woojin Park, for their careful supervision in developing my dissertation. In particular, Dr. Jae Kun Shim as my academic grandfather inspired me to begin the doctoral course and provided the knowledge basis for the current study. I would like to thank my colleagues, including Sanghoon Park, Dohoon Koo, Kitae Kim, Jiseop Lee, Dawon Park, Dayuan Xu, Jiwon Park, Sungjune Lee, Narae Shin, Yoonseok Choi, Jong-ah Kim, Dong-gyu Baek, and Jiho Kim. Without their supports, this dissertation could never have been completed. My parents, Ki-Woon Song, Jong-Seon Bae, and my older brother Hyun-Kyung Song, have always been my greatest help. Finally, my fiancé, Yera Oh, has assisted me in the final stage of my degree. Now I will be a pillar of strength to you.

At this moment, if I had to repeat the earlier question about the control mechanism of human motor behavior, my answer would be “still don’t know”. I might not be able to answer the question until the end of my life. Perhaps being a good researcher is not in having all the answers, but in pursuing the unanswerable questions. Just what I hope that this dissertation will be a handful of clues to approach the solution to the problem.